Genetic Analysis of Consanguineous South Indian Families with Leber Congenital Amaurosis and Retinitis Pigmentosa using Homozygosity Mapping

THESIS

Submitted in partial fulfillment

of the requirements for the degree of

DOCTOR OF PHILOSOPHY

By

S. Srilekha

2011PHXF101H

Under the Supervision of

Associate Prof. Dr. N. Soumittra

&

Under the Co-supervision of

Prof. Dr. Suman Kapur

BIRLA INSTITUTE OF TECHNOLOGY AND SCIENCE
HYDERABAD

2016

BIRLA INSTITUTE OF TECHNOLOGY AND SCIENCE HYDERABAD

CERTIFICATE

This is to certify that the thesis entitled **"Genetic Analysis of Consanguineous South Indian Families with Leber Congenital Amaurosis and Retinitis Pigmentosa using Homozygosity Mapping"** submitted by **Ms. S. Srilekha** ID No **2011PHXF101H** for the award of Ph.D. degree of the Institute embodies original work done by her under my supervision.

Signature in full of the Supervisor:

Dr. N. Soumittra
Principal Scientist &
Associate Professor
SNONGC Department of Genetics
and Molecular Biology
Vision Research Foundation
Chennai - 600006

Date:

Signature in full of the Co-Supervisor:

Prof. Dr. Suman Kapur
Dean, International Programmes and
Collaborations/Senior Professor
Head Department of Biological Science
BITS – Pilani, Hyderabad Campus
Hyderabad - 500078

Date:

ACKNOWLEDGEMENTS

I would like to begin with my tribute to the **Almighty**, who has given the strength, blessing me throughout my work, by giving such wonderful people around me including my teachers, friends and family. I acknowledge each and every one of them, though I could give a special mention only to few.

I have been blessed to be a part of Sankara Nethralaya and BITS, PILANI. The Vision Research Foundation, Sankara Nethralaya gave me an excellent infrastructure to work and BITS guided me in my journey towards PhD. I acknowledge Padmabhushan **Dr. S.S. Badrinath**, the Chairman Emeritus, **Dr. S.B. Vasanthi Badrinath** Director of Lab services and **Prof. B.N. Jain**, Vice chancellor and Director BITS Pilani, for giving me an opportunity to be a part of their esteemed institutions.

I extend my acknowledgement to **Dr. S.K. Verma**, Dean, Research and Consultancy Division Pilani, **Prof. V.S. Rao** Director of BITS Pilani, Hyderabad, **Dr. Lingam Gopal**, President of Vision Research Foundation (VRF), **Dr. Tarun Sharma** Honorary Secretary of VRF, **Dr. H.N. Madhavan** Director of Microbiology, **Dr. Ronnie George**, Director of Research, **Dr. Rama Rajagopal**, Advisor VRF, **Mr. S. Narayanan**, Manager VRF, for their support. I also thank **Dr. S. Meenakshi**, Director of Academics.

I extend my acknowledgment to **Indian Council of Medical Research (ICMR)**, Govt. of India for the grant 54/1/2010-BMS and SRF Fellowship - N0.45/2/2014-HUM-BMS and all the **patients** and their family for their kind co-operation.

I take this opportunity to acknowledge my supervisor **Dr. N. Soumittra**, Associate Professor in Genetics and Molecular Biology for carving my carrier with her valuable suggestion, clear ideas, and extensively analyzing the research work. I am in indebted to her for reviewing of my thesis patiently. She has been a very good friend, valuable philosopher and unforgettable guide. I am very blessed to have her as my PhD guide.

I take my privilege to acknowledge my co-supervisor **Prof. Suman kapur**, HOD, Department of Biological Sciences, BITS PILANI, Hyderabad for her understanding, timely guidance, and support. She has always been inspirational and I admire her enthusiasm in translational research. My sincere thanks to **Dr. P.R. Deepa**, BITS co-ordinator for her support and valuable advice.

I take this opportunity to thank **Dr. S. Meenakshi** for her clinical diagnosis on the project patients and **Dr. Parveen Sen** for helping me in the phenotype documentation of the affected patients.

I express my sincere thanks to **Mrs. R. Punitham** Manager of Lab services who had taught me the sincerity and dedication towards work and utilizing my potentials in the right way and also encouraging me for my P.G course.

I express my sense of gratitude to **Dr. G. Kumaramanickavel** who has been instrumental in recommending me towards M.S.MLT course conducted by BITS-Pilani along with Sankara Nethralaya and also my appreciation to **Dr. J. Madhavan** who had been my guide during my dissertation work in M.S and paved the right path for my PhD.

I acknowledge **Dr. A.J Pandian,** HOD, Department of Genetics and Molecular Biology for his enthusiastic support.

I am grateful to **Dr. S. Sripriya,** Associate Professor in Genetics and Molecular Biology for her moral support.

I sincerely acknowledge **Mr. T. Arokiasamy** social worker for identifying and motivating the patients to participate in the study. I also thank **Mr. M. Jayaprakash** for his continuous support and encouragement during my needy hours. They both gave me a moral support which I needed at many times.

My sincere thanks to my PhD partner **Mrs. N. N. Srikrupa,** who had been with me throughout my journey of PhD. She had been with me at many difficult moments and

accompanied me at many situations. I am grateful to her and **Mrs. Shabna** who were with me during my travel to BITS-Hyderabad and made my journey memorable.

I am thankful to my colleagues **Ms. D. Sudha and Dr. Divya Rao** who had been as a source of motivation when I felt lonely and depressed. They both brought in me a new source of energy and enthusiasm.

I sincerely thank my colleagues **Dr. Ferdina Marie Sharmila, Dr. C. Sathya priya, Mr. S. Malaichamy, Dr. Vinita Kumari, Mrs. Bhavna S Rao, Mrs. K. Sudha**, **Mrs T. Karthiyayene**, **Ms. P. Porkodi**, **Mrs. N. JeevaJothi, Mr. G. Venkatesan, Ms. Srividya**, **Mrs. V. Kavitha**, **Mrs. S. Jothi Lakshmi**, **Mr. N. Babu** and **Mr. O. Prabhu** for their sincere encouragement and inspiration; especially in extending their help in various ways possible.

I sincerely acknowledge my DAC members **Dr. Jayati Ray Dutta**, **Prof. Ramakrishna Vadrevu** for spending their valuable time and giving their suggestions in PhD presentations and **Dr. Kumar Pranav Narayan** and **Dr. K.N. Mohan** for scheduling presentations in each semester. I also acknowledge **Dr. Vidya Rajesh** (Associate Dean, ARCD), **Dr. Sridev Mohapatra and Dr. Debashree Bandyopathyay** for giving their valuable suggestion during my end sem presentation

I thank **Dr. K. Lily Therese**, VIBS co-ordinator for their continued support and encouragement. My extended sense of gratitude to **Drs. K.N. Sulochana, N. Angayarkanni, Dorien Gracious, S. Krishnakumar, A.S. Badrinath, J. Malathi, B. Mahalakshmi, K. Coral, S. Bharathi, J. Subbulakshmi, V. Umashankar, Nivedita Chatterjee** for evaluating my practice lectures.

I also acknowledge my friends and colleagues **Dr. E. Anuradha**, **Dr. G. Mamatha**, **Mr. M. Rajesh**, **Mrs. Salomi Christopher, Mrs. Amali John, Mrs. S. Sumathi** and **Mrs. C. Sacikala** for their support and friendship.

I acknowledge my friends from Genomics lab, BITS Pilani, Hyderabad **Ms. Sai Chinmayi**, **Ms. Anuradha Pal**, **Ms. Shivani Guptha**, **Ms. Padma**, **Ms. Sruthi Varier**, **Ms. Minal**, **Dr. Blesson**, **Mr. Pavan**, **Mr. Rupak** and **Pooja mam** for their support and encouragement. The time spent with them was joyful and informative.

I thank my husband **Mr. D. Anandakrishnan** who encouraged and supported me with all my decisions. I had the opportunity to do my P.G as well as PhD only after my marriage and he was there with me at all difficult situations. I also thank my little ones **A. Rakshan** and **A. Anjana** for bearing with their busy mother and accommodating themselves according to my lifestyle. I thank my in laws for their continued support and patience.

I also thank my uncle **Mr. L.R. Sadhasivam**, his wife **Mrs. Usha** and the little one **Srija Sadhasivam** for their continued support, guidance and encouragement. Their family had been a moral support to me.

I am in-debted to my brother **Mr. Rajesh** and my sister in-law **Mrs. Gajalakshmi** for their help in supporting me and taking care of my children during my absence. I also thank my little nephew **R. Naveen** for making me smile at all my difficult moments.

Last but not least my dear parents, **Mr. R. Sundaramurthy** my father who is a great source of inspiration giving me moral support and making me realize my own potentials. He had been with me where ever I had to go, still taking care of me and my family. My mother **Mrs. R. Selvi** who encouraged me to do PhD, took care of my children during the hour of need. I am indebted to both of them for their unconditional love and support. Without both of them, this wouldn't have been possible at all. I whole heartedly **dedicate** my thesis to my **parents.**

S.Srilekha

ABSTRACT

Background

Inherited retinal degenerations (IRD) are the major cause of incurable blindness and, diseases like Leber congenital amaurosis (LCA), Retinitis pigmentosa (RP) and Cone Rod dystrophy (CRD) are among this group of retinal dystrophies affecting the photoreceptors, the rods and cones. LCA is mostly inherited in autosomal recessive form contributing to 5% of all retinal dystrophies and 20% of childhood blindness, whereas RP and CRD is inherited in all patterns of Mendelian inheritance like autosomal dominant, autosomal recessive and X-linked recessive and both are the leading causes of visual impairment in children and young adults. There is also a clinical overlap between the juvenile RP which is diagnosed later to one year of age and LCA, both categorized as Early Onset Retinal Dystrophy (EORD) and there also exists a genotype overlap which involves *CRB1* and *RDH12*. Other retinal disease genes such as *TULP1, SPATA7, KCNJ13,* and *IQCB1* are known to cause LCA and autosomal recessive RP (arRP) and *ABCA4* is known to cause Stargardts, arRP and CRD. Due to this remarkable genetic and phenotypic heterogeneity, accurate molecular diagnosis would aid in the clinical diagnosis, predict the prognosis of the disease, and in genetic counseling. Various technologies have been widely used to identify the causative gene/loci. Homozygosity mapping with SNP or microsatellite markers is one such tool that exploits the fact that stretches of markers would be homozygous and identical by descent in cases of autosomal recessive diseases both in consanguineous and non-consanguineous families. This technology had been widely used in cases of autosomal recessively inherited disease and there are reports from India as well. The current study was done on consanguineous recessive LCA, arRP and arCRD south Indian families to know the prevalence of mutations in known genes and also to know the involvement of novel loci, if any and to correlate the observed phenotype with the genotype determined in the study.

Aim:

To perform homozygosity mapping in inherited retinal degenerative cases like LCA, arRP and arCRD inorder to identify the causative mutations in known gene or identify novel locus.

Objectives:

- To perform homozygosity mapping on consanguineous recessive families with inherited retinal degenerative disease using Affymetrix Gene chip to identify the disease loci involved.
- Screening the shortlisted candidate gene(s) by Sanger sequencing, identifying the causative gene(s) and/or mutations, performing the segregation analysis in the families, control screening and *in silico* analyses to confirm the pathogencity of the identified mutations.
- To correlate the observed phenotype with the genotype determined in the study.

Methodology:

Twelve LCA families, two arRP families and one arCRD family were included in the study. Complete ophthalmic examination was done for all the affected individuals including electroretinogram, fundus photograph, fundus autofluorescence, and optical coherence tomography where possible. Heparinised blood sample (10ml) was collected from all the affected individuals, unaffected siblings and parents after obtaining informed consent. Homozygosity mapping using Affymetrix 250K HMA Genechip was done for eleven LCA families and with 10K Genechip on one arRP family.

Following genotyping using 250K NspI GeneChip, the homozygous regions were analysed using Genotyping Console v4.0. Homozygous stretches between the affected and unaffected were compared by loss of heterozygosity (LOH) status. The homozygous blocks in the known LCA candidate genes region and all other homozygous blocks were noted. The known LCA candidate genes present in the largest homozygous blocks were screened by Sanger sequencing. For the arRP family genotyped by 10K HMA GeneChip, .CEL files generated for each sample was analyzed using GTYPE software. Homozygous stretches between the affected individuals were compared with the unaffected and known candidate gene was screened. If the causative mutation was identified on screening the candidate gene(s) within the homozygous block, segregation analysis, control screening and bioinformatics analyses were performed to confirm its pathogenecity.

A LCA, arCRD and arRP family each were taken for homozygosity mapping with 250K NspI GeneChip and analysis revealed 1-8 known candidate genes within homozygous blocks in each family. Since more than one candidate genes were to be screened, the proband from each family was subjected to targeted re-sequencing on Illumina MiSeq Next Generation sequencing (NGS) platform for IRD gene panel at Strand centre for genomics and personalized medicine, Bangalore, India. Library preparation was done according to the "Nexetra" protocol where DNA is tagmented and subjected to enrichment using target specific probes. The reads were aligned against the whole genome build hg19 using STRAND® NGS v1.6. (http://www.avadis-ngs.com). Reads which failed the QC, reads with average quality less than 20, were filtered out. Variations were then imported into Strandomics, annotation and prioritization of variants was done by automated pipelines using STRAND® NGS variant caller. These likely pathogenic variations were validated by Sanger sequencing and segregation analysis, control screening and bioinformatics analyses were also performed to confirm the pathogenecity of the identified mutations.

Results:

For the eleven LCA families and one arRP family homozygosity mapping followed by Sanger sequencing of the candidate gene was done. We identified the causative mutation in ten LCA families (90%); *AIPL1* mutation in three, *RPE65* mutation in two, and one each of *CRB1*, *GUCY2D, IQCB1, RDH12, SPATA7* and *MERTK* in the arRP family. In one LCA family we were unable to identify the causative mutation in known LCA candidate gene(s) screened. The causative mutation can either be in any one of the retinal disease genes or it could also involve a novel locus.

In the another set of families; LCA, arCRD and arRP each homozygosity mapping was followed by NGS analysis and three novel mutations, one each in *RDH12, ABCA4, CDHR1*, respectively were identified.

Segregation analysis was performed in all the families and the identified mutation segregated with the disease in the families, with all the affected being homozygous for mutation, parent(s) being heterozygous carriers and the unaffected being either heterozygous for mutation or wild type. One hundred normal controls (200 chromosomes) were screened for all the identified mutations and were wild type.

The phenotype documented were correlated with the genotype determined from the study, certain classical phenotype correlation such as para-arteriolar preservation of the retinal pigment epithelium (PPRPE) in *CRB1*, macular atrophy with bony spicules in *AIPL1*, bony spicules with salt and pepper fundus for *RPE65,* prononounced maculopathy and bony spicules for *RDH12,* macular atrophy with bony spicule pigmentation in *ABCA4,* were observed.

Conclusion:

In the study we had taken fifteen retinal disease families; twelve LCA, two arRP and one arCRD. We were able to identify the mutation in fourteen out of fifteen (93%) families. We had also identified mutations in seven different genes contributing to LCA, *AIPL1* in three families, *RPE65* in two families, *RDH12* in two families, *CRB1, GUCY2D*, *IQCB1*, *SPATA7* in one family each. In two arRP families, causative mutations were identified in *MERTK* and *CDHR1*. For arCRD family the causative mutation was identified in *ABCA4*. Of the fourteen pathogenic or likely pathogenic mutations, ten were novel (10/14) (71%). The molecular diagnosis in these families helps in predicting the disease prognosis and also in appropriate counseling like carrier testing, risk of other systemic diseases if any, recommendation for appropriate management of the systemic condition if possible and prenatal testing. Absence of mutation in the known LCA candidate gene in one family, indicate the involvement of novel locus, further analyses like whole exome or whole genome sequencing and overlapping with homozygosity mapping data would help identify the same. Studying genotype-phenotype correlation in larger cohort would aid in specific gene screening. Homozygosity mapping followed by candidate genes screening either by direct sequencing or by high through put NGS is a very efficient strategy for mutation identification in autosomal recessive diseases and the current study adds further strength to it.

TABLE OF CONTENTS

LIST OF TABLES

LIST OF FIGURES

LIST OF ABBREVIATIONS/SYMBOLS

WHO	World Health Organization
IRD	Inherited Retinal Degeneration
RDD	Retinal Degenerative Diseases
LCA	Leber Congenital Amaurosis
arRP	Autosomal recessive Retinitis pigmentosa
arCRD	Autosomal recessive Cone-Rod Dystrophy
NGS	Next Generation Sequencing
ERG	Electroretinogram
FAF	Fundus Autofluorescence
OCT	Ocular Coherence Tomography
HMA	Human Mapping Array
SNP	Single Nucleotide Polymorphism
STR	Short tandem repeat
IBD	Identity by Descent
HM	Homozygosity mapping
XbaI	Restriction enzyme
NspI	Restriction enzyme
.CEL	.Cel Intensity File
bp	base pair
Mb	Megabyte
µl	microlitre
TdT	Terminal deoxy nucelotidyl transferase
OCR	Oligo Control Reagent
TMACL	Tetramethyl Ammonium Chloride
QC	Quality Control
GUCY2D	Retinal guanylyl cyclase 1
RPE65	Retinoid isomerohydrolase
SPATA7	Spermatogenesis-associated protein 7
AIPL1	Aryl-hydrocarbon-interacting protein-like 1

CRB1	Crumbs homolog 1
RDH12	Retinol dehydrogenase 12
IQCB1	IQ calmodulin-binding motif containing protein 1
MERTK	Mer Tyrosine kinase proto-oncogene
ABCA4	ATP-Binding Cassette, Subfamily A Member 4
CDHR1	Cadherin-related family member 1
RPGRIP1	X-linked retinitis pigmentosa GTPase regulator-interacting protein 1
IMPDH1	Inosine 5' monophosphate dehydrogenase
RD3	Protein RD3
TE	Tris EDTA buffer
BSA	Bovine Serum Albumin
EB	Elution Buffer
TBE	Tris Boricacid EDTA buffer
SAPE	Streptavidin Phycoerythrin
GTYPE	Genotyping Analysis Software
GCOS	GeneChip Operating Software
HSF	Human Splice Finder
Polyphen 2	Polymorphism Phenotyping
SIFT	Sorting Intolerant from Tolerant
PMut	Pathogenic mutation prediction
RetNet	Retinal Information Network
UCSC	University of California, Santa Cruz
UTR	Untranslated region
VUS	Variation of Unknown Significance

CHAPTER 1

Introduction

The global data on visual impairment 2010 by WHO reveals that including people of all ages, the number of visually impaired is estimated to be 285 million, of whom 39 million are blind and 246 million have low vision and about 90% live in low income settings [1] where India ranks the second highest contributing to about 62.6 million people (21.9%) [2].

Globally the commonest cause of blindness as estimated by the WHO is cataract, accounting to about 51% and the other age related retinal dystrophies such as age related macular degeneration (AMD) and diabetic retinopathy (DR) contributing to about 5 and 1%, respectively [1] .

1.1 Human eye system

The eye is an optical system that works like a camera. The light rays enter the eye through the cornea, passes through the aqueous humor and enters the pupil to reach the lens. Then lens adjusts the thickness of the light to focus it on the retina, the light sensitive layer that lines inside the eye which then sends visual messages through the optic nerve to the brain. (Fig1.1)

Fig:1.1 Cross section of the human eye [3]

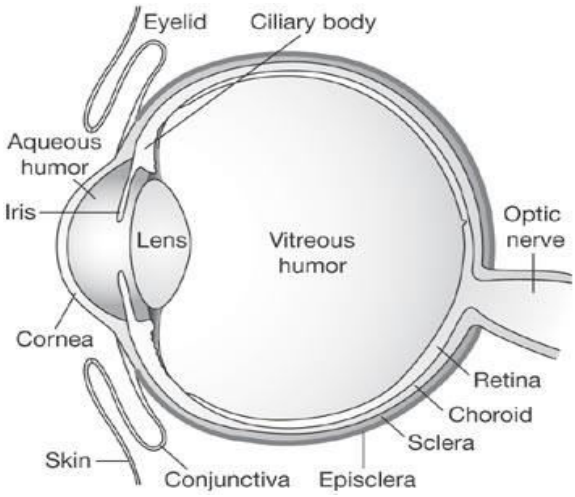

Retina: The retina is of about 0.5mm thickness and lines the back of the eye. The radial section of retina reveals ganglion cells that lie innermost and the photoreceptor cells on the outer most. When light strikes, it passes through all the layers of the retina to the photoreceptors where the photons are absorbed by the visual pigments of the photoreceptors, and then the biochemical message is converted into an electrical signal stimulating the succeeding neurons of the retina. Thus the retinal messages from the photoreceptors and preliminary organization of the visual image are transmitted to the brain through the optic nerve [4]. The structures of human retinal layers are shown in Fig 1.2.

Fig: 1.2 Structure of human retinal layers, the different types of cell; retinal pigment epithelium, photoreceptors (rods and cones), bipolar cells, ganglion cells, amacrine cells, horizontal cell and Muller glia [4].

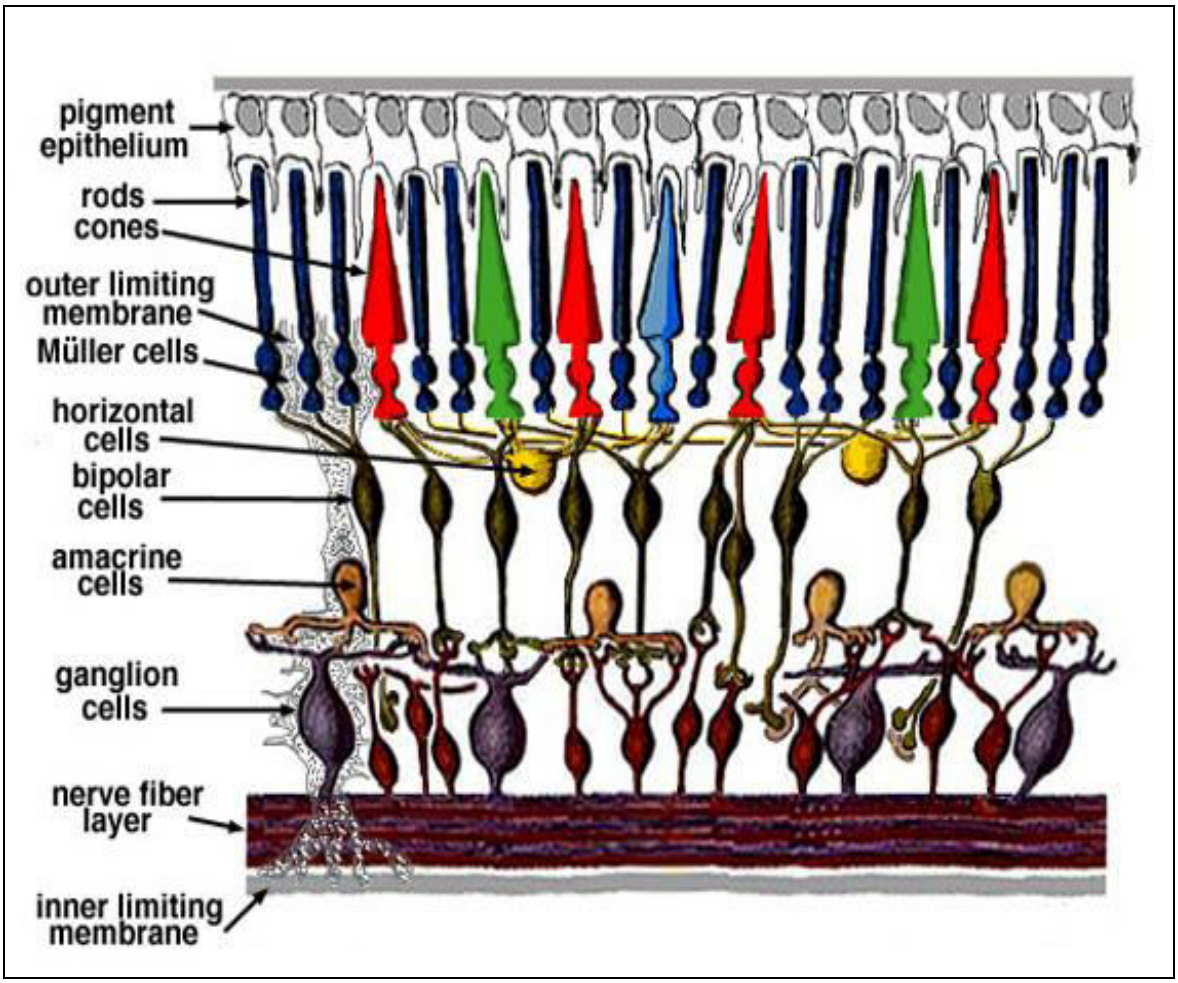

Photoreceptors: Rods and cones are the photoreceptor cells. They are specialized neurons which are primary cells for the vision. Rods contribute to scotopic vision i.e vision under dim and dark condition whereas cones contribute to photopic (bright light) and colour vision. The number of rods in the human retina is about 91 million far exceeding the cones which are about 4-5 million and due to this reason the density of the rods is much greater throughout than the cones. However, in the foveal region the cone density increases to about 200 fold and this helps the region to mediate high visual acuity. The rods are present at a high density away from the fovea; hence a faint object can be viewed at a distance with the help of rods by peripheral vision [5].
Both rods and cones (Fig:1.3) have an outer segment and an inner segment connected by a connecting cilium [5]. The inner segment contains the cell organelles such as the mitochondria and the nucleus. The outer segment contains stack of membranous disc which contains the light absorbing photo pigment. The rods contain a visual pigment, rhodopsin which is sensitive to blue-green light with peak sensitivity of around 500nm. There are three types of cone pigments, each corresponding to absorption of a different wavelengths of light, short (blue), medium (green), long (red), their wavelengths; 419, 531, 559 nm, respectively and their combined response helps in the color vision. Both the rods and cones have synaptic terminal which synapses with another neuron such as a bipolar cell to transmit the signal from the visual cycle [6].

Fig: 1.3 Diagrammatic representation of detailed structure of photoreceptors (rods and cones) [7]

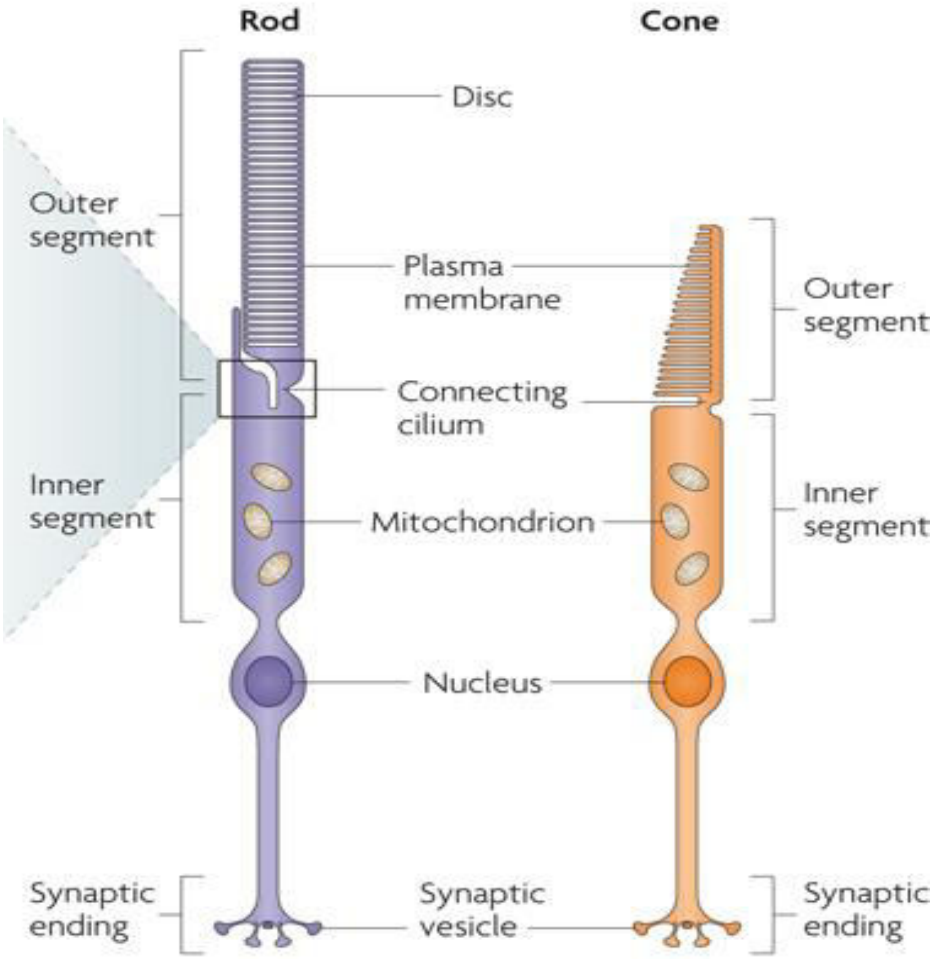

1.2 Visual Cycle

The rod visual pigment rhodopsin is made of chromophore 11-cis-retinal and protein opsin. Absorption of light by rhodopsin causes isomerisation of 11-cis-retinal to all-trans-retinal triggering the visual cycle. The activated rhodopsin yields opsin and all-trans-retinal, all-trans-retinal is released into the cytosol of the disc membrane by photoreceptor specific ATP-binding transporter (ABCA4). The all-trans-retinal gets reduced to all-trans-retinol by all-trans-retinal dehydrogenases (RDH8 and RDH12). Interphotoreceptor retinoid binding protein (IRBP), a soluble protein, present in the interphotoreceptor matrix (IPM) functions as the two way carrier of the retinoids from photoreceptors to RPE and from the RPE to photoreceptors.

The all-trans-retinol that is transported into the RPE by IRBP is esterified by lecithin retinol acyltransferase (LRAT) to all-trans-retinyl esters. The esters are then isomerized to 11-cis-retinol by RPE-specific protein, RPE65. The visual cycle is completed when 11-cis-retinol is oxidized by 11-cis-retinal specific dehydrogenase (RDH5) to 11-cis-retinal, which is transported back to photoreceptor by IRBP where it combines with opsin to regenerate visual pigments [8]. The representation of visual cycle is shown in Fig 1.4.

Fig: 1.4 Representation of visual cycle

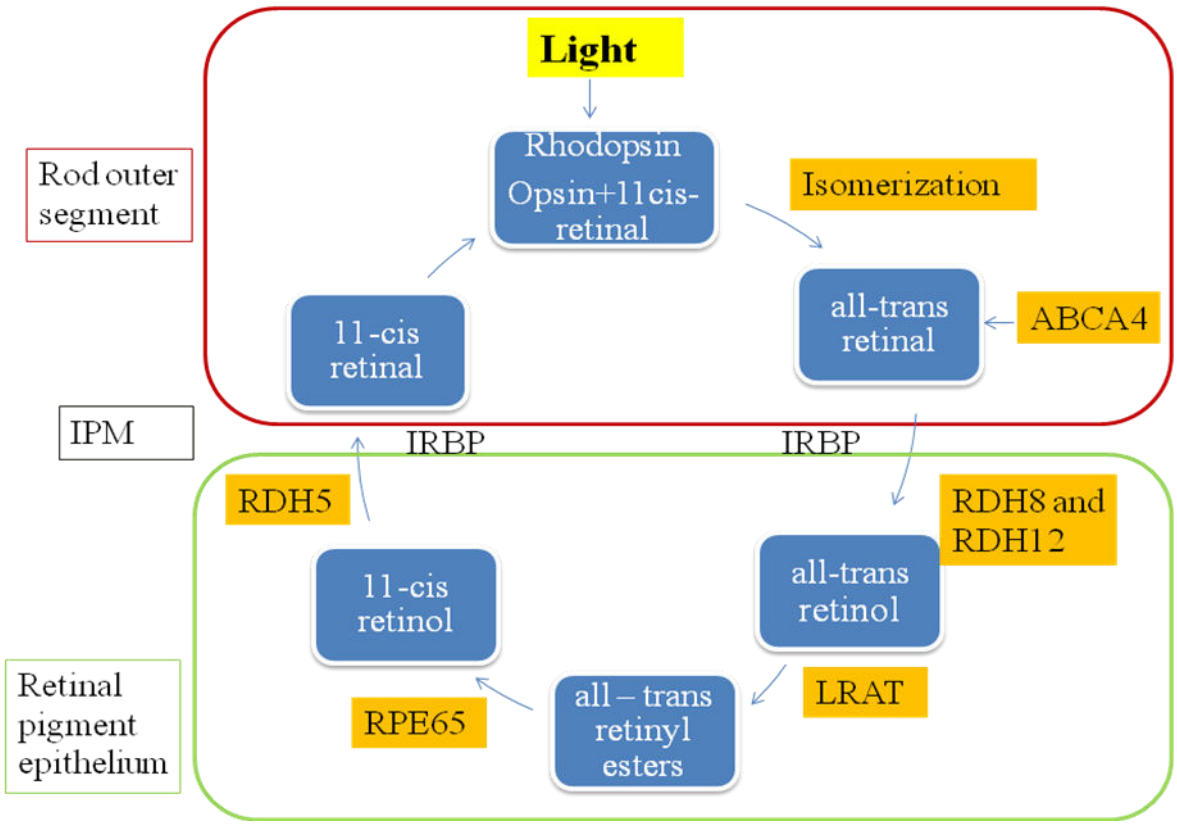

1.2.1 Phototransduction

It is a process, by which the photons in the light are converted into electrical signals. This occurs in the retina through the photoreceptors (Fig.1.5). According to light and dark adaptation the photoreceptors either hyperpolarizes or depolarizes. Rhodopsin is a G-protein coupled receptor consisting of opsin, a seven transmembrane domain protein and a chromophore 11-cis retinal.

A cascade of events takes place in the photoreceptor outer segment membrane when light activates rhodopsin, activating G-protein, transducin. The GTP bound alpha subunit of transducin further activates the cGMP phosphodiesterase (PDE) that hydrolyzes cGMP reducing its concentration and leading to the closure of Na^+ channels in the hyperpolarized state [9].

Three main biochemical events that takes place during the phototransduction:

a) When light enters the eye it causes the activation of rhodopsin molecules in the photoreceptors
b) Activated rhodopsin through a series of steps in turn results in a reduction of the cGMP intracellular concentration.
c) Decrease in the levels of cGMP causes the closure of the cGMP gated channels leading to the hyperpolarisation [9].

1.2.2 Termination of Phototransduction Pathway

The response to the light can be terminated through several mechanisms

i. Inactivation of rhodopsion occurs through phosophorylation by the rhodopsin kinase followed by binding of arrestin to phosphorylated rhodopsin leading to its inactivation.
ii. Inactivation of transducin occurs by the hydrolysis of GTP to GDP through GTPase activity.
iii. Inactivation of phosphodiesterase is also related with inactivation of transducin, where inactivated transducin disassociates from phosphodiesterase resulting in termination of PDE mediated cGMP hydrolysis.
iv. Activation of guanylate cyclase by guanylate cyclase activated protein (GCAP) will restore the cGMP level promoting the re-opening of the cGMP gated channels.

Fig: 1.5 Phototransduction cascade [10]

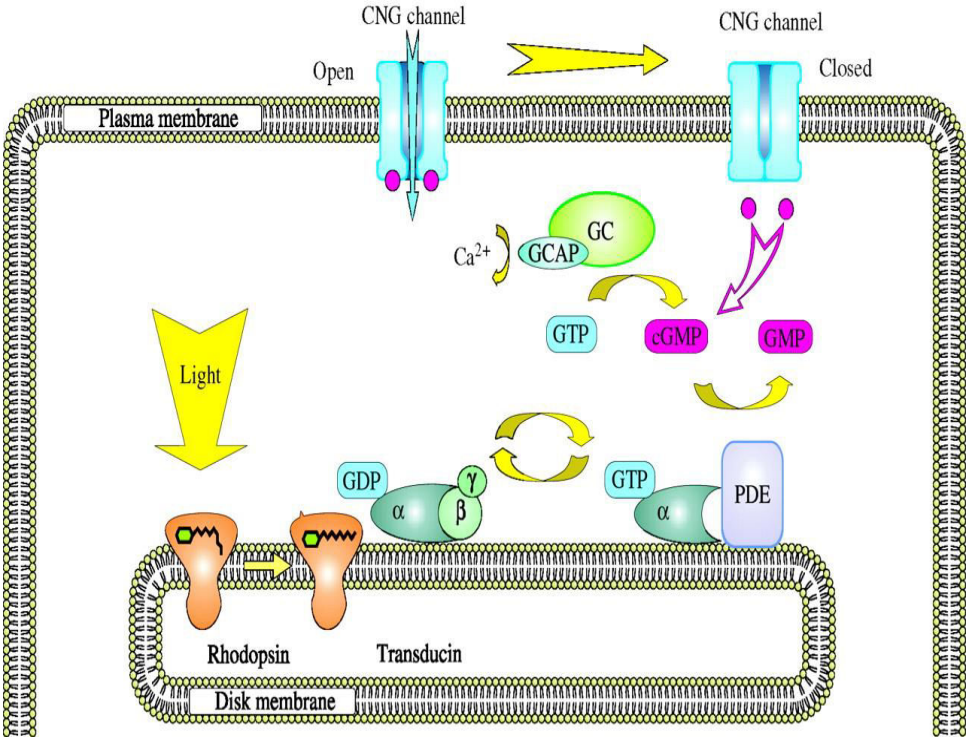

1.3 Inherited Retinal Degeneration (IRD)

IRD or retinal degenerative diseases (RDD) are the major group of incurable blindness characterized by loss of retinal photoreceptor cells or the adjacent retinal pigment epithelium, affecting millions of people worldwide [11]. It affects approximately 1 in 3000 people worldwide leading to either partial or total blindness [12]. The IRD include many retinal diseases such as retinitis pigmentosa (RP), Leber congenital amaurosis (LCA), Stargardt disease, Cone-rod dystrophy (CRD), Rod-cone dystrophy (RCD) and also some syndromic forms that have other systemic features [13]. Retinal degeneration is also seen in the more common complex diseases like age related macular degeneration (AMD) and diabetic retinopathy (DR) [14].

1.3.1 Genetics of Inherited Retinal Degeneration

The tremendous genetic heterogeneity in inherited retinal diseases makes the molecular diagnosis of the disease too complex thereby impeding genetic counseling and research on gene specific treatment strategies. There are about twelve different types of inherited retinal diseases (single gene disorders) with various modes of inheritance; either autosomal dominant, autosomal recessive or X-linked recessive and very rarely mitochondrial. Two- hundred and sixty loci and 220 different genes contribute to these diseases [RetNet, the Retinal Information Network] involving various functions such as phototransduction pathway, the visual cycle, photoreceptor structure or development, photoreceptor gene transcription, cell adhesion, cellular metabolism, protein folding and subunit assembly. In spite of the enormous amount of genes and variants having diversified disease mechanisms, all converge ultimately to photoreceptor or RPE cell death as a common pathway [7].

1.3.2 Genetic and Phenotypic Heterogeneity of IRD

The phenotype and genetic heterogeneity of IRD or RDD are immense and these contribute to the complexity in the clinical diagnosis and makes molecular testing technically challenging. There is also a considerable overlap between the phenotype and genotype; the same gene may show different phenotypes as in the case of *CRX* which can cause autosomal dominant LCA, autosomal dominant RP and autosomal dominant cone-rod dystrophy, this is defined as allelic heterogeneity. Locus heterogeneity, where mutations in many different genes cause the same phenotype is again a very common aspect of all RDD. Twenty-seven genes for LCA, sixty-nine genes for RP have been identified and the list continuous to grow with better and rapid genotyping methodologies. Also there are reports where a single gene can show a particular phenotype with different inheritance pattern e.g *RPE65* which is one of the candidate gene for autosomal recessive RP (arRP) was also identified as causative in an autosomal dominant RP family [15]. In some cases the same gene can cause an isolated RDD or systemic disease along with RDD as in the case of *AHI1* which was previously reported to be causative of Joubert syndrome and later also found to be

causing sporadic RP without any systemic manifestation [16]. In all forms of retinal degenerations, eventually apoptosis of the photoreceptor results [17], but the mechanism which leads to the death of the photoreceptors varies. The four major mechanisms are a) disruption of outer segment morphogenesis b) metabolic overload c) dysfunction of retinal pigment epithelial cells d) chronic activation of phototransduction [18].

1.4 Lebers Congenital Amaurosis

The form of congenital or early-infantile blindness known as Leber congenital amaurosis (LCA) was first defined by Theodor Leber in 1869 on the basis of typical clinical findings such as severe visual loss at birth, nystagmus, a variety of fundus changes, and minimal or absent recordable responses on the electroretinogram (ERG) before or by one year of age, accounting for 5% of all retinal dystrophies. LCA is usually inherited as an autosomal recessive disease but few cases of autosomal dominant inheritance is also reported [19, 20]. The disease affects about 1:30000 [21] to 1:81000 subjects [22] across various populations. The Table 1.1 shows the genes contributing to LCA and their protein function.

Table 1.1 Genes contributing to LCA and their Protein Function

S.NO	Gene	Protein	Protein Function	Gene/Locus OMIM/ Phenotype OMIM
1.	*GUCY2D*	Retinal guanylyl cyclase 1	Hydrolysis cGMP	600179,204000
2.	*RPE65*	Retinoid isomerohydrolase	Isomerohydrolase in Vitamin A visual cycle	180069,204100
3.	*SPATA7*	Spermatogenesis-associated protein 7	Possible vesicular transport	604232,609868
4.	*AIPL1*	Aryl-hydrocarbon-interacting protein-like 1	Rod PDE chaperone	604392,604393
5.	*LCA5*	Lebercilin	Ciliary Function	611408,604537
6.	*RPGRIP1*	X-linked retinitis pigmentosa GTPase regulator-interacting protein 1	Connecting cilium disc morphogenesis	605446,613826
7.	*CRX*	Cone-rod homeobox protein	Elongation of photoreceptor	602225,613829

			outer segment, photoreceptor development	
8.	*CRB1*	Crumbs homolog 1	Determining and maintaining photoreceptor architecture.	604210,613835
9.	*NMNAT1*	Nicotinamide mononucleotide adenylyltransferase 1	Rate - limiting enzyme NAD (+) biosynthesis	608700,608553
10.	*CEP290*	Centrosomal protein of 290 kDa	Ciliary function	610142,611755
11.	*IMPDH1*	Inosine 5' monophosphate dehydrogenase	De novo synthesis of gauanine nucleotide	613937.146690
12.	*RD3*	Protein RD3	Transcription and splicing. Suppress membrane guanylate cylcase activity	610612,180040
13.	*RDH12*	Retinol dehydrogenase 12	Unusual dual specificity for all-trans retinol and 11-cis retinol	608830,612712
14.	*LRAT*	Lecithin retinol acyltransferase	Esterification essential for Vitamin A visual cycle	604863,613341
15.	*TULP1*	Tubby-related protein 1	Protein transport from the photoreceptor inner segment to outer segment	602280,613843
16.	*KCNJ13*	Inward rectifier potassium channel 13	Maintaining resting membrane potential	603208, 614186
17.	*GDF6*	Growth Differentiation factor 6	Codes for widely expressed growth factor in the TGF-β pathway specifying the dorso-ventral retinal axis	601147,615360
18.	*IQCB1*	IQ calmodulin-binding motif containing protein 1	Ciliary function	609237, 609254
19.	*CABP4*	Calcium - Binding protein 4	Modulate voltage	610427,608965

			dependent calcium channel	
20.	*CNGA3*	Cyclic nucleotide-gated channel,alpha-3	Important for normal vision and olphatory signaling transduction.	600053, 216900
21.	*ALMS1*	Almstrom syndrome 1	Defective ciliogenesis	606844, 203800
22.	*MYO7A*	Myosin V11A	Distriution and mignration of retinal pigment epithelial melanosomes and phagosomes & required for normal hearing	600060, 276903
23.	*DTHD1*	Death domain containing protein 1	Functions in signaling pathway and apoptosis pathway	-
24.	*PRPH2*	Peripherin 2	Essential for disc morphogenesis	608133,179605
25.	*OTX2*	Orthodenticle, drosophila, homolog of 2	Plays a role in the development of brain and sense organs	610125, 600037
26.	*MERTK*	Mer Tyrosine kinase proto-oncogene	Essential for retinal pigment epithelium phagocytosis pathway	604705, 613862
27.	*IFT140*	Intraflagellar transport 140	Ciliary function	614620, 266920

1.4.1 Molecular Genetics of LCA

So far twenty-seven genes are implicated in LCA. These candidate genes have been identified by using various methodoliges like, either by candidate gene screening, or linkage studies on large families or homozygosity mapping on nuclear families using either microsatellite markers or SNP microarrays, or screening genes which are involved in retinal function/tissue specific expression, or recently by whole exome seqeuncing [23-26].

Combination approaches such as homozygosity mapping and exome sequencing have also helped in successfully identifying novel LCA genes such as *ALMS, CNGA3, MYO7A* [27]. These genes contribute to about 50-70% of LCA, but the mutation frequency varies among different ethnic populations [28].

1.5 Retinitis Pigmentosa

Retinitis pigmentosa is the most common of all the IRD [29]. RP starts with symptoms of night blindness, difficulty in the mid-periphery vision and advances towards the fovea and macula, primarily due to degeneration of the rods and in later stages affecting the cone photoreceptors as well and leading to complete blindness in some [30]. The estimated worldwide prevalence of the disease is 1:3000 to 1:7000. The prevalence also differs among different ethnic populations [31]. RP is broadly classified as non-syndromic or simple (not affecting any other organ other than eye) and systemic (other multiple tissues) or syndromic (affecting other organs systems) [29]. Non- syndromic RP may be inherited as autosomal dominant (adRP) contributing to about 15-25%, autosomal recessive (arRP) - 5-20%, or X-linked recessive forms (xlRP) - 5-15%, and rare digenic forms are also reported [32]. The other unknown or simplex forms comprise the major and contribute to about 40-50% of the RP [33].

1.5.1 Syndromic RP

The most frequent reported syndromic forms of RP include Ushers syndrome (USH) and Bardet Biedel syndrome (BBS). Ushers syndrome is an autosomal recessive disease characterized by hearing loss, RP and in some cases vestibular dysfunction. This syndrome accounts for more than 50% of the individual who are both deaf and blind, and affects between 1 in 12,000 - 1 in 13,000 people in different populations. The USH represent between 10-13% of all RP cases [34, 35]. BBS is also an autosomal recessive disease characterized by rod-cone dystrophy (>90%), truncal obesity (72%), postaxial polydactyl, cognitive impairment, male hypogonadotrophic hypogonadism, complex female genitourinary malformations and renal abnormalities.

It affects about 1 in 120,000 in Caucasian population and a higher incidence is reported in Newfoundland population with a reported prevalence of 1 in 13000 [36].
The other less frequent syndromes include Senior-Loken syndrome; an oculo-renal disease characterized by severe RP and nephronophthisis [37], rare dysmorphic syndrome include Cohen syndrome with facial dysmorphism, short stature, mental retardation, long and narrow hands and neutropenia and RP [38]. Jeune Syndrome with RP, thoracic hypoplasia, brachydactyl and chronic nephritis [39] and Cockayne Syndrome defined by hearing loss, eye abnormalities (retinopathy with fine granular spots), severe tooth decay, bone abnormalities, and changes in the brain [40], thiamine responsive megaloblastic anemia (TRMA), an autosomal recessive disorder characterized by hearing loss, diabetes, megaloblastic anemia, rarely RP with nystagmus and developmental delay [41].

1.6 Cone Rod dystrophy

In an IRD belonging to the group of pigmentary retinopathies, Cone-Rod dystrophies are characterized with pigmentary deposits predominantly in the macular region [42]. In contrast to RP (also called as the Rod Cone dystrophies (RCD)) which primarily results in the loss of rod then followed by cones, in Cone Rod dystrophy (CRD) primarily cones are affected followed by rods [42]. The major symptoms include photoaversion, decrease in visual acuity, with or without nystagmus, colour vision defects and decreased sensitivity to central visual fields, lately night blindness and peripheral visual loss also occur because of the involvement of rods [43]. However, in advanced RP (RCD) or CRD when the degeneration is widespread it is difficult to distinguish between the two forms [13].
The diagnosis of CRD is mainly based on the ERG response where mainly cones (photopic) response is severely reduced or equally as reduced as rods (scotopic) response [42, 44]. CRD occurs in 1:40,000 individuals [42, 43]. CRD too is inherited in all Mendelian patterns of inheritance, like autosomal dominant, autosomal recessive and X-linked recessive. Mutations in five genes have been implicated in about 50% of the non-syndromic autosomal recessive CRD (arCRD) i.e *ABCA4* [45], *ADAM9* [46], *CDHR1* [47], *CERKL* [48] and *RPGRIP1* [49].

1.7 Genotype-Phenotype correlation

LCA, RP and CRD presents a wide variety of clinical features, phenotype-genotype correlations have indicated that some fundus features like macular atrophy, nummular pigments may be specific to individual genetic abnormalities, providing a quick means of determining which gene may be causative. Some of the other clinical features include nyctalopia, photoaversion, keratoconus, cataract, etc. and these are also correlated with particular genotype. For e.g. nyctalopia and photaversion are common in *LCA5* patients whereas these symptoms are rare in *AIPL1* and *RPGRIP1* positive patients. Severe keratoconus are common in cases of *CRB1* and *AIPL1*. Similarly cataracts are more prevalent with increasing age in cases of *RPGRIP1*, *AIPL1*, and *TULP1* [50]. Macular atrophy is common in *AIPL1*, *TULP1*, *CRB1, ABCA4*, *CDHR1* and *LCA5* positive cases whereas nummular pigmentation is common finding of *RPE65*, *LCA5* and *CRB1* [42, 47, 50]. Pigmentary retinopathy is more prevalent in cases of *RPE65* and *LCA9* [50].

1.8 Genetic Mapping

It is also known as 'Linkage Mapping or meiotic mapping' and refers to determining the relative position and distance between the markers along the chromosomes based on the principle that genes (marker/loci) segregate by chromosomal recombination during meiosis thus allowing the analysis of the progeny [51]. There are two kinds of genome map; genetic linkage map and physical linkage map.

1.8.1 Genetic Linkage Mapping

Genetic linkage maps represent the crossing over which happens during meiosis resulting in recombinants that expresses new or modified trait in the offspring. This linkage maps also reveals that the traits/loci that are inherited together, are most often by genes that are close to each other, and genes which are far apart are more likely to undergo recombination [51].

The genetic linkage mapping is possible by genotyping using restriction fragment length polymorphisms (RFLPs), simple sequence length polymorphisms (SSLPs) and single nucleotide polymorphisms (SNPs).

Restriction length polymorphism: RFLPS were the first DNA markers to be studied. The restriction enzymes (RE) cut the genomic DNA based on specific sequence. A wild type allele may be recognized by the RE and the alternate allele may not, resulting in length polymorphism post RE treatment. This pattern of length polymorphism is used to define the position of any marker on the genome map [52].

Simple sequence length polymorphism: SSLPs are arrays that display length variations, different alleles containing different number of repeat units. The minisatellites are variable number tandem repeats of about 25 bp long. The microsatellites or simple tandem repeats are shorter, mostly dinucleotide or trinucleotide repeats, and are more advantageous than minisatellites because they are evenly spread across the genome and can be easily typed with the help of PCR [52] . The haplotype or the order of these SSLP markers is used to map the gene/marker.

Single Nucleotide Polymorphisms: There are vast numbers of SNPs in the human genome, some of them are recognized by restriction enzyme and many of them are not [52]. A high throughput oligonucleotide based hybridization; the microarray has evolved utilizing these SNPs for gene mapping and linkage analysis.

1.8.2 Physical Linkage Mapping

The physical map gives the physical DNA base pair distances from one landmark to another or between two loci, these landmarks are expressed in terms of ‘sequence tagged sites’ (STS).

These STS are unique sequences which range hundred base pair long and are found only in one place of the genome. Hence if these STS are found in the DNA their site of origin can be identified. The STS are detected by means of polymerase chain reaction (PCR) using specific primers. Now more and more STS are being mapped inorder to create maps that are more closely, evenly and accurately spaced [53].

Restriction mapping and fluorescent in situ hybridization (FISH) are other techniques which are used to map the position on the DNA.

Restriction mapping: It is used to map the unknown segment of the DNA molecule by subjecting them to restriction endonucleases and then by identifying the location of the breakpoints. It is also helpful in locating the position of non-polymorphic restriction sites [52] .

Fluorescent insitu hybridization: The metaphase chromosomes are utilized for this technique, with the help of fluorescent signal obtained by FISH, mapping is done by measuring its position relative to the end of the short arm of chromosome [54].

The flowchart depicting the methods available for Gene Mapping is shown in Fig: 1.6.

Fig: 1.6 Flowchart depicting the methods available for Gene Mapping

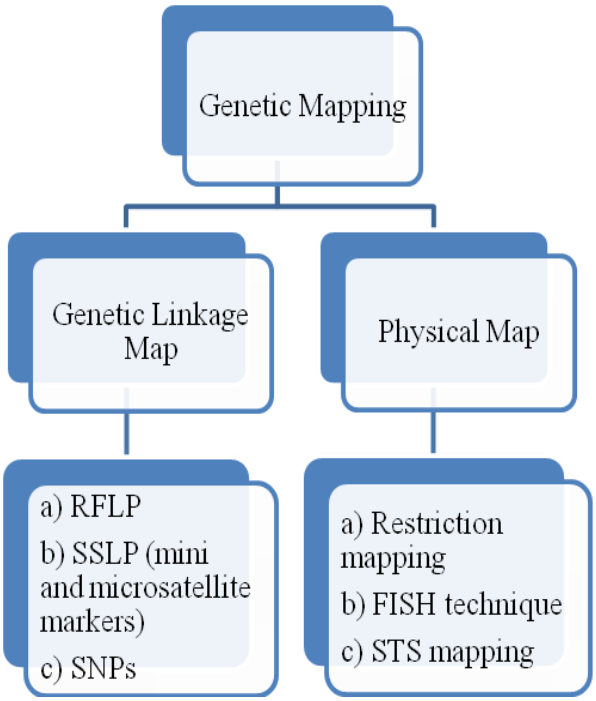

1.9 Linkage analysis

The term linkage analysis was conceived by Sturtevant in 1913 while working on fruit flies [55]. Linkage analysis involves the study of crosses between the parents with varying Mendelian traits and polymorphic variants (markers) and where because of the meiotic recombination, any marker showing co-segregation (linkage) with the trait indicate proximity between the two in the genome. Thus the presence of specific marker or set of markers occurring with a given trait or a disease indicate the possibility of disease gene in that given locus. In 1980 Botstein and colleagues proposed the use of naturally occurring DNA sequence polymorphism as a marker to create a human genetic map and also to trace the transmission of chromosomal region in families [56]. Then in 1990 through pilot studies thousands of single nucleotide polymorphisms (SNP) were identified and began to be used as markers to perform highly multiplexed genotyping through DNA microarrays [57].

1.9.1 LOD score

The (logarithm (base 10) of odds) is a statistical test developed by Newton E Morton for linkage analysis. The LOD score compares the likelihood of obtaining a test data whether the two loci are linked, and to know if the likelihood occurred by chance or not. By convention a positive LOD score of greater than 3.0 is considered evidence for linkage, as it indicates 1000 to 1 odds that the linkage being observed did not occur by chance and LOD score of >-2 is considered to exclude the linkage [58]. LOD score between -2 and 3 is suggestive of linkage.

1.10 Homozygosity mapping

Homozygosity or autozygosity mapping, is a powerful tool to identify recessively inherited disease gene locus because of high probability of stretches of homozygous regions inherited by descent more so in consanguineous or endogamous marriages [59, 60]. This utilizes the fact that adjacent regions surrounding the disease locus too will preferentially be homozygous by descent (HBD) [61].

Fig: 1.7 Homozygosity mapping of recessive disease genes [62]

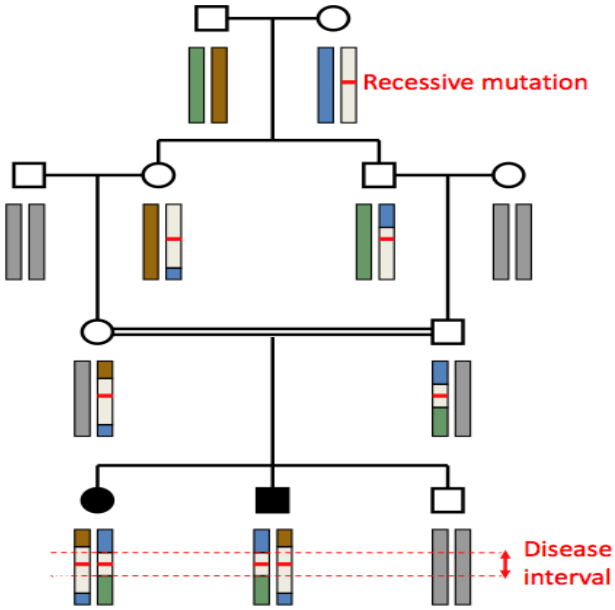

The affected individual for an autosomal recessive disease (Fig 1.7) is likely to be homozygous for the disease allele when the parents are married in consanguinity because they may inherit the disease allele from a common ancestor. Hence in homozygosity mapping the homozygous regions common between the affected individuals are analysed in order to map the causative disease gene. Homozygosity mapping which was previously performed with short tandem repeats (STR) markers is now achieved by using high throughput SNP based microarray [63].

1.10.1 Homozygosity mapping strategies also have the following advantages

- Large multi-generation families with many affected individuals are not required as in the case of conventional linkage studies. Genotyping one or two affected individuals along with an unaffected individual are sufficient to identify the disease locus.
- Homozygosity mapping is efficient in identifying the causative gene/mutation for a recessive disease in singleton case even in outbred population [64].

- When a known candidate gene is indicated by homozygosity mapping, screening the entire gene leads of identification of both novel and reported mutations. If the causative mutations are not identified in known candidate gene(s) the presence of various other homozygous regions gives a clue about the location of novel locus/gene [65]. Many novel loci/genes have been identified through homozygosity/autogyosity guided candidate gene screening or exome sequencing [25].

1.10.2 Consanguinity in Homozygosity mapping

Consanguineous marriages (union between related individuals) are a common practice among many populations; prevalence being highest in North Africa, the Middle East, South Asia and among migrant communities in North America, Europe and Australia [66]. Individuals who are born out of consanguineous marriages have an increased percentage of homozygous regions due to identity by descent [67] and hence also an increased prevalence of autosomal recessive diseases among consanguineous families. On an average in a first cousin marriage the homozygous segment would be 20cM and due to prolonged parental inbreeding the levels of homozygosity might be increased to 5% in consanguineous marriages [67]. Hence for an autosomal recessive disease in consanguineous families, homozygosity mapping is a very effective tool in identifying disease gene/loci [68, 69].

1.10.3 Pitfalls and limitations of Homozygosity mapping

- The main disadvantage of homozygosity mapping is, it will not detect compound heterozygous mutation i.e. allelic heterogeneity which can occur within the same family in which affected individuals can carry two different heterozygous mutations in the same gene [70].

- Loci heterogeneity which can occur within the same family where a part of the family are harboring homozygous mutation in one particular gene and others have the causative mutation in another gene. This is also difficult to identify using homozygosity mapping [70].

- Identifying digenic variations (two different genes carrying heterozygous variation and contributing to the disease) and Triallelism (three deleterious allele, i.e a homozygous mutation in a gene and a heterozygous variation in another gene) are challenging using homozygosity mapping and are pitfalls of homozygosity mapping [71].

1.11 Next Generation Sequencing (NGS)

NGS platforms perform massively parallel sequencing where millions of fragments of target regions of DNA are sequenced. It is a now the most widely used technology in genomics. The single bases that are incorporated into growing DNA strands are either detected by pH changes induced by the release of a hydrogen ion upon the incorporation of a nucleotide into a growing strand of DNA (Ion Torrent PGM) or the fluorescence is detected by the incorporation of fluorescently labeled nucleotides in the growing strand (Illumina NGS platforms) [72]. The ability to tag samples with sequence specific indices thus allowing multiplexing has revolutionized the genotyping technology in terms of speed, amount of data generated and the cost effectiveness. The applications of NGS cover a wide range [73].

- High throughput exome and whole genome sequencing facilitating the discovery of genes and regulatory elements associated with the disease.
- Targeted sequencing for the identification of disease causing mutations in molecular diagnosis of genetically heterogenous diseases.
- RNA-Seq which provides information on the entire transcriptome in a single analysis where novel transcripts too are identified.

  Also NGS is being widely used in the field of microbial, plant and animal genomics as well.

1.12 Clinical Diagnosis of LCA, RP and CRD

The diagnosis of LCA, RP and CRD is established by various clinical examinations.

Ophthalmoscopy: By means of indirect opthalmoscope the viewer can examine the retina, retinal blood vessels, optic nerve head and to less extent the choroid. Here the pupil is dilated to get a easier view of the retinal changes and for the macular examination [74].

Electroretinogram (ERG): It measures the electrical response of the retina to a light stimulus. The different cell types of the retina, the photoreceptors, and second order neurons like the bipolar, amacrine and the ganglion cells respond to the light stimulus which is recorded as a waveform with the help of electrodes [75].

Visual Field Testing: It is done to detect the defects in the central and peripheral vision. In RP, initially a ring scotoma is usually present at the mid periphery of the visual field, while as the disease progresses the outer edge from the periphery expands and moves towards the centre contracting the inner margin and producing a "tunnel vision". Thus this test is useful not only for the diagnosis of the diseases but also to know the stage of the disease [76]. This test will not be useful in cases of LCA where the vision loss is very severe from the birth.

Fundus Appearance: The fundus examination of the eye includes examining the appearance of retina, optic disc, macula, fovea and posterior pole. This procedure is done either by opthalmoscopy or fundus photography in which the details are documented as a photograph [77].

Fundus Autofluorescence (FAF): It is retinal imaging, the images encompassing the entire macular area with at least a portion of the optic disc. It is mainly done for mapping lipofuscin changes in the RPE and monitoring the retinal degeneration [78].

Optical Coherence Tomography (OCT): The cross section of the different retinal layers in micrometer resolution and in three-dimension is imaged non-invasively using low coherence interferometry [79].

1.13 Various Therapies under Investigation

Research on various therapeutic modalities like gene therapy, pharmacologic treatment, cell transplantation, and neuro-prosthetic devices are being done [80].

1.13.1 Gene Replacement Therapy

Gene therapy works best by replacing the abnormal gene with the therapeutic gene by the use of viral or non-viral vectors to produce the therapeutic effect. Gene therapy strategies differ depending on the type of the mutation present. The gene replacement therapies are classified into two groups 1) gene augmentation therapy 2) gene silencing therapy [81].

Gene Augmentation Therapy: In autosomal recessive and X-linked recessive diseases, the mutation in the gene usually leads to a loss of function and absence of normal protein product. Successful introduction of the wild type gene with the help of vectors in these cases would result in the production of normal functional protein compensating for the lost function [82]. Human gene therapy trials began for LCA with *RPE65* mutation following the success of preliminarily trails done in Briard dogs [83]. In 2007 the first human clinical phase I trial of AAV-mediated *RPE65* gene therapy treatment in humans was started at three places simultaneously; Moorefields Eye Hospital, London [84], Children's Hospital of Philadelphia, Pennsylvania [85] and University of Florida [86], to assess the effect and safety of gene transfer in humans. Results from these studies elucidated that the therapy demonstrated safety and showed slight improvements in vision. In 2009, investigators published one year follow-up results of the three patients who received the therapy and statistically significant increases in light sensitivity were found in the first three months of the trial in all patients and remained unchanged at one year [87, 88]. In 2013 results have been published by the scientists that there is substantial visual improvement in short term and there is no detectable decline in spite of continued retinal degeneration at retinal sites where the therapy was not administered [89].

However, recent report reveal that, gene therapy vector improves retinal sensitivity in humans but temporarily and the amount of *RPE65* dose required varied between the species (dogs and humans) and hence higher dose might bring a durable and robust improvement [90].

Phase I clinical study of gene therapy for six arRP patients with *MERTK* mutations to test the safety and efficacy of gene therapy via subretinal injection of rAAV2-VMD2-hMERTK have shown no major side effects and has shown mild clinical improvement in three patients [91].

Combined Gene replacement and Gene silencing therapies: It is done mainly for autosomal dominant diseases where there is toxic gain of function due to mutated protein or a dominant negative effect of the encoded protein [81]. Two approaches have been proposed to silence the abnormal gene, i) ribozymes [92] and ii) RNA interference (siRNA) [93].

Ribozymes: They are catalytic RNA molecules with the ability to cleave the complementary mRNA thus directed towards the mRNA from the mutated allele. This kind of ribozyme mediated gene silencing was tested on rat models for *RHO* gene [92].

RNA interference: In another study, suppression of the mutant transcript in a site independent manner along with codon modified gene replacement was achieved in Pro23His$^{+/-}$ *Rho*$^{+/-}$ mouse models. This was done by delivering shRNA and codon modified *RHO* replacement genes through subretinal injection of AAV vectors. This study represents the first in vivo indication that both suppression and replacement strategies can provide therapeutic benefit for dominantly inherited genetic conditions [93].

1.13.2 Pharmacological Treatment

Pharmacological agents are used for treatment in cases where there is a biochemical defect and when the patho-physiological mechanisms are known.

Oral administration of 9-cis-retinal: *RPE65* deficiency causes block in the visual cycle due to failure in the regeneration of 11-cis-retinal and accumulation of all-trans-retinyl esters [94]. Studies have been conducted in mice, where oral administration of 9-cis-retinyl acetate have shown to increase the light sensitivity, supported and evidenced by ERG recordings and vision sustained upto six months after treatment [95]. Oral administration of synthetic 9-cis retinal were given to 14 patients who were aged 6-38 years with *RPE65* and *LRAT* positive mutation, it was found that the therapy was well tolerated resulting in rapid improvement of the visual function in some of these patients with LCA [96].

Neurotrophic factors: There are number of neurotrophic agents which have shown to slow down the photoreceptor death in animal models. These are basic fibroblast-derived growth factor (bFGF), brain-derived neurotrophic factor (BDNF), cardiotrophin-1, nerve growth factor (NGF), fibroblast growth factor (FGF) and ciliary neurotophic factor (CNTF) [97]. In Phase I safety trial, human CNTF was delivered by human retinal pigment epithelium cells transfected with human CNTF gene sequestered within the capsules and surgically implanted into the vitreous of the patient's eye. The results indicated that CNTF is safe for human retina even with severely comprised photoreceptor [98].

1.13.3 Retinal Transplant

It is another therapeutic strategy to restore vision in patients with retinal degenerative disease. Different sources of cells are used for transplantation such as fetal tissue, embryonic stem cells, neural stem cells, somatic cells, induced pluripotent stem cells and RPE [99]. Several ocular clinical trial have been started in humans to establish the safety and efficacy using these stem cells [100] and results are awaited.

Fetal Tissue: Whole sheets of fetal neural retina are transplanted into the subretinal space and they have shown to improve the vision in mice models by enhanced survival of host photoreceptors by trophic signals from the donor tissue. The main disadvantage of this kind of transplantation is disorganization of the host neural retina, hence only sheets of immature photoreceptors are transplanted [101, 102]. Whereas human studies of transplanting the intact sheets of fetal neural retina with its

retinal pigment epithelium in RP patients have not shown much improvement in vision possibly due to the severe retinal degeneration in patients but there was no evidence of rejection [103].

Stem Cells: The stem cells used are embryonic stem cells and neural stem cells which are triggered to differentiate into photoreceptors. These have their limitation to differentiate into specific adult cell types with their proper function [102]. Transplantation of human embryonic stem cell (hESC) into the subretinal space of Royal College of Surgeons (RCS) rat showed to slow down the degeneration of photoreceptor and improve visual performance [104]. Stem cell transplantation for retinal disease is currently transitioning from preclinical research to phaseI/II clinical trials [104].

Somatic Cell Nuclear Transfer (SCNT): The basis of somatic cell nuclear transfer is to transfer the DNA from an adult somatic cell into an oocyte in which its original chromosomal material is removed. Then oocyte is electrically stimulated to generate the embryonic stem cell and kept in vitro or can be implanted into a uterus and by using this technique 200 different types of cells can be created. The main advantage of this technique is that the patients' somatic cell can be used and they would be the ideal match for transplantation back into the donor [102].

Induced Pluripotent stem cell: These are the cells artificially derived from non-pluripotent stem cells preferably adult stem cell. They are induced artificially to differentiate into photoreceptor.

Gene editing technologies like TALEN or CRISPER –Cas 9 opens another possibility in using patient specific cells for transplantation therapies as the genetic defect is corrected/ repaired [105].

Need for the current study

Till date about twenty-seven genes have been identified for LCA, about 77 genes and 7 loci for retinitis pigmentosa and 33 genes and 5 loci for CRD [106]. Candidate gene screening approaches, linkage mapping, homozygosity mapping and targeted next generation sequencing have identified mutations in 50-70% of the cohorts studied, nonetheless in about 30-50% no genetic cause has still been identified [28]. From a recent study in a Chinese LCA cohort using next generation sequencing, mutation was identified in 76.6% of the cases [107]. There have been few reports on LCA and arRP from India.

Our previous report on candidate gene screening of *RPE65* in 60 LCA cases had identified mutation in 1/60 (1.7%) case. We have also reported a case study where *LCA5* was identified as the causative gene in a consanguineous family using homozygosity mapping [108]. Other reports on LCA from India wherein either candidate gene screening alone or combined with Asper chip using APEX technology revealed fewer percentage of mutation (36%) positive cases [109]. A study from an Indian cohort of 38 cases revealed only 2.6% (1/38) with mutations that are more common in North American population [110]. Multicentre studies on candidate gene screening for LCA for fewer genes and where smaller cohorts from India have also been a part are reported. In a study on 176 probands, *CRX*, *GUCY2D* and *RPE65* were screened by SSCP analysis and 28 harbored possible disease causing mutation (15.9%) [111]. Exome sequencing identified a novel gene, *NMNAT1* in a Pakistani family, subsequently Sanger sequencing was done to screen *NMNAT1* in 284 unrelated cases which included cases from India and identified a mutation frequency of 4.9% (14/284) for this gene [112]. Autosomal recessive RP families from India have been part of multicentric studies where they identified novel candidate genes; *TTC8* in a single arRP family and *FAM161A* in two consanguineous Indian families. These were identified either by homozygosity mapping or by whole exome sequencing or a combination of both [113, 114]. Reports on homozygosity mapping in autosomal recessive RP families from India have identified the causative gene in approximately 15% (5/34 and 4/26) of the families studied, indicating that still newer causative genes have to be identified [63, 115].

There are two clinical case reports on CRD from India, correlating the manifestation of keratoconus and vertical nystagmus [116, 117]. But no reports on mutational screening, except for an autosomal recessive retinal dystrophy study where of the 14 families analysed by homozygosity mapping using microsatellite markers, two families revealed mutations in *ABCA4* gene [118].

Since LCA and a considerable portion of RP and other retinal dystrophies are predominantly inherited in recessive pattern, homozygosity mapping was used for identifying disease loci with the advantage of identifying novel loci, if any in the current study.

Documenting the phenotype to correlate with the identified genotype would help in better prediction of the prognosis in the patients and in genetic counseling of the patients and their family members. Genotype data would especially be mandatory for any potential gene based therapies in future.

Objectives of the study:

1. To perform homozygosity mapping on consanguineous families with inherited retinal degenerative disease using high through put microarray and to identify the disease loci involved.
2. Identification of causative gene(s) and/or mutations in the families studied.
3. To correlate the observed phenotype with the genotype determined in the study.

Organization of the thesis:

This thesis documents the genetics of autosomal recessive LCA, arRP and arCRD using homozygosity mapping. Chapter1 gives a brief introduction, review of literature on inherited retinal diseases, LCA, RP and CRD followed by Chapter 2 materials and methods for the study, Chapter 3 the results of the experiments followed by Chapter 4 the discussion with respect to the results obtained and available literature. The flowchart depicting the organization of thesis is shown in Fig: 1.8.

Fig: 1.8 Flowchart depicting the organization of thesis

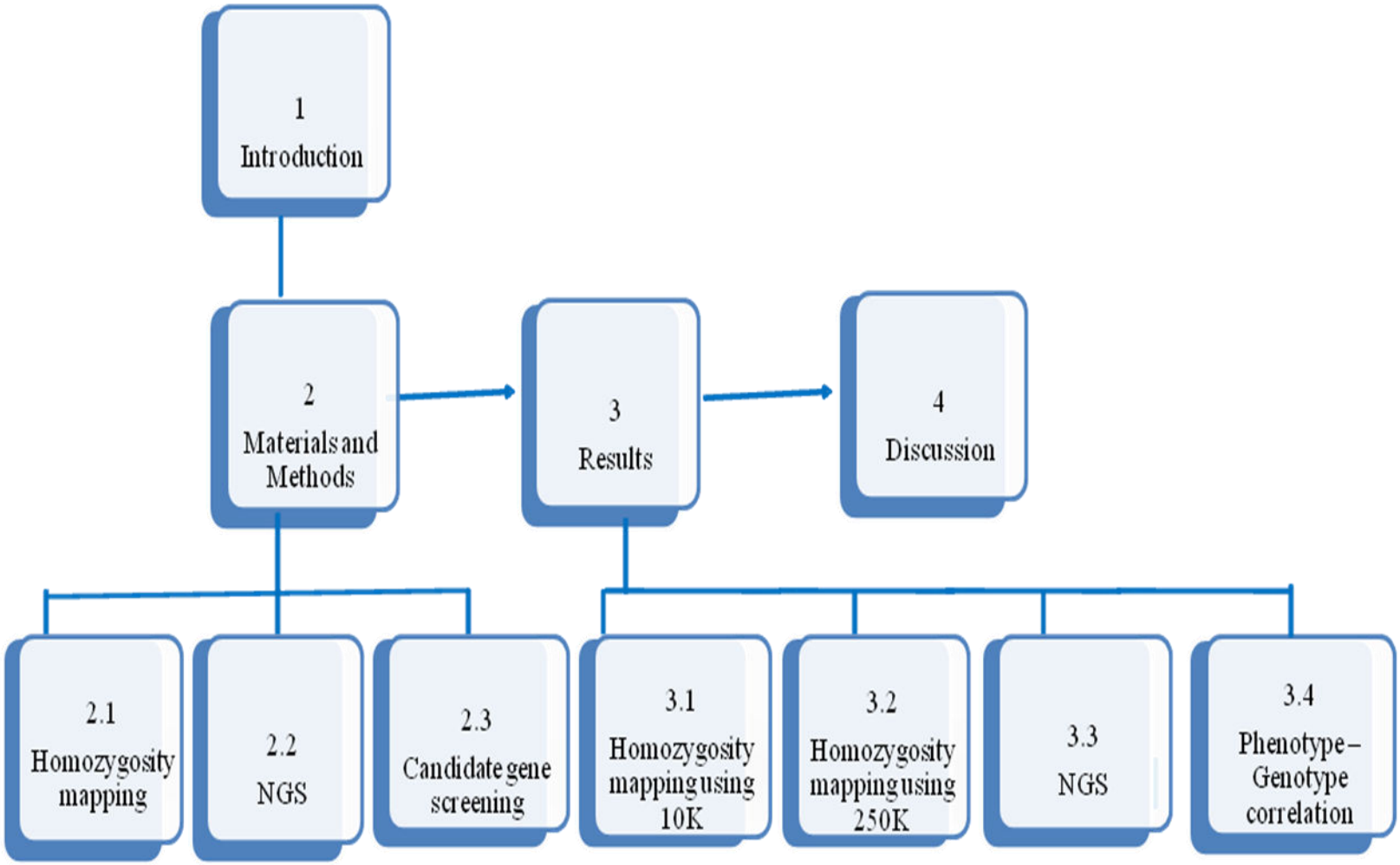

CHAPTER 2

Materials and Methods

Subjects

Patient recruitment and clinical examinations

Twelve LCA, two arRP and one arCRD consanguineous south Indian families with at least one unaffected sib were enrolled in the study. Complete ophthalmic examination was carried out for all the affected individuals that included slit-lamp examination, electroretinogram (ERG), fundus photograph, fundus auto fluorescence (FAF) in all patients and optical coherence tomography (OCT) where ever possible. Blood (10ml) was collected from all the affected individuals, unaffected siblings and parents after obtaining written informed consent. The study was approved by the Vision Research Foundation's Institutional Review Board (IRB) and ethics committee and all the procedures were performed in accordance with institutional guidelines and the Declaration of Helsinki.

Methods

Blood collection, DNA extraction using Nucleospin Blood XL kit (Macherey-Nagel, GmbH, Düren, Germany), quantification of extracted DNA, are detailed in Appendices 1-3. The overview of methodologies adopted are shown in Fig: 2.1

Fig: 2.1 Overview of the methodologies adopted

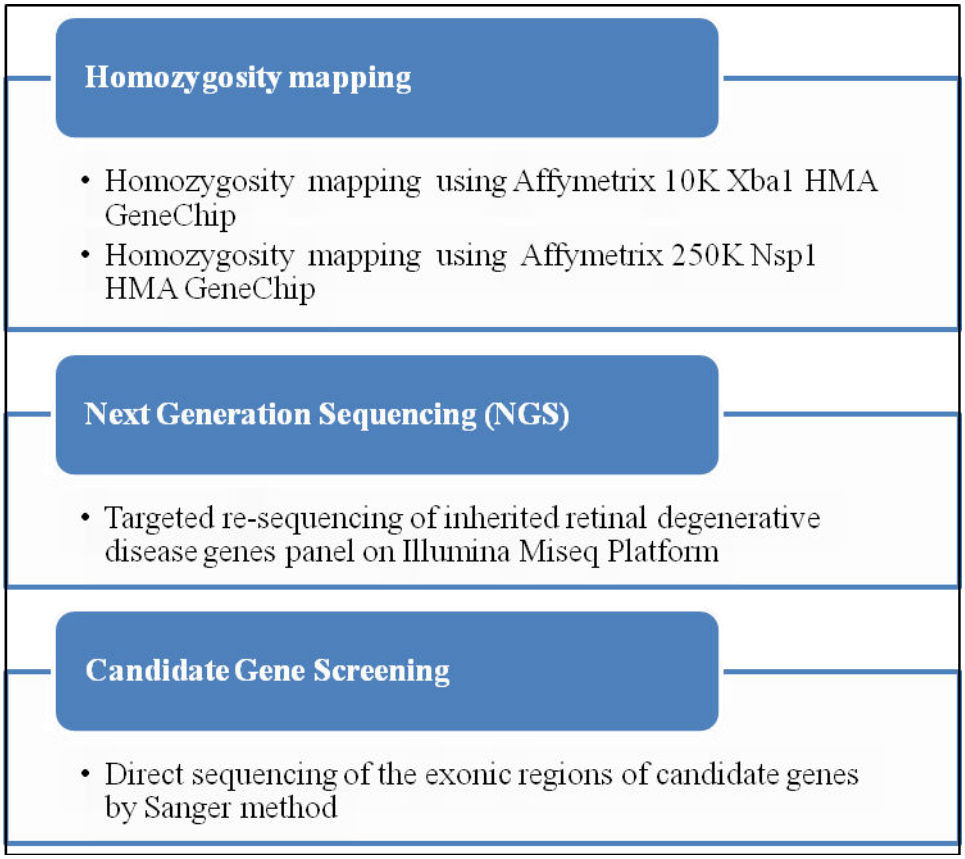

2.1 Homozygosity mapping

Homozygosity mapping was done using Affymetrix 10K Xba1 and 250K Nsp1 HMA GeneChips.

The Affymetrix GeneChip mapping assay is designed to detect approximately 10,000 for 10K and 2,50,000 for 250K single nucleotide polymorphisms (SNP) from samples of genomic DNA. This assay mainly utilizes the strategy of reducing the complexity of genomic DNA by digesting the genomic DNA with specific restriction enzyme(s), followed by ligating the digested fragments with specific adapter sequence. Then PCR is performed which is optimized for fragments of a specified range. PCR is followed by fragmentation and end labeling with biotin.

The labeled fragments are hybridized overnight i.e for 16-18hrs on specific GeneChip. Post hybridization washing and staining is performed in the Affymetrix fluidics station.

Finally the GeneChips are scanned and the raw data generated as .CEL files. The .CEL files are taken for further analysis using specialized software. Table 2.1 illustrates the number of affected people taken for GeneChip analysis.

Table 2.1 Illustrates the family ID, diagnosis and number of affected people taken for GeneChip analysis.

Family ID	Diagnosis	Number of affected people taken for high through put SNP genotyping analysis
Fam-01	arRP	3
Fam-02	LCA	2
Fam-03	LCA	4
Fam-04	LCA	2
Fam-05	LCA	2
Fam-06	LCA	2
Fam-07	LCA	2
Fam-08	LCA	2
Fam-09	LCA	1
Fam-10	LCA	2
Fam-11	LCA	2
Fam-12	LCA	2
Fam-13	LCA	2
Fam-14	arCRD	2
Fam-15	arRP	1

2.1.1 Homozygosity mapping using Affymetrix 10K Xba1 GeneChip

The detailed protocol followed for genotyping using Affymetrix 10K array is given in Appendice 4 and flowchart of the overall steps involved are given below

Genomic DNA of 50ng/µl was digested with Xba1 restriction enzyme

↓

Ligation with specific adaptor

↓

PCR to amplify fragments of size ranging from 200 – 1000bp

↓

Purification of the amplified PCR product using vacuum manifold

↓

Quantification of the purified PCR product and normalization to 20µg per 45µl with elution buffer

↓

Fragmentation of the PCR product using Fragmentation Reagent

↓

Biotin end labeling of the fragmented PCR products using Terminal deoxynucleotidyl transferase enzyme

↓

Hybridization of the end labeled products on the specific GeneChip using Affymetrix GeneChip®Hybridization Oven 640 for 16-18 hours

↓

Washing, staining in the Affymetrix Fluidics Station 450 and scanning (Affymetrix, GeneChip Scanner 3000 7G) of the 10K array

Data analysis for 10K GeneChip

For the arRP1 family; Fam-01, three affected and one unaffected members were genotyped using 10K HMA GeneChip. The internal quality control check for the microarray analysis was set as 90%. .CEL files generated for each sample were analyzed using GTYPE software. The genotype generated was exported to excel sheet for further analysis. Here, the data was first sorted according to chromosome number and then by cytoband position (p arm and q arm). The sorted data was compared between the affected and unaffected for large continuous stretch of homozygous regions (consecutive SNP being homozygous). Chromosomal segments were considered to be homozygous if they had ≥39 consecutive SNPs homozygous since the likelihood of this to occur by chance is 1:100 in consanguineous families.

2.1.2 Homozygosity mapping using Affymetrix 250K Nsp1 GeneChip

The detailed protocol followed for genotyping using Affymetrix 250K HMA array is given in Appendice 4. Flowcharts of the overall steps involved are as below

Genomic DNA of 50ng/µl was digested with NspI restriction enzyme

↓

Ligation with specific adaptor

↓

PCR to amplify fragments of sizes ranging from 250bp to 1100bp

↓

Purification of the amplified PCR product using vacuum manifold

↓

Quantification of the purified PCR product and normalization to 90µg per 45µl with RB buffer

↓

Fragmentation of the PCR product using Fragmentation Reagent

↓

Biotin end labeling of the fragmented PCR product using Terminal deoxynucleotidyl transferase enzyme

Hybridization of the end labeled products on specific GeneChip using Affymetrix, GeneChip®Hybridization Oven 640 for 16-18 hours

Washing, staining in the Affymetrix Fluidics Station 450 and scanning (GeneChip Scanner 3000 7G) of the 250K array

Data analysis for 250K GeneChip

Fam-02 – Fam-15, SNP genotyping was done on one or more affected family members along with an unaffected sibling using 250K NspI GeneChip. The raw data generated as .CEL files were further analyzed using GCOS v4.0 (Affymetrix, Santa Clara, CA) software. The internal quality control check was set as 90%. Loss of heterozygosity (LOH) score is a measure for the likelihood of a stretch of SNPs to be homozygous based on the population SNP allele frequencies and a score of ≥15 is considered to be significant. Homozygous stretches between the affected and the unaffected were compared by LOH status. The homozygous blocks with the known LCA candidate genes loci and all other homozygous blocks were noted. We first screened the known LCA gene present in the largest homozygous block, followed by others, if required. When the causative mutation was identified, segregation analysis in the family members and control screening was performed to confirm its pathogenicity.

2.2 Next Generation Sequencing (NGS)

The targeted re-sequencing and the initial NGS data analysis was done for 184 inherited retinal disease genes at Strand Centre for Genomics & Personalized Medicine, Bengaluru, India, on Illumina MiSeq platform.

a) **NGS – library preparation and sequencing:** Nextera DNA library preparation protocol (Illumina, USA) was used to convert input genomic DNA (gDNA) into adapter-tagged indexed libraries. Approximately 50 ng of input gDNA was used in the tagmentation process, which involves simultaneous fragmentation and adapter tagging of gDNA followed by adapter ligation. This was followed by limited cycles of PCR (ABI 9700, Life Technologies, USA) to allow the incorporation of sample specific indices or multiplex identifier (MID) barcodes. The quality of the library was assessed using the BioAnalyzer (Agilent, USA). Next, 500 ng of individual libraries were pooled and hybridized to biotin-labeled probes specific to the targeted regions. The pool was enriched for the target genomic regions by adding streptavidin beads that bind to the biotinylated probes. The biotinylated gDNA fragments bound to the streptavidin beads were magnetically pulled down from the solution. The tagged and amplified sample libraries were checked for quality and quantified using the BioAnalyzer (Agilent, USA). Upto 6-10 pM of the pooled library was loaded and sequenced on the MiSeq platform (Illumina, USA), according to the manufacturer's instructions.

b) **NGS – data analysis and interpretation**: The trimmed FASTQ files were generated using MiSeq Reporter (Illumina, USA). The reads were aligned against the whole genome build: hg19 using Strand NGS v2.1.6 (http://www.strand-ngs.com/). Briefly, the 150 bp paired-end reads were first aligned against the hg19 reference genome. Five base pairs from the 3' end of the reads were trimmed, as were 3' end bases with base quality below 10. Reads with length less than 25 bp after trimming were not considered for alignment. A maximum of 5 matches of alignment score at least 90% were computed. Post alignment, the reads were re-aligned using the local

realignment functionality in Strand NGS v2.1.6. Following this, reads that failed vendor QC (quality control), reads with average quality less than 20, reads with ambiguous characters and all duplicate reads were filtered out. The variant detection algorithm in Strand NGS v2.1.6 was then used to detect variants in the target regions covered by a minimum of 20 reads with at least 2 variants reads. Variants with a decibel score of at least 50 were reported and consecutive single base variants (SBVs) were merged to create multi-base variants (MBVs) in the final variant call format (VCF) file. The VCF file along with a low coverage (<20 reads) file generated using the filtered read list were uploaded into StrandOmics v3.0 (http://www.strandls.com/strandomics/; (a proprietary clinical genomics interpretation and reporting platform from Strand Life Sciences) for all subsequent analysis and variant interpretation. The 'interpretation interface' in StrandOmics v3.0 allows quick filtering and evaluation of variants identified in a sample.

2.3 Candidate genes screening

The candidate genes were screened by direct sequencing using Sanger method. The entire coding region along with 100bp of introns was amplified and screened for identifying the causative mutations in Fam-01 - Fam-15. The primers encompassing the exons of the gene were designed using Primer 3 (v. 0.4.0) software. The primer sequences for all the genes screened are listed in Appendice 5.

A 12.5µl PCR reaction was set up with 10pmol of forward primer and reverse primer, 1X Taq Buffer A (Bangalore Genei, Bengaluru, India), 500µM dNTPs (Applied Biosystems, Foster City, California), 0.3U TaqDNA polymerase (Bangalore Genei, Bengaluru, India) and 25ng of genomic DNA. The PCR reaction protocol is illustrated in Table 2.2 and Thermal cycler profile is shown in Table 2.3.

Table 2.2 PCR reaction protocol

Reagents	Concentration	Volume(µl)
DNA	25ng	0.5
Froward primer	10pmol	1.0
Reverse primer	10pmol	1.0
Taq	0.3units	0.1
dNTPs	500µM	0.5
Taq buffer A(10X)	1X	1.25
Water	-	8.15
Total Reaction Volume	-	12.5

Table 2.3 Thermal cycler profile

Phase of the cycle	Temperature ˚C	Time (secs)	Cycles
Initial Denaturation	95	180	1x
Denaturation	95	20	35 cycles
Annealing	Annealing Temperature (AT)	20	
Extension	72	30	
Final extension	72	300	
Hold	4	Infinity	

A touch-down PCR was performed for some exons, where the annealing temperature was set at 0.5ºC decrement for the first 14 cycles followed by constant temperature for the rest of 21 cycles.

The annealing temperature and reaction conditions for all the coding regions of nine candidate genes along with exon 11 and exon 13 of *ABCA4* and *CDHR1* gene respectively were standardized. The details are given in Appendice 6.

The amplified PCR products were subjected to 2% agarose gel electrophoresis, ExoSAP treatment, Cycle sequencing using BigDye terminator v3.1 kit (Applied Biosystems, Foster City, California), purification of the cycle sequenced extension products and then capillary electrophoresis in ABI Prism 3100 AVANT Genetic Analyzer (Applied Biosystems, Foster City, California). The details of the protocol are given in Appendice 7, 8, 9, 10, 11, respectively.

2.4 RNA extraction and cDNA analysis

Ten ml of heparin blood samples were allowed to stand at room temperature for one hour and then the buffy coat was collected. RNA was extracted using Nucleospin RNA II kit (Macherey-Nagel, GmbH, Düren, Germany). The RNA was converted to cDNA using Verso cDNA kit (Fischer Scientific, Surrey, U.K) and the cDNA amplified using specific primers encompassing exons 11, 12, and 13 of *IQCB1* gene giving a 487bp product. The cDNA primer sequences are listed in Appendice 12. The cDNA synthesis protocol, Thermal cycler profile for cDNA synthesis, cDNA amplification reaction protocol and Thermal cycler profile for cDNA amplification are listed in Table 2.4, 2.5, 2.6 and 2.7 respectively.

Table 2.4 cDNA synthesis protocol

Reagents	**Concentration**	**Volume(µl)**
RNA	150ng	3.0
cDNA synthesis buffer (5x)	1x	4.0
dNTP Mix	500µM	2.0
RNA Primer	400ng	1.0
RT Enhancer	-	1.0
Verso enzyme	-	1.0
Water (Nuclease free)		8.0
Total Reaction Volume		20

Table 2.5 Thermal cycler profile for cDNA synthesis

Phase of the cycle	**Temperature ˚C**	**Time (mins)**	**Cycles**
cDNA synthesis	42	30	1x
Inactivation	95	2	1x
Hold	4	Infinity	-

Table 2.6 cDNA amplification reaction protocol

Reagents	**Concentration**	**Volume(µl)**
cDNA	25ng	0.5
Froward primer	10pmol	1.0
Reverse primer	10pmol	1.0
Taq	0.6units	0.2
dNTPs	500 µM	0.5
Taq buffer A(10x)	1x	2.0
Water	-	14.8
Total Reaction Volume	-	20

Table 2.7 Thermal cycler profile for cDNA amplification

Phase of the cycle	**Temperature ˚C**	**Time (secs)**	**Cycles**
Initial Denaturation	95	180	1x
Denaturation	95	20	14/21 cycles
Annealing	65/58-58 with 0.5 decrement	20	
Extension	72	30	
Final extension	72	300	
Hold	4		

2.5 Control Screening

Hundred unrelated healthy controls with no ocular involvement were taken for control screening. The control samples were available from epidemiology projects conducted by our institute, Medical Research Foundation [119, 120]. For the mutations identified in Fam-02 – Fam-08 and Fam10 - Fam15 control screening was performed by direct Sanger sequencing.

2.5.1 Allele specific PCR

The control screening for the identified causative mutation in Fam-01 and Fam-09 was done by allele specific PCR.

This method allows an efficient genotyping of a sinlge SNP in a PCR reaction. Here, apart fron the common forward and reverse primer two different allele specific forward primers were used. The 3' end of the mutant and wild type specific forward primer were complementary for the specific alleles. Futher, the specificity and stringency was enhanced by changing the fifth base from the 3'end of allele specific primer, from purine to pyrimidine or vise versa.

The reaction protocol, thermal cycle profile for allele specific PCR for the identified mutation in *MERTK* c.721C>T p.(Gln241Ter), *AIPL1* c.247G>A p.(Glu83Lys) in Fam-01 and Fam-09, respectively are given below. The primer sequence and the corresponding amplified product size are given in Appendice 13. The allele specific reaction protocol and thermal cycler profile are listed in Table 2.8 and 2.9 respectively.

Table 2.8 Allele Specific Reaction Protocol

Reagents	**Wild type Volume (ul)**	**Mutant Volume (ul)**	**Final Concentration**
DNA	0.5	0.5	25ng
Froward primer	1.0	1.0	10pmol
Reverse primer	1.0	1.0	10pmol
Wild type /Mutant primer	1.0	1.0	10pmol
Taq	0.1	0.1	0.3units
dNTPs	0.5	0.5	500µM
Taq buffer A(10x)	1.25	1.25	1X
Water	7.15	7.15	
Total Reaction Volume	12.5	12.5	

- For a single sample, two reactions were set up, one labelled as wild type and other as mutant
- For the wild type all the above mentioned reagents were added along with the wild-type allele specific primer
- For the mutant, all the above mentioned reagents along with the mutant allele specific primer was used.

Table 2.9 Thermal cycler profile for allele specific PCR

Phase of the cycle	**Temperature ˚C**	**Time (secs)**	**Cycles**
Initial Denaturation	95	180	1x
Denaturation	95	20	35x
Annealing	60	20	
Extension	72	30	
Final extension	72	300	1x
Hold	4		

2.6 Bioinformatics analyses

The identified nine novel variations were checked in Human Genome Mutation Database (HGMD), dbSNP, ClinVar, 1000 Genomes database, Exome Variant Server (EVS) and the Exome Aggregation Consortium (ExAC). In addition the three missense mutations also were checked in UCSC Genome Browser across 46 vertebrates. The intronic mutations were analysed by Human Splice Finder 2.4.1 [121] and Mutation taster [122] for possible splicing defects and the missense mutations were anlaysed by PolyPhen-2 [123] SIFT [124], Mutation Taster [122], Mutation Accessor [125], MutPred [126], PMUT [127] to predict their possible effect on structure and function of the protein. The details of the bioinformatics tools have been listed in Appendice 14.

CHAPTER 3

Results

The results chapter has been divided as; 3.1 - Homozygosity mapping using 10K GeneChip, 3.2 - Homozygosity mapping using 250K GeneChip, 3.3 - Homozygosity mapping using 250K GeneChip followed by NGS analysis, 3.4 - Genotype-phenotype correlation of mutation positive LCA, arRP and arCRD cases/families.

3.1 Homozygosity mapping using 10K GeneChip

We had taken three affected members and one unaffected sibling of the Fam-01 diagnosed with arRP, for Homozygosity mapping using Affymetrix 10K XbaI GeneChip.

- The genotype was called using GTYPE software and the analysis done as detailed in the methods section.
- The sorted data was compared between the affected and unaffected for large continuous stretch of homozygous regions (consecutive SNP being homozygous).
- Comparison between the three affected members and one unaffected sib identified a longest region of 48 consecutive SNPs spanning 2q12.1-2q14.1 (rs722475 -rs1586794) to be homozygous in all affected members as shown in Fig 3.1.
- By using the UCSC genome browser we found 49 annotated genes in this interval and one of the possible candidate gene; *MERTK* in 2q13 region. *MERTK* is previously associated with arRP.

Fig: 3.1. Snapshot of homozygous block common between the affected individuals and the same stretch of SNPs being heterozygous in the unaffected. The homozygous block is highlighted.

2	q12.1	103802308	rs726653	AA	AA	AA	AA
2	q12.1	104558489	rs2375936	NoCall	NoCall	NoCall	NoCall
2	q12.1	105404701	rs445077	AA	AA	NoCall	NoCall
2	q12.1	105404580	rs409542	AA	AA	AA	AB
2	q12.1	105404967	rs435852	AA	AA	AA	AB
2	q12.1	102932512	rs950881	BB	BB	BB	BB
2	q12.1	102822879	rs1922296	AA	AA	AA	AA
2	q12.1	103813615	rs2310401	BB	BB	BB	AB
2	q12.1	104308545	rs264962	AA	AA	AA	AB
2	q12.1	102932293	rs953934	BB	BB	BB	BB
2	q12.1	103208610	rs1861229	BB	NoCall	BB	BB
2	q12.2	106235889	rs721656	BB	BB	BB	AB
2	q12.2	107463422	rs1375002	BB	BB	BB	AB
2	q12.3	108114345	rs187861	BB	BB	BB	AB
2	q12.3	108219963	rs2203581	BB	BB	BB	BB
2	q12.3	108808424	rs855034	AA	AA	AA	AA
2	q12.3	108537623	rs1820558	BB	BB	BB	BB
2	q12.3	108537591	rs1820559	BB	BB	BB	BB
2	q12.3	107671404	rs1524289	NoCall	NoCall	BB	NoCall
2	q12.3	108051330	rs266175	BB	BB	BB	NoCall
2	q12.3	109056609	rs1112806	AA	AA	NoCall	AA
2	q12.3	108051515	rs266177	BB	BB	BB	AB
2	q12.3	107607039	rs725999	AA	AA	AA	AA
2	q12.3	109489365	rs1073893	BB	BB	BB	BB
2	q12.3	109489429	rs1073895	AA	AA	AA	AA
2	q12.3	109170839	rs920264	AA	AA	AA	AA
2	q13	111801402	rs967895	BB	BB	BB	BB
2	q13	112995810	rs2254860	BB	NoCall	BB	BB

The entire coding region along with 100bp introns of the *MERTK* gene was screened for identifying the causative mutation in Fam-01. A novel non-sense mutation was identified in exon4 c.721C>T p.(Gln241Ter) (Table 3.1). Segregation analysis was performed in the family, all the affected were homozygous for mutation, parent(s) being heterozygous carriers and the unaffected either heterozygous carriers or wild type, shown in Fig: 3.2.

Table: 3.1 Pathogenic mutation identified in the Fam-01 (arRP-01 family)

Homozygous region by size	Chromosome	Known candidate gene	Exons /intron	Mutation identified	Predicted change in protein
48 Consecutive SNP	2	*MERTK*	Exon 4	c.721C>T **Novel**	p.(Gln241Ter)

Fig: 3.2 Fam-01 *MERTK* c.721C>T

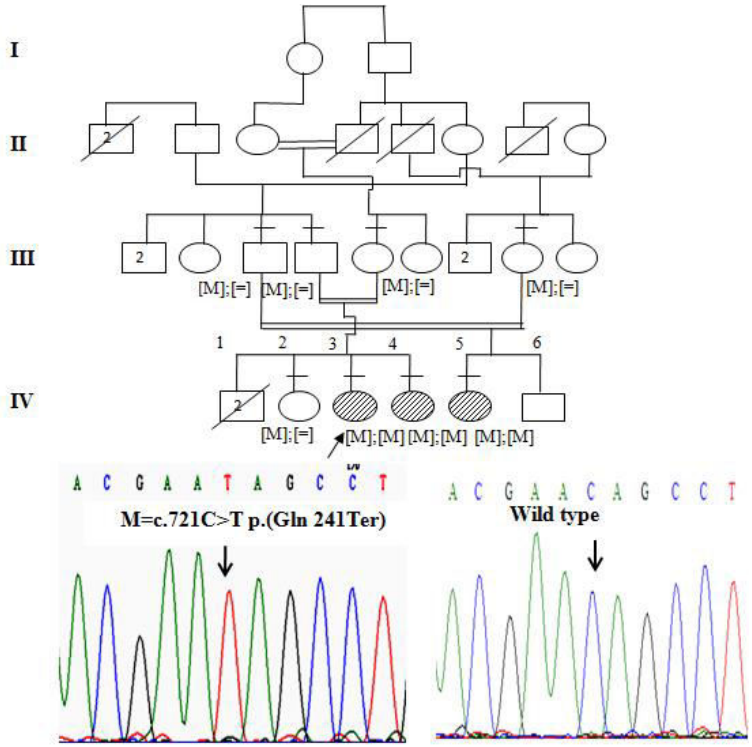

Control screening

Allele specific PCR was performed for control screening for the identified *MERTK* c.721C>T mutation. It was also done for proband, parents and unaffected sibs with mutant and wild type specific primers, respectively. Since the proband is homozygous for mutant, amplification with mutant specific primer alone is observed. Whereas the homozygous wild type controls had amplified only for the wild type but not for the mutant specific primer and in heterozygous carrier parents and unaffected sib both the wild type and the mutant specific primers amplified (Fig: 3.3). One hundred normal controls (200 chromosomes) were screened and all were wild type.

Fig: 3.3 Agarose gel photograph of allele specific PCR of *MERTK* c.721C>T mutation for control screening

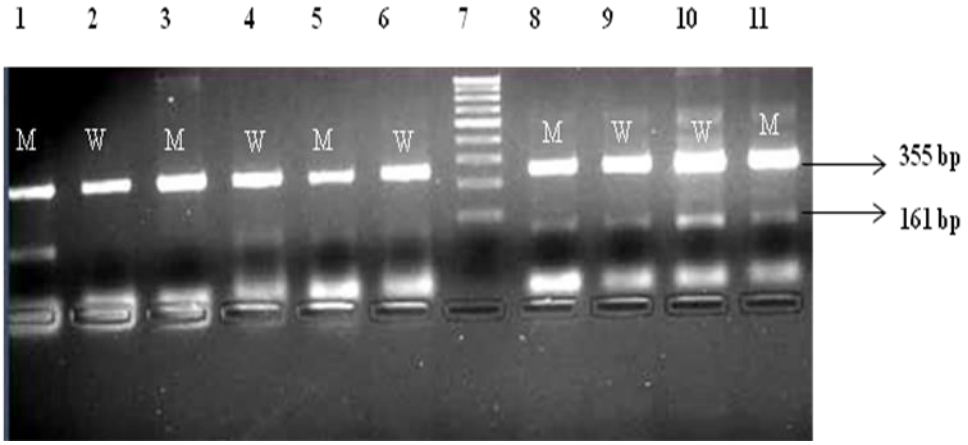

Legend

M – Amplification with mutant specific primer

W – Amplification with wild type specific primer

Lane 1 and 2: Homozygous mutant Proband – allele specific primer amplified for mutant but not for wild type

Lane 3 and 4: Homozygous wild type control – allele specific primer not amplified for mutant but only for wild type.

Lane 5 and 6: Heterozygous carrier father – allele specific primer amplified for both mutant and wild type.

Lane 7: 100 – 1000 bp ladder

Lane 8 and 9: Heterozygous carrier mother - allele specific primer amplified for both mutant and wild type.

Lane 10 and 11: Heterozygous carrier unaffected sibling - allele specific primer amplified for both mutant and wild type.

3.2 Homozygosity mapping using 250K GeneChip

Eleven consanguineous LCA families were analysed. Homozygosity mapping was performed for the eleven LCA families with Affymetrix 250K Nsp1 HMA GeneChip on 32 individuals of which 23 were affected and 9 unaffected siblings. In each of the LCA family, we were able to identify on an average of about fifteen to twenty homozygous blocks ranging in size from 1Mb to 30Mb. Families with more than 1Mb block are listed in Table 3.2. Out of eleven LCA families, we identified the causative mutation in ten families (90%), *AIPL1* mutation in three, *RPE65* mutation in two, and *CRB1*, *GUCY2D, IQCB1, RDH12, SPATA7* mutation in one family each, respectively. Table 3.3 shows the list of known LCA candidate genes present within the homozygous blocks in these LCA families. Table 3.4 shows the pathogenic mutation identified in LCA families.

Table 3.2: Total number of homozygous blocks >1Mb in the eleven LCA families

S.No	Family ID	Number of blocks >1Mb in size
1.	Fam-02	8
2.	Fam-03	7
3.	Fam-04	15
4.	Fam-05	8
5.	Fam-06	20
6.	Fam-07	16
7.	Fam-08	33
8.	Fam-09	28
9.	Fam-10	9
10.	Fam-11	15
11.	Fam-12	18

Table 3.3: Size of homozygous blocks and the known LCA candidate genes identified in the eleven LCA families

S.No	Family ID	Number of Affected individuals taken for analysis	Size of the homozygous block in which known LCA candidate gene(s) were present (Mb)	Chromosome location	Genes Screened	Gene reference ID
1.	Fam-02	2	13	1p31.3	*RPE65*	NM_000329.2
2.	Fam-03	4	26	1q31.3	*CRB1*	NM_001257965.1
3.	Fam-04	2	3	17p31.1	*GUCY2D*	NM_000180.3
4.	Fam-05	2	4.7	3q13.3	*IQCB1*	NM_001023570.2
5.	Fam-06	2	3.7	17p13.2	*AIPL1*	NM_014226.3
				17p31.1	*GUCY2D*	NM_000180.3
6.	Fam-07	2	4.05	14q11.2	*RPGRIP1*	NM_020366.3
			1	2q13	*MERTK*	NM_006343.2
7.	Fam-08	2	6	14q11.2	*RPGRIP1*	NM_020366.3
			1.8	7q32.1	*IMPDH1*	NM_000883.3
			1.3	14q24.1	*RDH12*	NM_152443.2
8.	Fam-09	1	5	17p13.2	*AIPL1*	NM_014226.3
			3	1q32.3	*RD3*	NM_183059.2
			2	14q24.1	*RDH12*	NM_152443.2
9.	Fam-10	2	30	1p31.3	*RPE65*	NM_000329.2
			1	14q11.2	*RPGRIP1*	NM_020366.3
10.	Fam-11	2	4.9	17p13.2	*AIPL1*	NM_014226.3
				17p31.1	*GUCY2D*	NM_000180.3
11.	Fam-12	2	6	14q31.3	*SPATA7*	NM_018418.4
			1	1p31.3	*RPE65*	NM_000329.2

Table 3.4: Pathogenic mutations identified in the eleven LCA families.

S.No	Family ID	Genes Screened	Exon/intron	Mutation identified (in homozygous state)	Predicted change in protein	Effect of identified sequence variation
1.	Fam-02	*RPE65*	intron 8	c.850+1G>T Reported	(r.spl?)	Pathogenic
2.	Fam-03	*CRB1*	Exon 9	c.3307G>A Reported	p.(Gly991Arg)	Pathogenic
3.	Fam-04	*GUCY2D*	Exon 3	c.994delC **Novel**	p.(Arg332AlafsTer63)	Pathogenic
4.	Fam-05	*IQCB1*	intron 12	c.1278+6T>A **Novel**	r.[1131_1278 del,1131_1278del] p.(Gln378AlafsTer2)	Pathogenic
5.	Fam-06	*AIPL1*	Exon 6	c.824G>A Reported	p.(Trp278Ter)	Pathogenic
6.	Fam-07	*RPGRIP1 MERTK*	-	Not identified	-	-
7.	Fam-08	*RPGRIP1 RDH12*	*RDH12* intron 3	c.344-8C>T **Novel**	(r.spl?)	Likely pathogenic
8.	Fam-09	*AIPL1*	Exon 2	c.247G>A **Novel**	p.(Glu83Lys)	Pathogenic
9.	Fam-10	*RPE65*	Exon 13	c.1409C>T Reported	p.(Pro470Leu)	Pathogenic
10.	Fam-11	*AIPL1*	Exon 4	c.613_622 delATCATCT GCC **Novel**	p.(Ile205Ter)	Pathogenic
11.	Fam-12	*SPATA7*	intron 7	c.913-2A>G **Novel**	(r.spl?)	Pathogenic

Segregation Analysis and Control Screening

Segregation analysis was performed in all the families (Fig:3.4-.3.13) and the mutation segregated with the disease in the family, with all the affected being homozygous for mutation, parent(s) being heterozygous carriers and the unaffected being either heterozygous for mutation or wild type. One hundred normal healthy controls (200 chromosomes) were screened by Sanger sequencing for the identified mutations and all were wild type.

Fig: 3.4 -3.13 Segregation analysis

Fig 3.4: Fam-02 *RPE65* c.850+1G>T, **3.5**: Fam-03 *CRB1* c.3307G>A, **3.6:** Fam-04 *GUCY2D* c.994delC, **3.7:** Fam-05 *IQCB1* c.1278+6T>A, **3.8**: Fam-06 *AIPL1* c.824G>A, **3.9**: Fam-08 *RDH12* c.344-8C>T, **3.10**: Fam-09 *AIPL1* c.247G>A, **3.11**: Fam-10 *RPE65* c.1409C>T, **3.12**: Fam-11 *AIPL1* c.613_622 delATCATCTGCC, **3.13**: Fam-12 *SPATA7* c.913-2A>G

The arrow indicates the index case. The filled in circles and squares are affected females and males respectively. [M];[M] – affected with homozygous mutation, [M];[=] – carries for any given mutation and [=];[=] – wild type. Lines above the individual indicate availability of genotype.

Fig 3.4: Fam-02 *RPE65* c.850+1G>T

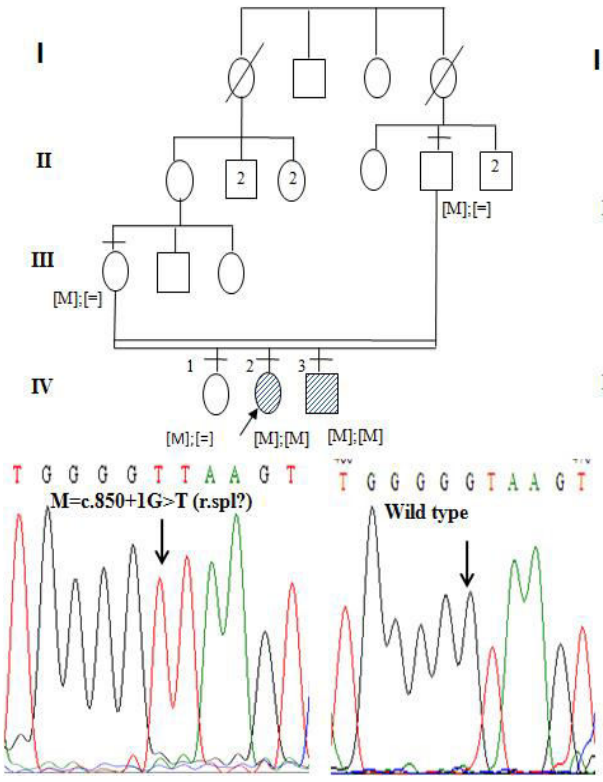

Fig 3.5: Fam-03 *CRB1* c.3307G>A

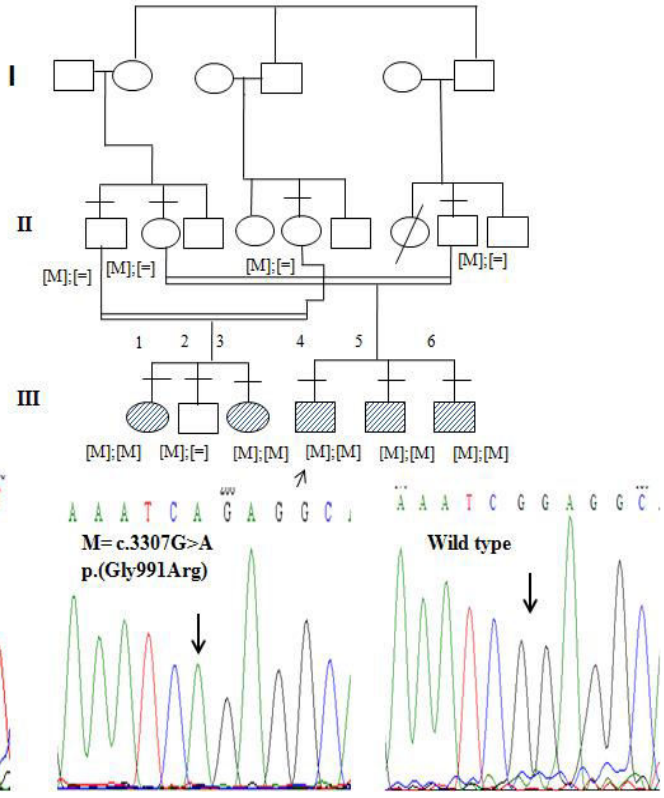

Fig 3.6 Fam-04 *GUCY2D* c.994delC

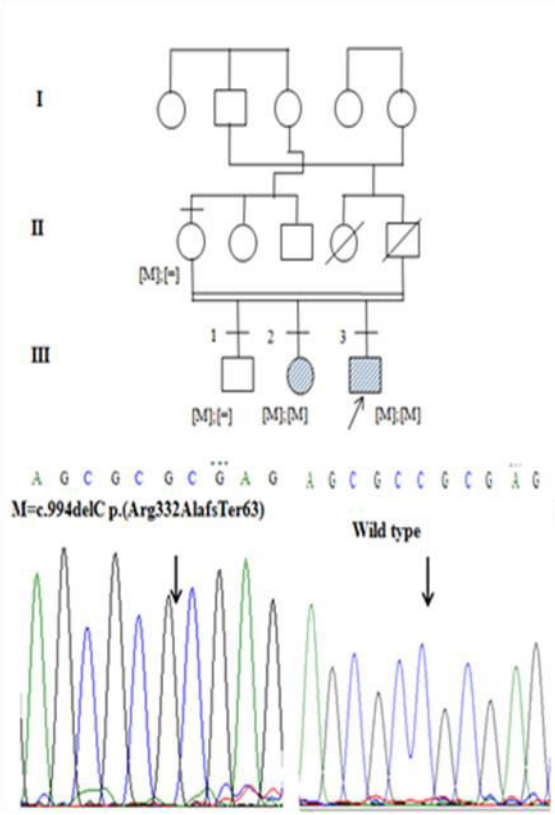

Fig 3.7 Fam-05 *IQCB1* c.1278+6T>A

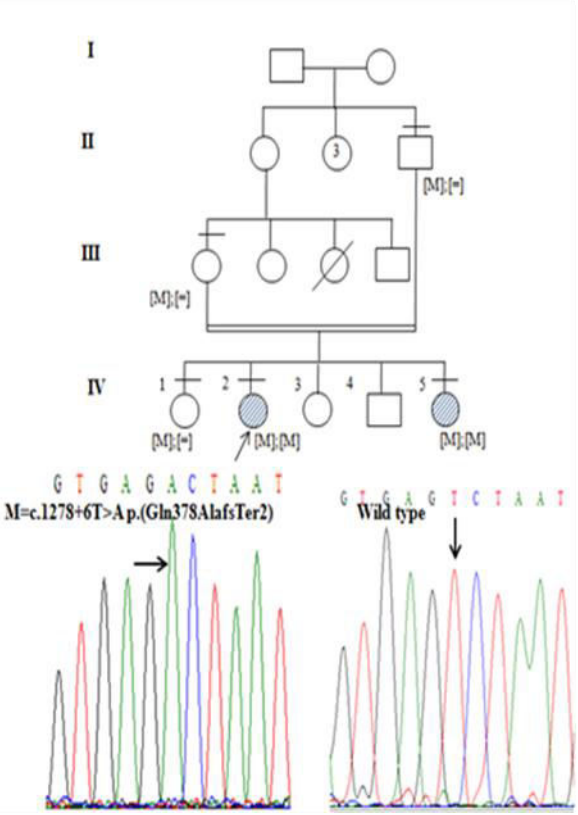

Fig 3.8 Fam-06 *AIPL1* c.824G>A

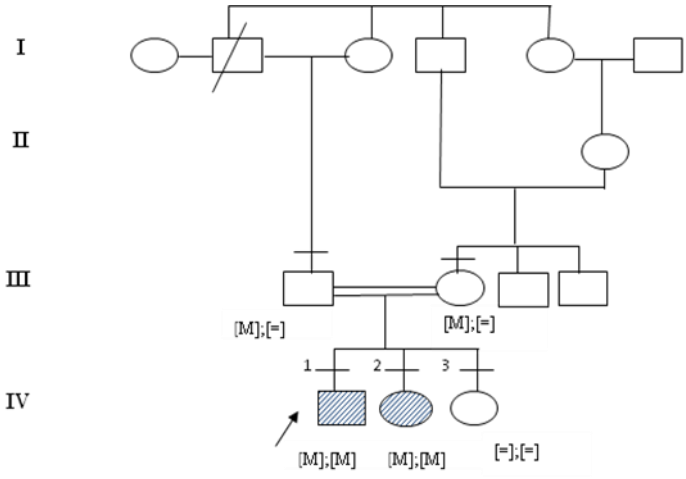

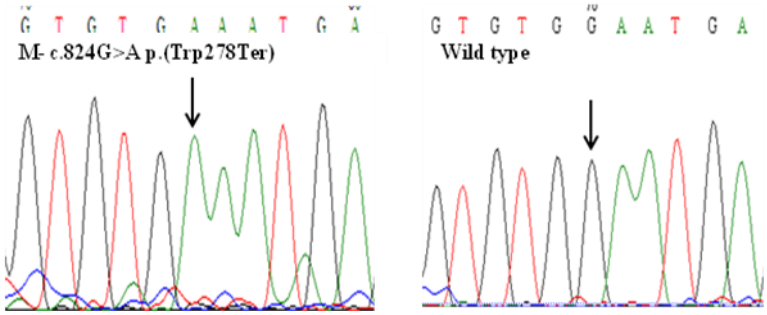

Fig 3.9 Fam-08 *RDH12* c.344-8 C>T

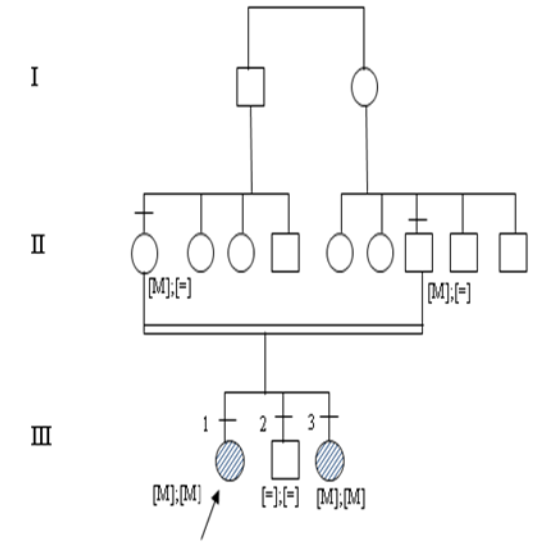

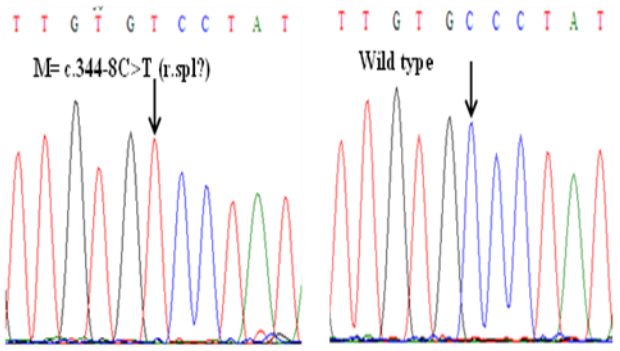

Fig 3.10 Fam-09 *AIPL1* c.247G>A

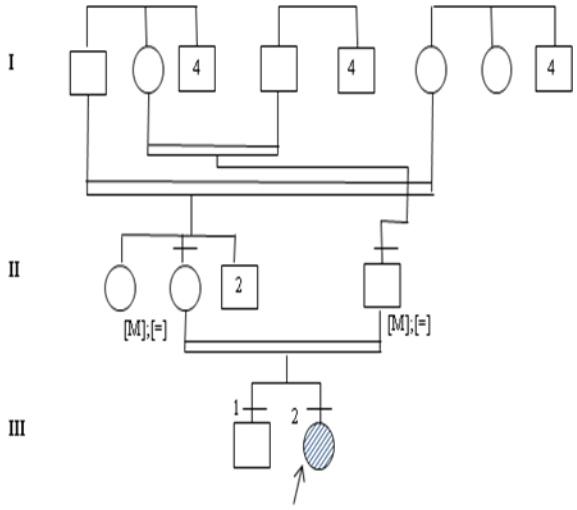

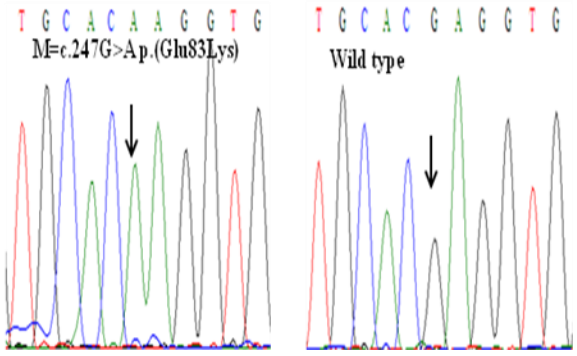

Fig 3.11 Fam-10 *RPE65* c.1409C>T

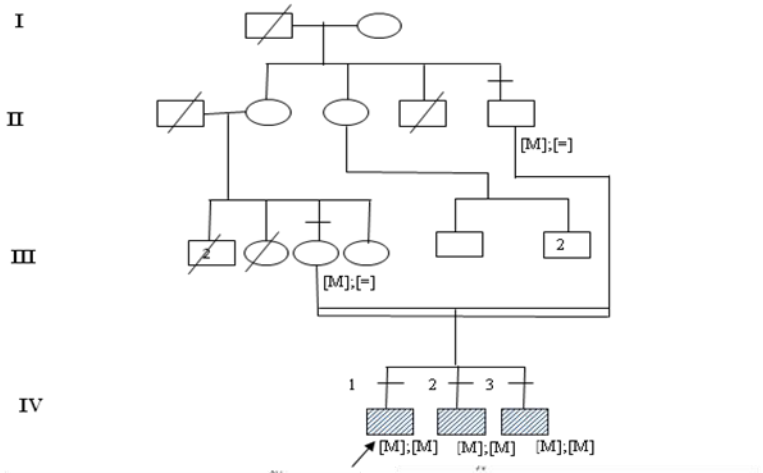

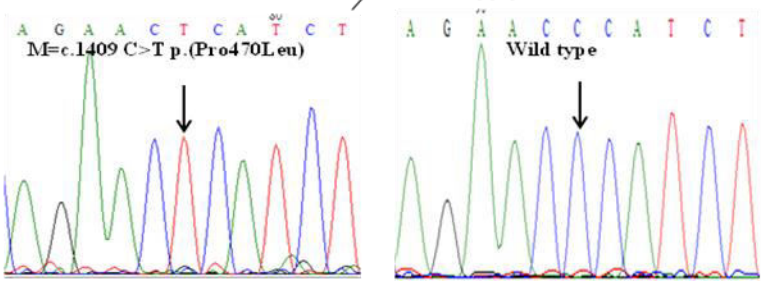

Fig 3.12 Fam-11 *AIPL1* c.613_622 delATCATCTGCC

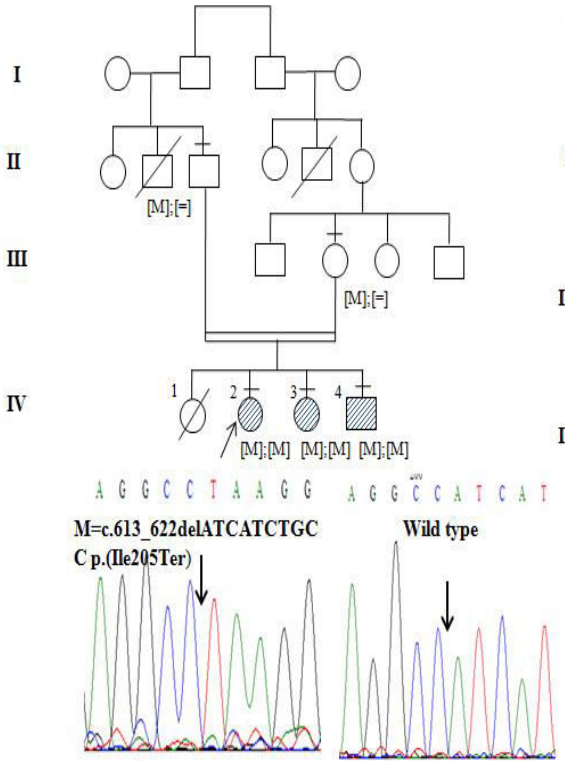

Fig 3.13 Fam-12 *SPATA7* c.913-2A>G

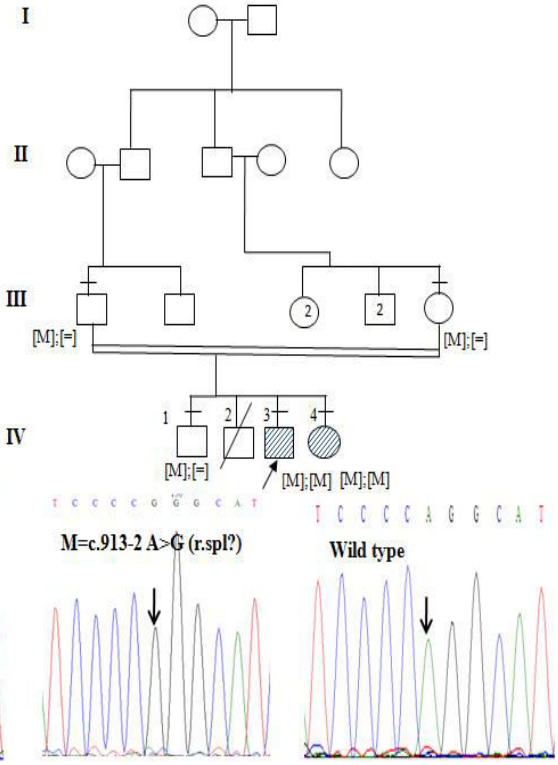

cDNA analysis: *IQCB1* is a ciliopathic gene and is also expressed in lymphocytes; cDNA analysis for the identified *IQCB1* intronic mutation was done for one of the affected and the carrier parents of the LCA family, Fam-05. cDNA amplified with specific primers encompassing exons 11-13, revealed a single transcript of 338bp in the affected, two transcripts of 338 and 487bp, respectively in the heterozygous carrier parents and a single transcript of 487bp in the normal control (Fig:3.14). The amplified products were sequenced. Direct sequencing revealed that in the proband, exon 12 has been completely deleted resulting in an amplicon of 338bp, both the parents were heterozygous carriers i.e in one allele exon 12 was completely deleted and in other allele exon 12 was present resulting in two amplicons of 338 and 487bp, respectively while in the normal control both the alleles had exon 12 (Figure 3.15). This skipping of exon 12 in the affected is predicted to result in a truncated protein, p.(Gln378AlafsTer2).

Fig: 3.14 2% Agarose gel electrophoresis showing cDNA amplification of exons 11-13 of *IQCB1:* Lane 1-100bp ladder, Lane 3-affected index case, Lane 5 and 7 - carrier parents, Lane 9 - control, Lane 2, 4, 6, 8 - empty wells

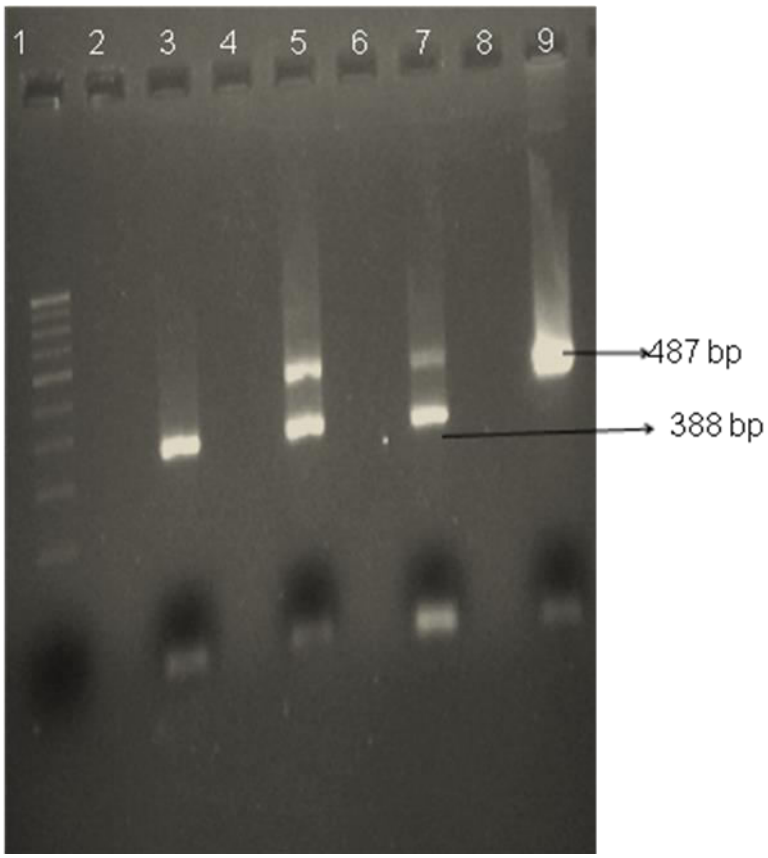

Fig: 3.15 Electrophoretogram trace showing the amplified cDNA of control and proband. In proband exon 11 is followed by exon 13 and exon 12 is completely deleted, whereas in control, exon 11, 12 and 13 is continuous. The end of exon 11 is marked in both the phoretograms.

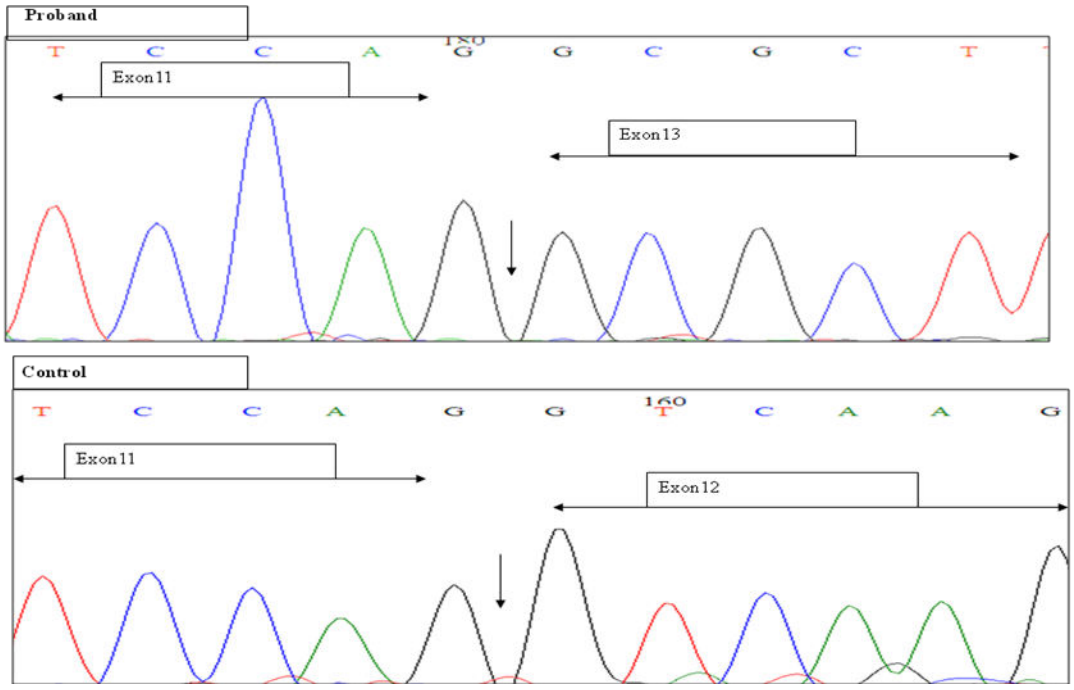

3.3 Homozygosity mapping using 250K GeneChip followed by targeted re-sequencing by NGS on three IRD families

Three consanguineous families with inherited retinal degenerative disease were studied. Fam-13 had LCA, Fam-14 had CRD and Fam-15 had arRP respectively. Totally seven individuals were taken; two, two and one affected individuals, from Fam-13, Fam-14 and Fam-15, respectively and two unaffected, one each from Fam-13 and Fam-14, respectively were genotyped using Affymetrix 250K Nsp1 HMA GeneChip.

Homozygosity mapping revealed known candidate genes for LCA, CRD and arRP that ranged from 1-8 in numbers within the homozygous blocks. Table 3.5 shows the known candidate genes within the homozygous blocks in the three families. In Fam-14 the shortlisted candidate gene *IQCB1* was screened by direct sequencing but no mutation was identified.

With the absence of mutation in *IQCB1* and more numbers of probable candidate genes in the other two families, targeted re-sequencing of the inherited retinal disease genes by NGS was taken up.

Table 3.5: Homozygous blocks with the known candidate genes in the three IRD families analysed

Family ID	Number of Affected individuals taken for analysis	Size of the homozygous block in which known candidate gene(s) were present (Mb)	Genes Present	Chromosome location	Gene Reference ID
Fam-13	2	8	*IQCB1*	3q13.3	NM_001023570.2
Fam-14	2	18	*LRAT*	4q32.1	NM_004744.4
		13	*RD3*	1q32.3	NM_183059.2
		8	*CNGA1*	4p12	NM_001142564.1
		6	*MERTK*	2q13	NM_006343.2
		1.5	*GPR125*	4p15.31	NM_145290.3
		1	*ABCA4*	1p22.1	NM_000350.2
		1	*NEK2*	1q32.3	NM_002497.3
		1	*RDH12*	14q24.1	NM_152443.2
Fam-15	1	40	*RP1*	8q12.1	NM_006269.1
			TTPA	8q12.3	NM_000370.3
		7	*CDHR1*	10q23.1	NM_033100.3
			RGR	10q23.1	NM_002921.3
		2	*PDE6G*	17q25.3	NM_002602.3
		1	*ABCA4*	1p22.1	NM_000350.2

NGS analysis identified three novel mutations; *RDH12* c.832A>C p.(Ser278Arg), *ABCA4* c.1462G>T p.(Glu488Ter) and *CDHR1* c.1384_1392delCTCCTGGACinsG p. (Leu462AspfsTer1) in the LCA (Fam-13), CRD (Fam-14) and arRP (Fam-15) family, respectively (Table 3.6). The identified mutations were validated by direct sequencing, also segregated with the disease in the families and were absent in the 200 control chromosomes screened (Fig 3.4 - 3.13). These genes were in the homozygous blocks identified by homozygosity mapping for Fam-14 and Fam-15.

Table 3.6: Mutations identified in IRD families

Family ID	**Diagnosis**	**Gene**	**Exon/ intron**	**Mutation identified (in homozygous state)**	**Predicted change in protein**	**Effect of identified sequence variation**
Fam-13	LCA	*RDH12*	Exon 6	c.832A>C **Novel**	p.(Ser278Arg)	Likely pathogenic
Fam-14	arCRD	*ABCA4*	Exon 11	c.1462G>T **Novel**	p.(Glu488Ter)	Pathogenic
Fam-15	arRP	*CDHR1*	Exon 13	c.1384_1392delCTCCTGGACinsG **Novel**	p.(Leu462AspfsTer1)	Pathogenic

Fig: 3.16 - 3.18 Segregation analysis

Fig 3.16: Fam-13 *RDH12* c.832A>C, 3.17: Fam-14 *ABCA4* c.1462G>T, 3.18: Fam-15 *CDHR1* c.1384_1392delCTCCTGGACinsG.

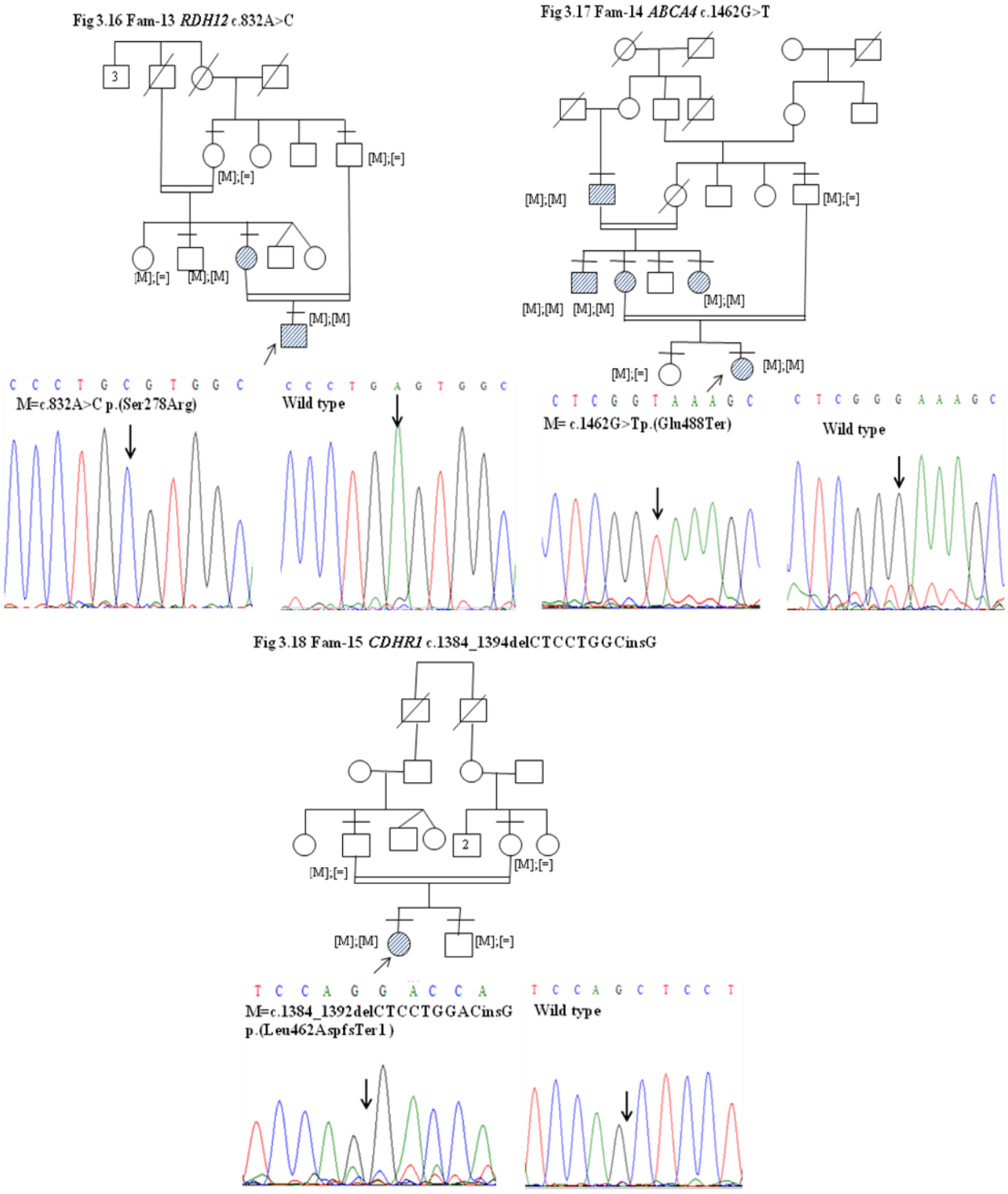

Whereas for Fam-13 the homozygous block encompassing *RDH12* was present in the two affected individuals (the index case and the affected mother) and was 23.9Mb in size and also in the unaffected maternal uncle of about 1.8cM (spanning the *RDH12* gene). Hence we did not screen *RDH12* gene in this family, but screened the other candidate gene, *IQCB1* and did not identify any mutation. Following the NGS results and to validate our homozygosity mapping data, we genotyped by direct sequencing the SNPs that spanned the *RDH12* gene present in the GeneChip and also the entire coding region of the gene. We genotyped the two affected; the index case (IV-1) and his mother (III-3); three unaffected; the index cases' father (II-2), maternal uncle (III-2), maternal grandmother (III-1). All members were homozygous for all the SNPs in the coding region and for the five SNPs that represent the *RDH12* gene in the GeneChip except for the unaffected father (II-2) whose was heterozygous for the SNP at 5'UTR (Fig 3.19).

Fig: 3.19 The zygosity and segregation of the SNPs that are probed in the GeneChip across *RDH12* gene and confirmed by direct sequencing.

The segregation of the SNPs explains the presence of homozygous block (analysed by LOH status in comparison with the affected individuals using Affymetrix 250K Nsp1 HMA array) encompassing the *RDH12* gene in the unaffected maternal uncle.

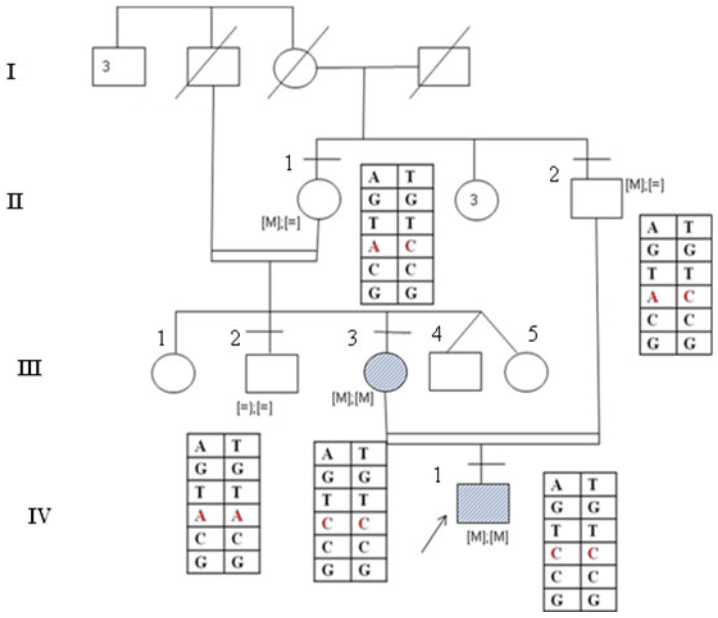

Variants of unknown significance identified from NGS

We had also identified variations of unknown significance (VUS) in Fam-13 – Fam-15 while performing the NGS analysis. Validation and segeregation for the same was performed in two of the three families to know if there was any modifier effect as shown in Table 3.7. In Fam-13, apart from the pathogenic mutation identified in *RDH12*, a heterozygous variant c.1928T>G p.(Val643Gly) was identified in exon13 of *ABCA4*. The variation was present in the heterozygous state in both the affected individuals. For Fam-14, few variations of unknown significance in *ZNF513, ROM1, OPA1, HMCN1* were observed but validation and segregation analysis was not performed for these. In Fam-15, a novel heterozygous missense variation in *MERTK* c.20C>T p.(Pro7Leu) and reported variation in *ARL6* p.(A161S) were present in the heterozygous state in the only affected proband.

Table 3.7: Segregation analysis performed for variations of unknown significance

ID	**Relationship to the Proband**	**Affected status**	***ABCA4* *c*.1928T>G p.(Val643Gly)**	
Fam-13	Proband	Affected	Heterozygous	
	Mother	Affected	Heterozygous	
	Father	Unaffected	Heterozygous	
	Maternal uncle	Unaffected	Heterozygous	
	Grandmother	Unaffected	Heterozygous	
			***MERTK* c.20C>T p.(Pro7Leu)**	***ARL6* c.481G>T p.(Ala161Ser)**
Fam-15	Proband	Affected	Heterozygous	Heterozygous
	Sibling	Unaffected	Heterozygous	Wild type
	Mother	Unaffected	Wild type	Wild type
	Father	Unaffected	Heterozygous	Heterozygous

3.4 Bioinformatics Analyses: We had checked all the identified nine novel variations in the following databases ENSEMBL, dbSNP, Clin Var, Human Genome Mutation Database (HGMD), 1000 Genomes database, Exome Variant Server (EVS) database and the Exome Aggregation Consortium (ExAC). None of them were reported in the above mentioned databases.

The four intronic mutations identified in the LCA families, which are present either in the conserved splice acceptor or donor site or within ten bases of the intron following the exon were analysed using the human splice finder (HSF 2.4.1) (Table 3.8). As the ΔCV is less than 10%, mutation is predicted to break the splice site.

These intronic mutations were also analysed with Mutation Taster (Table 3.9). The wild type and mutant is scored and a confidence score of >0.3 for the mutant indicates gain of completely new splice-site. In LCA families, Fam-05, 08 and 12 the mutation is predicted to change the splicing, i.e. activating cryptic splice site, affecting protein features, however, for the Fam-02, there was no score given and it was predicated that the mutation would disturb normal splicing as the sequence motif is lost.

The three missense mutations, *CRB1* c.3307G>A p.(Gly1103Arg), *AIPL1* c.247G>A p.(Glu83Lys) and *RDH12* c.832A>C p.(Ser278Arg) were analyzed with PolyPhen 2, SIFT, Mutation Taster, Mutation Assessor, pMUT and Mutpred (Table 3.10). In addition we also checked for the conservation of the amino acid residue among the 46 vertebrates using UCSC Genome Browser (Fig.3.20 - 3.22). *CRB1* mutation (p.(Gly1103Arg) in Fam 03), the glycine residue is conserved among 36 vertebrates (not in Angaroo-rat, Microbat, Shrew, Cat, Armadillo, Fugu, Stickleback, Medaka, Zebrafish, and Lamprey). In Fam-09 with *AIPL1* mutation (p.(Glu83Lys)) the glutamic acid residue is conserved among 34 vertebrates and not in 12 vertebrates (such as Gorilla, Tree-Shrew, Angaroo-rat, Squirrel, Cat, Microbat, Hedgehog, Armadillo, Sloth, Chicken, Zebrafinch and Lizard). For the Fam-13 with *RDH12* mutation (p.(Ser278Arg)), the serine residue is conserved among 39 vertebrates while not conserved among Tree-shrew, Cat, Rock-hyrax, Chicken, Zebra-finch, X.tropicalis and Lamphrey.

Table 3.8: Probable effects of splice-site mutations using HSF 2.4.1

S.No	Family ID	Gene	Mutation identified	Wild type consensous value (CV)	Mutant consensous value (CV)	△CV (%)	cDNA Analysis
1.	Fam-02	*RPE65*	c.850+1G>T	-	-	**-**	**Not done**
2.	Fam-05	*IQCB1*	c.1278+6T>A	79.28	75.78	-4.42	r.[1131_1278del,1131_1278del] **Exon12 skipping**
3.	Fam-08	*RDH12*	c.344-8C>T	73.62	70.25	-4.57	**Not done**
4.	Fam-12	*SPATA7*	c.913-2A>G	86.72	57.09	Site broken	**Not done**

Table 3.9: Probabale effects of splice-site mutations using *in silico* tool Mutation taster

S.No	Family ID	Gene	Mutation identified	Wild type scoring	Mutant scoring	Splice site change	Prediction
1.	Fam-02	*RPE65*	c.850+1G>T	-	**-**	Likely to disturb normal splicing, sequence motif lost	Splice site changes; Protein features might be affected
2.	Fam-05	*IQCB1*	c.1278+6T>A	0.36	0.95	Donor increased	
3.	Fam-08	*RDH12*	c.344-8C>T	0.55	0.76	Acceptor increased	
4.	Fam-12	*SPATA7*	c.913-2A>G	0.53	0.84	Acceptor increased	

Table 3.10 Predicted probable effect of missense mutations using insilico tools.

Family ID	Gene	Mutation	PolyPhen-2		SIFT		Mutation Taster (MT)		Mutation Assessor		PMut		MutPred		
			score	Predicted effect	score	Predicted effect	score	Prediction	Functional Impact score (FIS)	Functional Impact	Neural Network (NN) score	Prediction	General score (g)	Property score (p)	Molecular Mechanism disrupted
Fam-03	*CRB1*	c.3307G>A	0.91	Possibly Damaging	0	Damaging	125	Disease causing	3.2	Medium	-	-	0.837	0.1297	-
Fam-09	*AIPL1*	c.247G>A	1.0	Possibly Damaging	0	Damaging	56	Disease causing	1.96	Medium	-	-	0.784	0.023	Confident hypothesis
Fam-13	*RDH12*	c.832A>C	0.955	Possibly Damaging	0	Damaging	110	Disease causing	2.8	Medium	0.4117	Neutral	0.527	0.0171	Actionable hypothesis

We used 5 bioinformatic tools for analyzing the missense mutation *CRB1* p.(Gly1103Arg) and *AIPL1* (p.(Glu83Lys) in Fam-03 and Fam-09, respectively. Four tools predicted the variation to be damaging/disease causing for the *CRB1* p.(Gly991Arg) and five tools predicted the *AIPL1* p.(Glu83Lys) variation to be damaging/disease causing. The *RDH12* mutation p.(Ser278Arg) was analysed with six tools and five of them predicted it to be damaging/disease causing.

Figure: 3.20-3.22 Amino acid sequence alignment across 46 vertebrates for the three missense variations; *CRB1* p.(Gly1103Arg), *AIPL1* p.(Glu83Lys) and *RDH12* p.(Ser278Arg).

Fig: 3.20 Fam-03 *CRB1* c.3307G>A p.(Gly1103Arg)

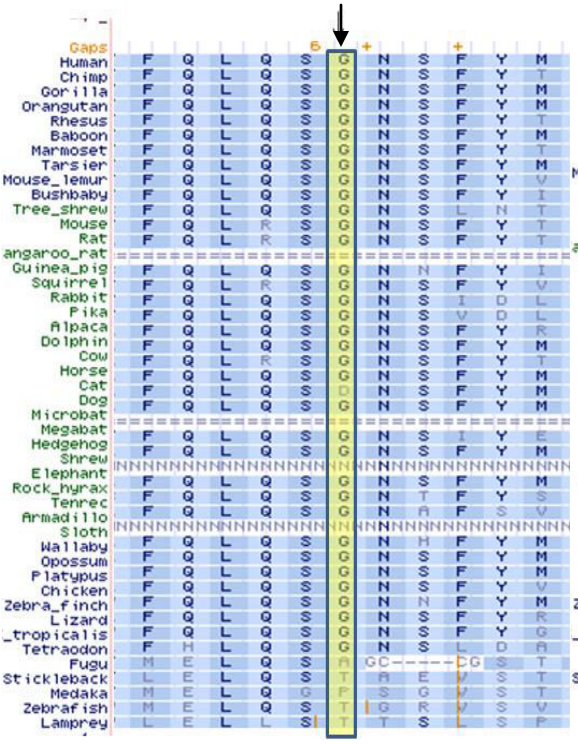

Fig:3.21 Fam-09 *AIPL1* c.247G>A p.(Glu83Lys)

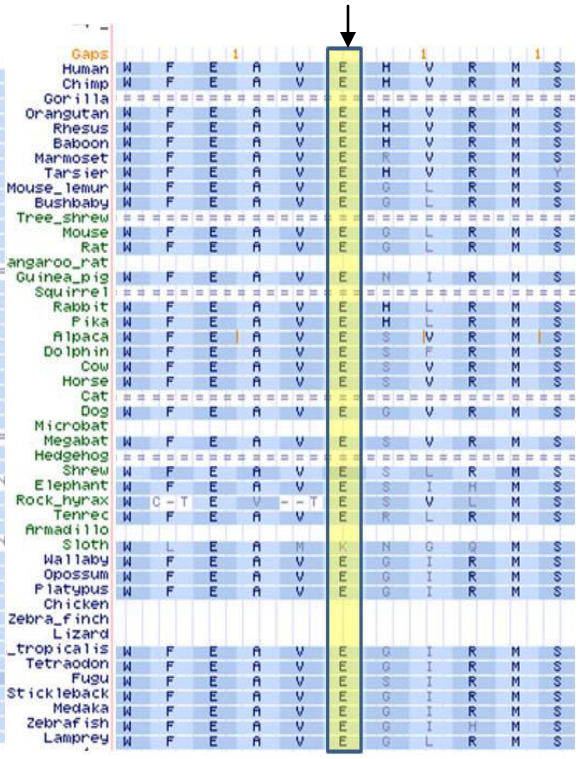

Fig:3.22 Fam-13 *RDH12* c.832A>C p.(Ser278Arg)

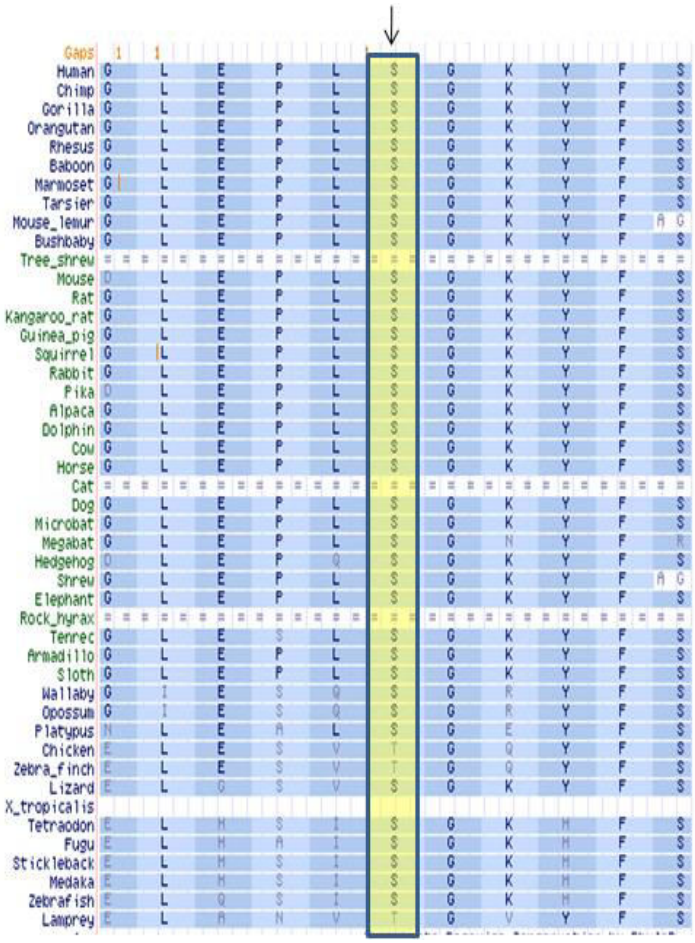

3.5 Phenotype – Genotype correlation

3.5.1 Phenotype-Genotype correlation of the LCA families from the study

We identified mutations in eleven of the twelve LCA families screened, three families with *AIPL1,* two families each with *RPE65* and *RDH12* and one family each with, *CRB1, GUCY2D, IQCB1* and *SPATA7*.

Patients with *AIPL1* mutations: In the three families, three different types of mutations were observed, a reported nonsense mutation, c.834G>A p.(Trp278Ter) in family Fam-06, a novel missense mutation, c.247G>A p.(Glu83Lys) in family Fam-09 and a novel 10-base pair deletion, c.613_622delATCATCTGCC p.(Ile205Ter) in family Fam-11.
In Fam-06, both the affected siblings had normal disc, and mildly attenuated vessels. Yellowish atrophic patches were seen in the macular area in the younger sibling (10 yrs) (Fig.3.23), while the elder sibling (14yrs) had atrophic macula with black pigments (Fig.3.24). Both the siblings had salt and pepper fundus with bony spicules. Additionally other than the ophthalmic findings both the children had delayed milestones, of which the elder sibling along with the delayed milestones had speech delay, involuntary movements and mental retardation. In Fam-09, there was only one affected person phenotyped for fundus features at the age of 5 years, had normal disc, mildly attenuated vessels, and atrophic macula with peripheral RPE granularity. The other non-ophthalmic abnormality was; the patient had cleft palate. In Fam-11, the three affected siblings also had atrophic macular degeneration with bony spicules, attenuated vessels, all seen in their third decade of life. The cases in the genotyped families revealed three different mutations but were similar phenotypically with severity of the retinal changes increasing with age reflecting the progressive nature of the disease and macular degeneration being a characteristic feature in *AILP1* mutation positive LCA cases.

***RPE65*:** In two families, we identified *RPE65* mutation, a reported splice-site mutation, c.858+1G>T (r.spl?) in Fam-02 and a reported missense mutation, c.1409C>T p.(Pro470Leu) in family Fam-10. In Fam-02, both the affected siblings phenotyped in their second decade had pale disc with attenuated vessels, salt and pepper fundus with peripheral RPE mottling. The elder sibling also revealed macular scarring (Fig.3.25) and the younger sibling had very few early alterations in the macula. In Fam-10, all the three affected siblings phenotyped in their third decade had pale disc, attenuated vessels, normal macula with salt and pepper appearance in the periphery.

In both the families affected individuals had profound visual loss. The eldest sibling (28yrs) of Fam-10 also showed presence of distinct pin head sized white spots at the posterior pole (Fig.3.26).

RDH12: Fam-08 had a novel possible pathogenic variant in *RDH12*, c.344-8C>T (r.spl?). The two affected siblings, one aged 26yrs and other 10yrs showed normal disc, attenuated arteriolar vessels, and macula revealed small horizontal oval area (bull's eye like lesion) along with metallic sheen in the background. Atrophic changes in the macula were seen in the first decade itself in the younger sibling. In Fam-13 the affected proband and his mother had a novel missense possibly pathogenic mutation, c.832A>C p.(Ser278Arg). The affected mother (40yrs) (Fig: 3.30) had pale disc and attenuated vessels with early macular RPE atrophy, extensive widespread bony spicule pigment in the periphery. The (Fig: 3.31) proband (20yrs) showed pale disc, attenuated vessels with prominent petal like macular coloboma with sloping sides and plenty of peripheral pigmentation.

***CRB1*:** In family Fam-03 with four affected members, a reported missense mutation, c.2971G>A p.(Gly991Arg) was identified in *CRB1*. All the four affected members in their second decade had profound visual loss and all had a typical fundus picture of pale disc, para-arteriolar preservation of the retinal pigment epithelium (PPRPE), and atrophic macula with nummular pigment clumps and greyish atrophic reflex along with coin shaped pigment clumps seen at the background (Fig: 3.27 - 3.29).

***GUCY2D*:** In family Fam-04 with two affected members, a novel frameshift mutation, c.994delC p.(Arg332AlafsTer63) was observed in *GUCY2D*. Both the siblings in their late teenage had profound visual loss and showed fundus picture of pale disc, minimal arteriolar attenuation and normal looking macula (Fig 3.32). The elder sibling had speech impairment in addition to the visual loss.

***IQCB1*:** A novel *IQCB1* splice mutation, c.1278+6T>A r.[1131_1278 del,1131_1278del] p.(Gln378Alafs*2) was seen in Fam-05. The two affected siblings showed pale disc, attenuated vessels, normal macula and plenty of hypo-pigmented lesion, tapetal reflex was seen at the background in the elder sibling (30y) (Fig 3.33), whereas the younger sibling (24yrs) had little hypo-pigmentation. The elder sibling had both kidneys failure at 31yrs but the younger sibling did not report of any kidney failure until 27yrs. As renal failure is observed along with LCA, the case is now re-diagnosed as Senior-Loken syndrome.

SPATA7: A novel spice-site mutation, c.913-2A>G (r.spl?) was seen in Fam-12, with two affected siblings aged 8yrs and 2yrs. Fundus picture of both the siblings revealed presence of mild disc pallor, arteriolar attenuation and peripheral RPE mottling (Fig 3.34).

Figure: 3.23 - 3.34 Fundus photographs of probands from LCA families, Fam-02-Fam-13 with mutations identified.

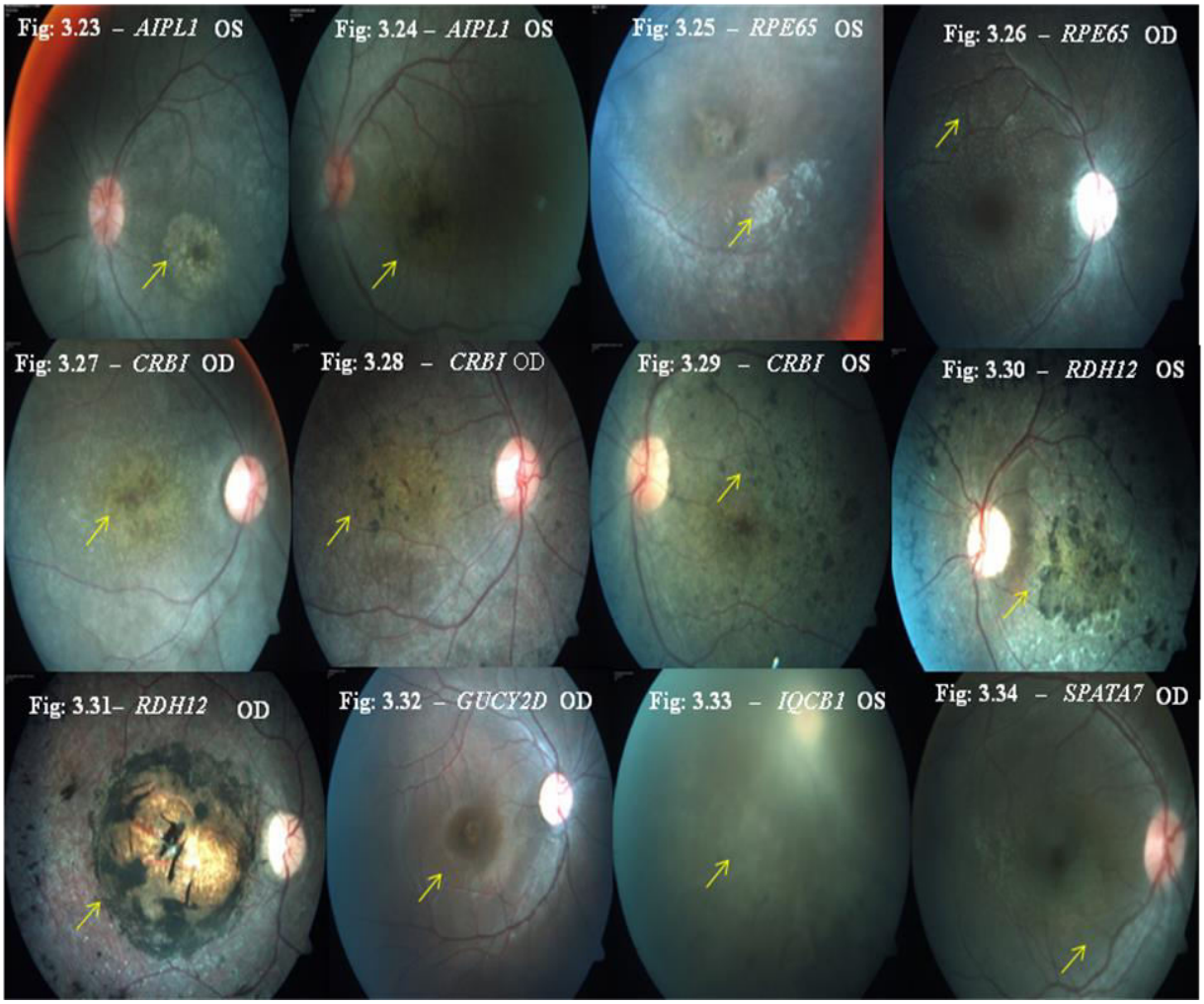

Figure 3.23: A 10yrs old female with c.824G>A p.(Trp278Ter) mutation in *AIPL1* (Fam-06) showed normal disc, attenuated vessels, yellow patches in macula.

Figure 3.24: A 14yrs old male with c.824G>A p.(Trp278Ter) mutation in *AIPL1* (Fam-06, proband's brother) showed normal disc, attenuated vessels, black pigments in macula.

Figure 3.25: A 18 yrs old female with c.850+1G>T (r.spl?) mutation in *RPE65* (Fam-02) showed pallor disc, attenuated vessels with scar in the macula, peripheral RPE mottling.

Figure 3.26: A 28yrs old male with c.1409C>T p.(Pro470Leu) mutation in *RPE65* (Fam-10 proband) showed pallor disc, attenuated vessels, normal macula, with salt and pepper fundus. Arrow mark shows distinct pin head size yellow white dot like spots at the posterior pole.

Figure 3.27: A 14 yrs old male with c.2971G>A p.(Gly991Arg) mutation in *CRB1* (Fam-03 proband) showed coin shaped pigment clumps and greyish atrophic changes seen in the macula, (arrow mark indicates the macula).

Figure 3.28: A 18 yrs old male with c.2971G>A p.(Gly991Arg) mutation in *CRB1* (Fam-03, proband's brother) showed pale disc, attenuated vessels, atrophic macula with nummular pigment clumps and greyish atrophic reflex (arrow mark indicates the macula).

Figure 3.29: A 19yrs old male with c.2971G>A p.(Gly991Arg) mutation in *CRB1* (Fam-03, proband's brother) showed coin shaped pigment clumps seen in the background (arrow mark indicates the coin shaped clumps). All the three affected siblings with *CRB1* mutation show progressive changes in macula with age.

Fig 3.30: A 40 year old female with c.832A>C p. (Ser278Arg) possible pathogenic mutation in *RDH12* (Fam-13 proband's mother) showed pale disc, attenuated vessels, early macular atrophy with wide spread bony spicule pigment in the periphery (arrow mark indicates the atrophic macula).

Fig 3.31: A 20 year old male with c.832A>C p.(Ser278Arg) possible pathogenic mutation in *RDH12* (Fam-13 proband) showed pale disc, attenuated vessels, prominent petal like macular coloboma with sloping sides and plenty of peripheral pigmentation (arrow mark indicates the macular coloboma).

Fig 3.32: A 19 year old male with c.994delC p.(Arg332AlafsTer63) mutation in *GUCY2D* (Fam-04 proband) showed pale disc, minimal arteriolar attenuation and normal looking macula (arrow mark indicates macula).

Fig: 3.33: A 34 year old female with c.1278+6T>A r. [1131_1278 del,1131_1278del] p. (Gln378AlafsTer2) mutation in *IQCB1* (Fam-05 proband) showed pale disc, attenuated

vessels, normal macula and plenty of hypo-pigmented lesion, tapetal reflex was seen at the background (arrow mark indicates the hypopigmented lesion).

Fig: 3.34: A 8 year old male with c.913-2A>G (r.spl?) mutation in *SPATA7* (Fam-12 proband) showed mild disc pallor, arteriolar attenuation and peripheral RPE mottling (arrow mark indicates the RPE mottling).

3.5.2 Phenotype features of arRP families

MERTK: In Fam-01 with arRP and mutation in *MERTK* c.721C>T p.(Gln241Ter) there were three affected siblings, two were in their second decade of life and the eldest sister was in her third decade of life. Fundus picture revealed pallor disc, marked attenuated vessels, atrophic macula, bone spicule pigment and widespread RPE atrophy. This family is marked by a progressive change in the fundus (Fig.3.35 - 3.37). ERG findings were non-recordable scotopic and photopic response for all the three affected siblings.

CDHR1: In case of Fam-15, a novel indel was identifed in *CDHR1,* c.1384_1392delCTCCTGGACinsG p.(Leu462AspfsTer1). ERG findings were non-recordable scotopic and photopic response. The (Fig:3.38) proband (27yrs) showed pale disc, attenuated vessels with atrophic macula and yellowish spots in the periphery.

Figure: 3.35 - 3.38 Fundus photographs of Fam-01 and Fam-15

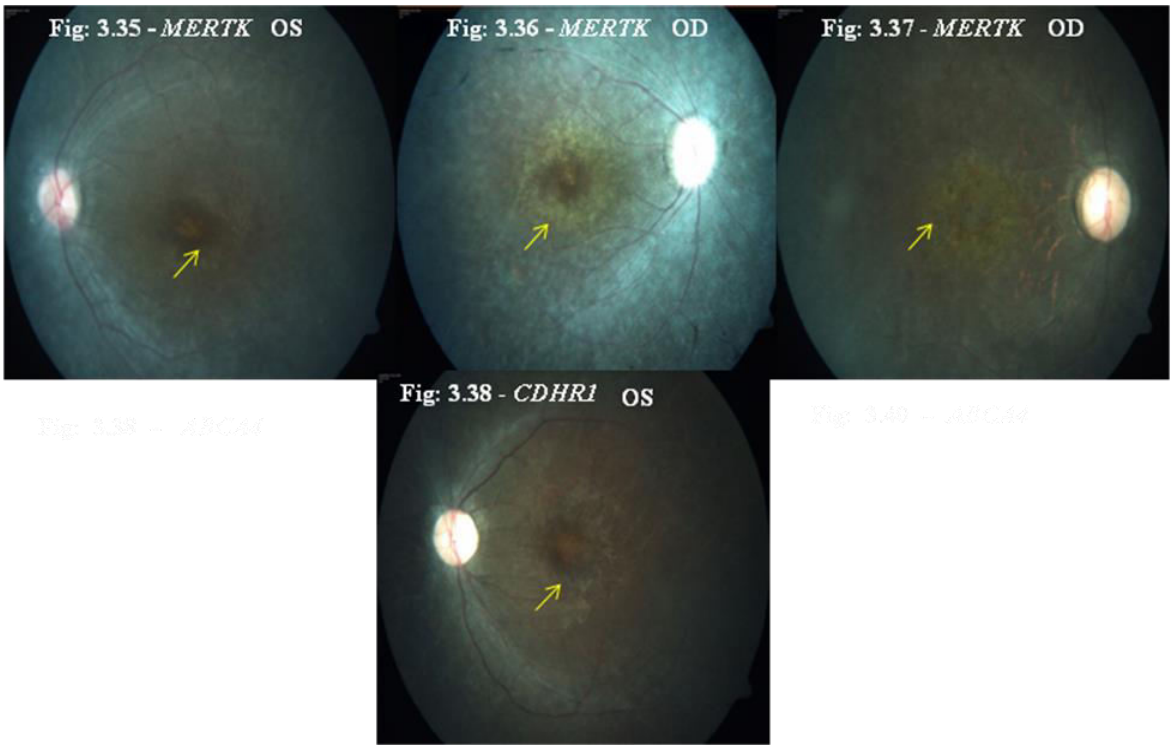

Figure 3.35: A 24 yrs old female with c.721C>T p.(Gln241Ter) mutation in *MERTK* (Fam-01) showed mild features of RP (arrow mark indicates the macula).

Figure 3.36: A 25 yrs old female with c.721C>T p.(Gln241Ter) mutation in *MERTK* (Fam-01, proband's sister) showed milder features of RP (arrow mark indicates the macula).

Figure 3.37: A 32 yrs old female with c.721C>T p.(Gln241Ter) mutation in *MERTK* (Fam-01, proband's eldest sister) showed marked features of RP. Progressive changes with age in the macula are observed (arrow mark indicates the macula).

Fig 3.38: A 27 year old female with c.1384_1392delCTCCTGGACinsG p.(Leu462AspfsTer1) in *CDHR1* (Fam-15) showed disc palor, arteriolar attenuation, atrophic macula with yellowish spots in the periphery (arrow mark indicates atrophic macula with yellowish spots).

3.5.3 Phenotype features of arCRD family

***ABCA4*:** In this CRDfamily, all the five affected individuals had novel *ABCA4* nonsense mutation c.1462G>T p.(Glu488Ter). All five patients had a profound visual loss with difficulty in night vision. The proband (15yrs) had well delineated RPE atrophy and pigment dispersal at the posterior pole (Fig 3.39). The proband's mother (40yrs) had extensive RPE atrophy and widespread pigment dispersal (Fig 3.40). ERG of the proband and mother (Fig 3.41, 3.42) showed progressive decrease in the amplitudes of photopic and scotopic response. Proband's grandfather (67yrs) and maternal uncle (41yrs) also had a picture of advanced disease with extinguished ERG. Since the photopic responses were reduced first (as seen in the proband) and the scotopic responses were found to be extinguished in older members of the family, a diagnosis of progressive arCRD was made. ERG pictures of the proband 15yrs (Fig:3.41) and proband's mother 40yrs (Fig:3.42) showed progressive decrease in the amplitudes of photopic and scotopic response.

Figure: 3.39 - 3.40 Montage fundus photographs of Fam-14 and ERG Trace pictures (Figure 3.41 - 3.42)

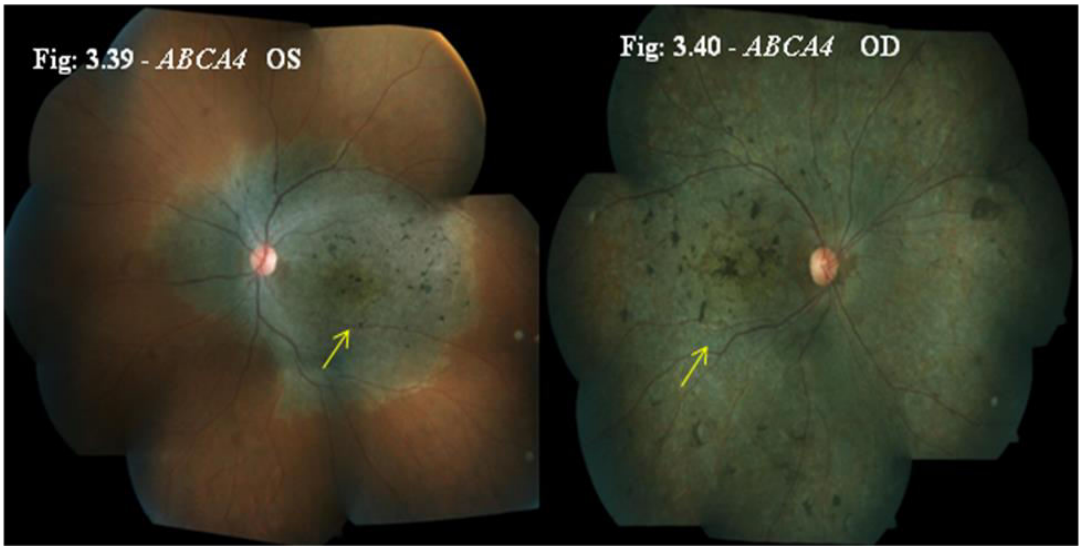

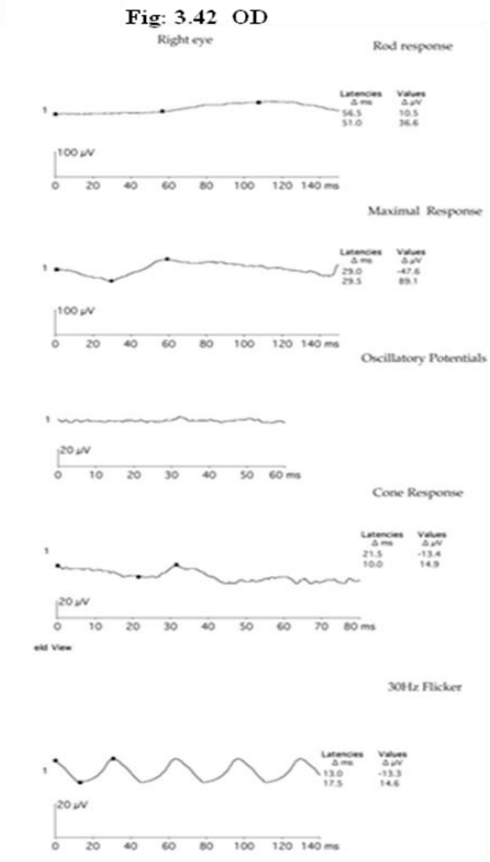

Fig: 3.39 A 15 year old female with c.1462G>T p.(Glu488Ter) mutation in *ABCA4* (Fam 14, Fundus montage of the left eye in proband) showed well delineated RPE atrophy and pigment dispersal at the posterior pole (arrow mark indicates the pigment dispersal).

Fig: 3.40 A 40 year old female with c.1462G>T p.(Glu488Ter) mutation in *ABCA4* (Fam 14, Fundus montage of the right eye in proband's mother) showed extensive RPE atrophy and widespread pigment dispersal (arrow mark indicates the widespread pigment).

Fig: 3.41 and 3.42 ERG pictures of the proband 15yrs (3.41) and proband's mother 40yrs (3.42) showed progressive decrease in the amplitudes of photopic and scotopic response.

Fig: 3.43 Genes identified as causative in the families studied and their functions in visual and phototransduction pathways, morphogenesis in retina

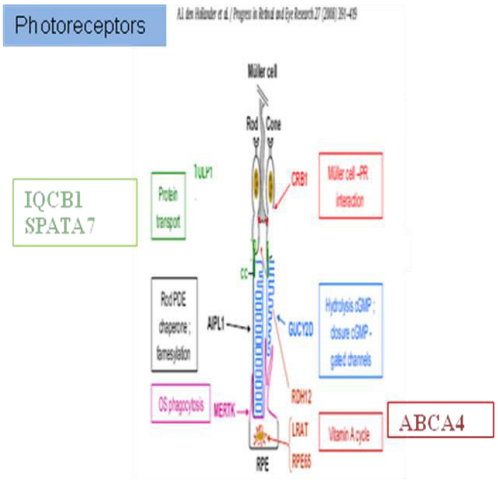

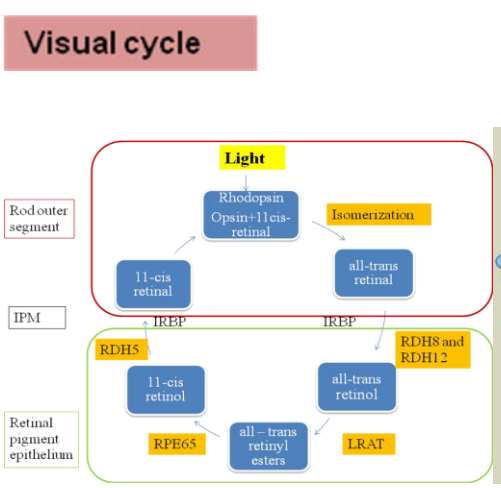

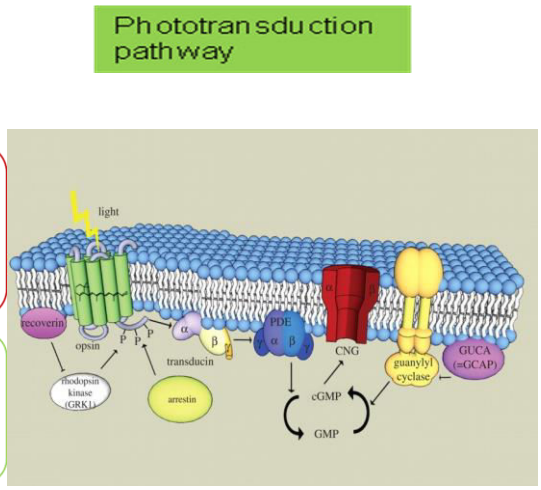

CHAPTER 4

Discussion

We have taken twelve LCA, two arRP and one arCRD families for homozygosity mapping and further analysis to identify the disease causative gene and mutation. We identified the causative mutation in fourteen out of fifteen families (93%). We also identified mutations in ten different genes in the LCA families studied; *AIPL1* in three families, *RPE65* in two families, *RDH12* in two families, *CRB1, GUCY2D*, *IQCB1*, *SPATA7* in one family each. In two arRP families, causative mutations were identified in *MERTK*, and *CDHR1*. *ABCA4* was identified in the arCRD family. Of the fourteen pathogenic or likely pathogenic mutations, ten are novel (71%). The discussion chapter is divided under three subheadings, Chapter 4.1 includes discussion on homozygosity mapping using 250K and 10K HMA array for eleven LCA and one arRP families, respectively. Chapter 4.2 includes homozygosity mapping followed by NGS analysis in each of LCA, arCRD and arRP families. Chapter 4.3 includes discussion on the phenotype-genotype features from the study.

Chapter 4.1

Homozygosity mapping using 250K HMA GeneChip in eleven LCA and one arRP families

In our study, of eleven consanguineous LCA families analyzed by homozygosity mapping followed by candidate gene screening, we identified the causative mutations in ten (90%). Also we identified the causative gene and mutation in one arRP family studied. Homozygosity mapping involves detecting the disease loci by exploiting the fact that the adjacent region i.e. short chromosomal segments surrounding the homozygous mutation had not been crossed over and hence the surrounding markers, i.e. the single nucleotide polymorphism (SNP) and STR would also be in a homozygous state as these regions would be inherited by descent (Identical by descent) from a common ancestor [64].

In our study, the significant homozygous blocks were in the average size from 1Mb to about 33Mb, differing for each family and harboring the candidate LCA gene(s). Also, when more number of affected members was genotyped, the number of homozygous blocks shared among the affected was less, enabling easier identification of the candidate locus/gene.

Seven of the eleven mutations identified are novel. There are six novel mutations in six LCA families and one novel mutation in the arRP family in this study; *AIPL1*-2 mutations, and one each in *GUCY2D*, *IQCB1, RDH12, SPATA7,* and *MERTK* (in arRP family). Of the ten mutations identified in the eleven LCA families, two are splice-site mutations, one each in *RPE65* and *SPATA7,* two intronic mutations within 10bp of the intron in *IQCB1* and *RDH12,* respectively, three missense, one nonsense and two deletion mutations resulting in frameshift. The three missense mutations, *CRB1* c.3307G>A p.(Gly1103Arg), *AIPL1* c.247G>A p.(Glu83Lys) and *RDH12* c.832A>C p.(Ser278Arg) were analyzed with PolyPhen 2, SIFT, Mutation Taster, Mutation Assessor, pMUT and Mutpred. All the three mutations were predicted to be possibly damaging, damaging, disease causing by PolyPhen 2, SIFT, Mutation Taster, respectively and Mutation Assessor predicted the Functional Impact to be medium for altering the function of the protein. As per the Mutpred score, for *AIPL1* c.247G>A, a confident hypothesis was predicted where the amino acid substitution is deleterious based on the g value, and certain structural and functional properties to be impacted based on the p value. In case of *RDH12* c.832A>C, an actionable hypothesis was predicted where the amino acid substitution is probably deleterious and certain structural and functional properties also might be affected. However for the *CRB1* c.3307G>A missense mutation, no hypothesis was predicted as the g value score was 0.837 (>0.75) predicting the amino acid change to be deleterious, but the p value score was 0.1297 (and not < 0.05) and thus the structure and functional impact was not predicted.

The splice-site mutations analyzed with bioinformatics tools, HSF2.4.1 and Mutation taster 2 were predicted to result in loss of splicing, whereas the mutations within 10bp of the intron in *RDH12* and *IQCB1* were predicted to activate cryptic splice-site. We performed cDNA analysis for the *IQCB1* mutation, as this gene is expressed in lymphocytes as well. *IQCB1* gene encodes for nephrocystin protein which interacts with calmodulin and retinitis GTPase regulator protein. Defects in this gene are reported in Senior-Loken Syndrome type 5 [128]. Splice-site mutations in *IQCB1* have been previously reported in nephronophthisis patients and also in two LCA families [27, 129]. In a study done by Estrada-Cuzcano et al [130], eleven *IQCB1* mutations were identified in a cohort of 150 LCA patients. During revaluation, seven of the mutation positive cases were found to have developed renal complications, thus re-diagnosed to have Senior-Loken Syndrome, while rest of the four patients reported no kidney abnormalities but they had similar mutations found in nephronophthsis patients. In our cohort, the family Fam-05 with two affected siblings (sisters) was initially diagnosed with LCA and reported no renal abnormalities. However, when we recalled the family for cDNA analysis after identification of the mutation, the family reported that the proband, now 34 years had a sudden onset of renal failure (both the kidneys) at the age of 31 years and is under treatment. We could perform the cDNA analysis in the younger affected sibling and the carrier parents only, and till now the younger sibling (29y) has no renal complications. cDNA analysis confirmed that the mutation, c.1278+6T>A activates cryptic splice-site leading to complete skipping of exon 12 resulting in a predicted truncated protein p.(Gln378AlafsTer2). *IQCB1* mutation positive LCA patients may be at risk of developing renal abnormalities, however the onset of the renal failure is highly variable [130] and need to be counseled and managed appropriately. cDNA analysis for *RDH12,* c.344-8C>T mutation could not be done because the gene is not expressed in lymphocytes and has exclusive retinal expression.

However, we consider this to be a likely pathogenic variant which might be causative for the disease phenotype; a) through homozygosity mapping we identified two large homozygous blocks spanning about 6Mb and 1.3 Mb containing two known LCA candidate genes, the larger block had *RPGRIP1* and the smaller block had *RDH12*. Firstly, screening *RPGRIP1* did not reveal any pathogenic variant, hence it was followed by screening *RDH12*, where we found the intronic variant, c.344-8C>T, which segregated with disease phenotype in the family and was absent in 200 control chromosomes screened. b) *in-silco* analysis predicted the variant to activate the cryptic splice-site affecting/altering the protein and c) phenotypically the fundus of both the affected sibs too showed maculopathy in the first decade of life, a feature previously observed in *RDH12* mutation positive cases [131].

Mutation negative family: In one family (Fam-07) we were unable to identify the causative gene/mutation in the known LCA candidate gene(s); there were two homozygous blocks with known LCA genes, *RPGRIP1* and *MERTK*. These two did not harbor any pathogenic mutation, however there are fourteen other homozygous blocks shared between the affected and ranging in size from 1-7Mb with no known LCA candidate genes. There was an autosomal recessive RP candidate gene *IMPG2* present in a homozygous block of about 0.6Mb in size. The gene at chromosome 3q12.3 contains 19 exons, we did not screen the gene due to non-availability of primers. Homozygosity mapping has revealed many homozygous blocks and the causative gene/mutation may either be a novel gene or a gene involved in other retinal disease and is most likely to be present in one of these blocks. We have however not screened the intronic and regulatory regions of the known candidate gene(s) in the family and hence cannot rule out the possibility of deep intronic mutations or mutations in regulatory regions that might be pathogenic. Nevertheless, homozygosity mapping has helped in indicating possible novel disease locus.

4.2 Homozygosity mapping followed by NGS

Three consanguineous families diagnosed with LCA, arCRD and arRP; Fam-13, Fam-14 and Fam-15 were analysed by homozygosity mapping followed by targeted gene screening using NGS to identify the causative mutation. We have identified the causative gene and mutation in all. Homozygosity mapping using 250K HMA GeneChip was done for all the three families, and in each family the number of known candidate genes present within the homozygous blocks ranged from 1-8 and the blocks were about 1-40Mb in size. Following homozygosity mapping, targeted re-sequencing on NGS for retinal gene panel was performed in the proband of all the families for rapid identification of the causative gene/mutation. The causative mutations identified by NGS were present in the gene within the homozygous blocks for Fam-14 and Fam-15.

In the Fam-13, totally 32 homozygous blocks were shared only between the affected with largest block being 23.9Mb and smallest 0.2Mb. An 8Mb block shared exclusively by the two affected, harbouring *IQCB1* gene was the only one with known LCA candidate gene. As screening of *IQCB1* did not identify any mutation, we proceeded with targeted NGS. Identification of novel mutation in *RDH12* in the proband and validation followed by segregation in the family confirming the NGS results lead us to re-analyze the homozygosity mapping data. The results explained the smaller homozygous block of 1.8Mb encompassing the *RDH12* gene in the unaffected maternal uncle. On an average 11% of genome of individuals with recessive disease and having first cousins as parents is homozygous with at least 20 homozygous blocks measuring >3cM. Also the number and runs of homozygosity is larger in consanguineous mating [67, 132]. Hildebrandt et al have demonstrated that homozygosity mapping with chip density of 250K can identify recessive disease genes in ~ 2 Mb regions even in an outbred population [64]. In this case (Fam-13) a higher density chip would have revealed closer regions of recombination which would have helped us pick *RDH12* for screening.

The identified novel missense mutation in *RDH12* c.832 A>C p.(Ser278Arg) segregated with the disease in the family, was absent in 200 control chromosomes, the serine residue at position 278 is conserved across most of the vetebrates and also five of the six *in silico* analyses predict the mutation to be damaging. However, *in vitro* functional analysis of the catalytic activity of the identified missense mutation would further confirm the pathogenicity of the mutation [133]. Phenotypically both the proband and mother had typical petal coloboma, a characteristic feature of *RDH12* mutation [134] and thus the novel missense mutation is defined as likely pathogenic.

In Fam-14 with novel nonsense mutation in *ABCA4* c.1462G>T p.(Glu488Ter), the younger members of this family showed preserved scotopic responses but the older members had a progressive decrease in the photopic as well as the scotopic response. Similar progression has been described in *ABCA4* mutations [45]. The phenotypic variability within the family could be due to progression with age [135] and modifying effects, either environmental or genetic or both [136].

In Fam-15 we had identified a novel indel in *CDHR1* c. 1384_1392delCTCCTGGACinsG p.(Leu462AspfsTer1). Mutations in *CDHR1* gene has been reported in autosomal recessive cone-rod dystrophy or retinal dystrophy and till date seven families have been decribed [47]. Here, for the first time we report *CDHR1* mutation in a case of arRP from India.

As mentioned VUS were observed in these families, some of which have been validated and checked for segregation. However, the phenotype or the severity did not specifically show any distinct feature that could be attributed to the modifier effect of the VUS and hence their contribution is not clear.

4.3 Identified mutations and the gene function

There were mutations identified in seven different genes namely *AIPL1, RDH12, RPE65, CRB1, GUCY2D, IQCB1, SPATA7* in LCA families, in *MERTK* and *CDHR1* in the two arRP families and in *ABCA4* in the autosomal recessive CRD family.

AIPL1: Aryl hydrocarbon - interacting receptor protein - like1 (OMIM: 604392), it is essential for the maintenance of rod photoreceptor function [137]. It is involved in nuclear transport or chaperone activity for rod phosphodiesterase (PDE) [28]. It is located at 17p13.1 region consisting of 4 exons [138]. The gene is responsible for the phenotype of autosomal recessive cone-rod dystrophy, autosomal recessive LCA, autosomal recessive juvenile RP, Mutation in *AIPL1* contributes to about 7% of LCA worldwide [137]. *AIPL1* expression is very specific to the human retina and restricted to the rod photoreceptor [139]. AIPL1 contains three tetratricopeptide repeat (TPR) domains [140]. The mutations are grouped into three classes. The class I are missense mutations in the N-terminal part of AIPL1, class II are missense mutations in TPR domain and non-sense mutation that lack one or more TPR domain, these are found to be associated with LCA [109]. Whereas class III mutation are deletion mutations located at the C-terminus of AIPL1 protein and are linked to autosomal recessive juvenile RP and cone-rod dystrophy [137, 141]. The identified reported p.(Trp278Ter) mutation resides in third TPR domain and thus categorized as class II mutation. Functional analyses have shown a markedly different secondary structure and thermal instability of this mutated protein [142]. The other identified novel mutations; p.(Glu83Lys) missense mutation in Fam-09 located at the N-terminal region belong to class I and p.(Ile205Ter) in Fam-11, located at the second TPR domain belong to class II type of mutation [142].

RDH12: Retinol Dehydrogenase 12 (OMIM: 608830) belongs to a family of dual specificity retinol dehydrogenases which metabolize both the all-trans and cis-retinols. The gene is located at 14q24.1 region containing 7 exons spanning 13kb [143] and mutation in *RDH12* contributes to about 4% of LCA [144]. *RDH12* is predominantly expressed in the eye but it is also expressed in kidney, brain, skeletal muscle and stomach. It consists of two motifs which are highly conserved among short chain alcohol dehydrogenase/reductases, the cofactor binding site and catalytic residues [143]. It consists of transmembrane domain at the N-terminus, phosphate-binding site and catalytic site [145]. In Fam-08 we had identified a novel intronic mutation in intron 3 and based on bioinformatics analyses using HSF and Mutation Taster, it was predicted to affect the splice-site and protein features. The novel missense possible pathogenic mutation at exon 6 in Fam-13, p.(Ser278Arg) lies at the catalytic domain which can disrupt the formation of the active site leading to loss of enzymatic activity [145], the bioinformatic tools too predicted it to be probably damaging, deleterious and disease causing.

RPE65: Retinal pigment epithelium-specific protein, 65-KD (OMIM: 180069), is an abundant protein in retinal pigment epithelium, with isomerohydrolase activity and critical for the regeneration of 11-cis retinol in the visual cycle. [146]. There are two forms of RPE65, a soluble form (sRPE65) and membrane form (mRPE65). The membrane form serves as the palmitoyl donor for lecithin retinyl transferase (LRAT), an enzyme required to cataylze the vitamin A to all-trans retinol and the soluble form serve as regulatory protein where the ratio and concentration play a very important role in the 11-cis retinal synthesis [147]. The gene contains 14 exons spanning about 20Kb located at 1p31.3-31.2 region.

The phenotype heterogeneity of the gene is immense; mutation in the gene is known to cause autosomal recessive LCA [148], autosomal recessive RP [149] and very rarely autosomal dominant RP [15]. The *RPE65* mutation contribute to about 3-16% of LCA in the western population [144]. In our study two mutations are identified in *RPE65*. A reported splice-site mutation, c.850+1G>T (r.spl?) in Fam-02, predicted to inactive splice-site resulting in a truncated protein or cause complete absence of the protein due to greatly reduced mRNA/protein stability [150]. The second mutation, also a reported missense mutation, c.1409C>T p.(Pro470Leu) at exon 13 in Fam-10 alters proline to leucine at codon 470 which is conserved across the six mammalian species. For this reported mutation the secondary structure prediction tool indicate decrease in stability of the mutant protein [151]. Human gene therapy trials for LCA with *RPE65* mutation began following the success of trails done in Briard dogs [83]. In 2007 the first human clinical phase I trial of AAV-mediated *RPE65* gene therapy treatment was started at three places simultaneously, Moorefields Eye Hospital, London [84], Children's Hospital of Philadelphia, Pennsylvania [85] and at University of Florida, Gainesville [86] to assess the effect and safety of gene transfer in humans. In 2013 results have been published reporting that there is substantial visual improvement in short term and there is no detectable decline in-spite of continued retinal degeneration at retinal site, where the therapy was not administered [89]. However, recent report reveal that, gene therapy vector improves retinal sensitivity in humans but temporarily and the amount of *RPE65* dose required varied between the species (dogs and humans) and hence higher dose might bring a durable and robust improvement [90].

CRB1: Crumbs, drosophila homolog of 1 (OMIM: 604210), is specifically expressed in the human retina and in the retinal pigment epithelium; and the gene is located in the region of 1q31.3 consisting 12 exons spanning of 40kb and yields two transcripts with the length of 1376 and 1406 amino acids, due to alternate splicing [152].

The crumbs protein mainly controls the position and integrity of photoreceptor adherens junction and the photosensitive organ in Drosophila [153] whereas CRB1 which is a homolog of crumbs in human is involved in maintaining the integrity of human retinal layers [154]. Mutation in this gene cause autosomal recessive LCA [155], autosomal recessive RP [152] and pigmented paravenous chorioretinal atrophy [156]. *CRB1* gene mutations cause about 9-13% of LCA [155, 157]. It consists of 19 Epidermal Growth factor (EGF) like domain, three laminin A globular (AG)-like domain and a signal peptide in the extracellular region of which some residues are conserved throughout the evolution. The first exon is untranslated, exons 2-6, 8-11 encode the 19 EGF like domains, while the first laminin AG-like domain is encoded by exon 6, second laminin AG-like domain by exon 6 and 7, and the third laminin AG-like domain by exon 9. The transmembrane and the cytoplasmic doimans are encoded by exon 12. [158]. The mutation p.(Gly1103Arg) found in Fam-03 in our study is present in exon 9 that encode laminin AG-like domain 3, the mutation at this domain is predicted to affect the protein-protein interaction, calcium binding and protein folding thus affecting retinal layer formation and function [158, 159].

GUCY2D: Guanylate cyclase 2D (OMIM: 600179), encodes for retinyl guanylate cyclase, a protein that plays an important role in phototransduction [160]. Human *GUCY2D* is located in the region of 17p13.1 and contains 20 exons spanning 16kb [161]. Mutations in *GUCY2D* gene may present with the phenotype of autosomal dominant cone-rod dystrophy [162], and autosomal recessive form of LCA [163]. It contributes to 6-21% of recessive LCA [164]. The gene encodes for a protein with extracellular, transmembrane and catalytic domains. It has been shown that mutations in catalytic domain result in marked reduction in cyclase activity whereas mutations in extracellular domain result in moderately reduced activity [165]. The identified novel mutation p.(Arg332AlafsTer63) resides in the extracellular domain [166] and is predicted to result in shifting of the reading frame leading to abrupt truncation of the protein with 393 aminoacids only instead of 1093 aminoacid residues.

It has been hypothesized that mutations in extracellular domain might result in misfolding of the mutant *retGC-1* protein during biosynthesis and subsequent degradation in the endoplasmic reticulum (ER). Nevertheless, it is a hypothesis and has not been proved by experiments [167]. Alternatively, the truncated transcript could undergo nonsense mediated decay (NMD) resulting in absence of the protein.

IQCB1: IQ-MOTIF-Containing Protein B1 (OMIM: 609237), the protein is localized in the connecting cilia of the photoreceptor and in the primary cilia of renal epithelial cells. Any dysfunction of the protein, leads to ciliary malfunction [168]. The gene is located at 3q13.33, containing 15 exons, spanning about 65.7kb. This gene is responsible for autosomal recessive form of Senior-Loken syndrome which presents with nephronophthisis along with RP [128, 168]. The encoded protein consists of central coiled-coil region and two calmodulin-binding IQ domains. *IQCB1* is expressed in all tissues except in pancreas [169]. In this study we had identified a novel mutation in intron 12 c.1278+6T>A. Since *IQCB1* a cilipothic gene and is also expressed in the lymphocytes, cDNA analysis has shown a complete skipping of exon 12 predicting to result in a truncated protein, p.(Gln378AlafsTer2) which could result in either loss of the second calmodulin binding domain [169] or absence of protein due to NMD of the truncated transcript.

SPATA7: Spermatogenesis – Associated 7 (OMIM: 609868) is a ciliopathy gene which is critical for RPGRIP1 localization and protein trafficking in retina [170]. It is located at 14q31.3 region containing 12 exons spanning about 52.8kb [171]. *SPATA7*, in addition to its original identified expression in testis, is also expressed in multiple layers of the retina and responsible for the autosomal recessive LCA and juvenile arRP [172]. This gene contributes to about 1.7% of LCA or early childhood-onset severe retinal dystrophy [173]. It encodes for a highly conserved vertebrate specific protein containing a single transmembrane domain [172]. From the study we had identified a novel intronic mutation (intron7) c.913-2A>G in Fam-12.

The bioinformatic tools predict this mutation to cause splice-site changes and affect the protein features, but whether the change would result in intron retention or exon skipping is unknown. Any such change in the reading frame usually causes a protein truncation which would be deleterious or result in absence of protein due to non-sense mediated decay of the aberrant transcript.

MERTK: MER Tyrosine Kinase proto-oncogene (OMIM: 604705) is involved in the phagocytosis of photoreceptor outer segment [174]. It is located at 2q13 region containing 19 exons [175]. *MERTK* mutations cause autosomal recessive RP and contribute to less than 1% for the disease. [176]. The exons 1-9 encodes for extracellular domain, exon 10 encode for transmembrane domain, while exons 11-19 encode for intracellular domain. Within the extracellular domain exons 2-5 encode a Ig domain (112-280 amino acid residues) and exons 6-9 encode a Fibronectin type III (FNIII) domain (284-478 amino acid residues) [175]. The identified novel nonsense mutation in *MERTK* (Fam-01) is present in exon4 p.(Gln241Ter) that codes for Ig domain. The wild type protein is 999 amino acids long whereas the mutant results in truncation of the protein at the 241st amino acid residue. Therefore the abrupt truncation of the protein might lead to loss of functionally important transmembrane and intracellular domain and/or could also lead to non-sense mediated mRNA decay. Phase I clinical study of gene therapy for six arRP patients with *MERTK* mutations is initiated to test the safety and efficacy of gene therapy via subretinal injection of rAAV2-VMD2-hMERTK and the two year follow up results have shown no major side effects and very mild clinical improvement in subset of patients (3/6 patients) [91].

ABCA4: ATP-Binding Cassette, Subfamily A Member 4 (OMIM: 601691) mediates the transport of an essential molecule (or ion) either into or out of the photoreceptor cells [177]. It is located at 1p22.1 containing 50 exons spanning about 150kb [178].

Mutations in *ABCA4* gene have been reported in autosomal recessive Stargardts disease in 66-80% of the cases [179] and in several other retinal phenotypes such as autosomal recessive RP [180] (incidence not reported), autosomal recessive cone-rod dystrophy (23.6%) [181], fundus flavimaculatus [182] (incidence not reported) and age-related macular degeneration (16%) [183]. The *ABCA4* gene transcribes a large retina specific protein with two transmembrane domains (TMD), two glycosylated extracellular domains (ECD), and two nucleotide binding domains (NBD) [184]. The transmembrane domain is responsible for binding to the substrate and forming the translocation path whereas NBDs provide energy for transport by hydrolyzing ATP to ADP [184]. In Fam-14 we have identified a nonsense mutation which encodes only for 488 amino acids p.(Glu488Ter) instead of 2273 aminoacids leading to a truncated protein comprising only the extracellular domain thereby possibly leading to inactivation of the *ABCA4* allele or NMD of the truncated transcript. ABCR knock-out mice model studies showed deposition of lipofuscin fluorophore (A2E) in retinal pigment epithelium with secondary photoreceptor degeneration [185]. In rodent models of recessive Stargardts disease, Isotretinoin (13-cis retinoic acid) was used for treatment, that showed delayed rhodopsin regeneration and slowing the recovery of rod sensitivity after light exposure, thus a lowered degeneration of photoreceptors [186]. The result suggests that the agent can also be used as an effective treatment for other retinal or macular degeneration.

CDHR1: Cadherin-related family member 1 (OMIM: 609502), a member of calcium dependent cadherin superfamily, exerts its function at the base of photoreceptor outer segment especially at the junction between the outer and inner segment opposite to the connecting cilium [187]. The gene is located at chromosome 10q22 containing 17 coding exons [188]. Mutations in *CDHR1* have been reported in autosomal recessive cone-rod dystrophy and autosomal recessive RP [189]. CDHR1 is composed of large extracelluar calcium (EC) binding domain (six ectodomains with linker region), one transmembrane and one intracellular domain.

Mutation reported in our study, the novel deletion at exon 13 predicted to result in p.(Leu462AspfsTer1) in Fam-15 is present in the fourth extracellular domain. The wild type codes for an 859 amino acids protein whereas the novel indel is predicted to cause abrupt truncation at 463rd amino acid residue after insertion of two novel amino acids. The novel indel is predicted to lead to loss of two ectodomains with the linker region along with the transmembrane and intracellular domain that may lead to loss of protein function or non-sense mediated decay due to truncated transcript. Till date there are seven mutations reported in *CDHR1* and interestingly six of them have been reported to result in the premature stop codon leading to nonsense mediated mRNA decay and thus no protein product [47]. Knock out mouse models exhibit compromised cone and rod outer segments thereby causing photoreceptor degeneration [187].

Although different proteins products of candidate genes LCA, arRP and CRD are involved in various functions such as phototransduction, visual cycle, morphogenesis and maintenance of the integrity of photoreceptors, ciliogenesis, the disruption of the protein function either due to truncation or misfolding or altered activity or absence, all eventually lead to the photoreceptor death and/or RPE degeneration.

4.4 Phenotype Genotype features from the study:

LCA Families

In patients with *AIPL1* mutations (three), atrophic macula and bony spicules were common features, as reported earlier [50, 190]. While, fine pigments were seen in the periphery only in elder patients but not in younger patients. Patients with *RPE65* mutation showed tapetal reflex, disc pallor, attenuated vessels, typical bony spicules with salt and pepper fundus and normal macula as described earlier [23]. Distinct yellow white dot like lesion appeared in eldest member of Fam-10 as well as in the other family who had the same mutation p.(Pro470Leu) as reported from our previous study [151].

Whether these particular RPE white dots are specific to this particular type of missense mutation or for mutations in exon 13 is not known. *CRB1* mutation positive siblings showed typically described mild para-arteriolar preservation of the retinal pigment epithelium (PPRPE) in their fundus [191] along with coin shaped pigment clumps at the background. In *RDH12* mutation positive patients too, pronounced maculopathy and bony spicules were observed [131]. *GUCY2D* mutation positive patients showed normal macula and vessels and *SPATA7* mutation positive patients showed mild disc pallor, arteriolar attenuation and peripheral RPE mottling.

arRP Families: In Fam-01 with *MERTK* mutation, the patients showed atrophic macula with bone spicule pigmentation as described [192]. In Fam-15, *CDHR1* positive patients showed macular atrophy and pigmentary deposits in the peripheral retina as reported [47].

arCRD Family: In Fam-14 *ABCA4* positive patients had arteriolar attenuation, atrophic macular patches and bone spicule pigmentation [193] but considerbale intrafamilial phenotypic variation between the affected individuals was observed.

Our observation is that, long term follow up of patients and phenotype documentation at regular intervals reveal the progressive nature of the disease in general and also increasing severity with age particularly for certain genes such as *MERTK*, *AIPL1* and *ABCA4*. The phenotype of LCA with *RDH12* variants showed macular atrophy with severe disease progression even during the first decade of life.

LIMITATIONS OF RESEARCH

- Homozygosity mapping strategy can be used for gene identification in autosomal recessive diseases only and not for autosomal dominant diseases [59].
- Homozygosity mapping will not detect compound heterozygous mutations [194].
- Locus heterogeneity that may occur within the same family [70], inability to identify digenic or triallelic variants are some of the pitfalls of homozygosity mapping [71].
- This study was on a small cohort of fifteen families that include twelve LCA, two arRP families and one arCRD family; a larger sample size could give a more thorough representation of the distribution and frequency of genes and mutations in our population.

GENERAL CONCLUSION

- Homozygosity mapping (HM) had been an efficient strategy for mapping the causative disease loci in autosomal recessive families with reported success rate of 93% [64], and our study also shows similar results.
- Next generation sequencing (NGS) technology using massively parallel sequencing of candidate genes has been widely used for molecular diagnosis of IRD with success of mutation identification in about 55-80% of the cases [195]. In our study also we had identified the causative mutation in all the three families analysed by NGS. The combined approach of HM and NGS based targeted re-sequencing is efficient and rapid method for mutation identification [196].
- The Phenotype-Genotype features observed in our study is similar to earlier reports.
- The molecular diagnosis in these families has helped in appropriate genetic counseling and also in offering carrier testing in the unaffected family members.

SPECIFIC CONCLUSION

- We were able to identify the causative mutation in 93% (14/15) of the IRD families studied.
- Using homozgosity mapping followed by screening of shortlisted known LCA candidate genes by direct sequencing, we were able to identify both the reported as well as novel mutations in our cohort. There are ten novel mutations identified from the study (10/15) .i.e 67%. This indicates screening methods that enable identification of both reported and novel mutations in candidate genes are appropriate for molecular diagnosis in our population rather than methods like APEX array chip technology which detects only the reported mutations [110].

- By homozygosity mapping approach we would be able to narrow down the known candidate genes, if the genotype-phenotype correlation can be well achieved it may help to determine the responsible gene rapidly, thus decreasing the number of genes to be analyzed and also the decreasing the cost and time for molecular testing.
- In one family we were unable to identify the pathogenic mutation in known LCA candidate genes. However, many homozygous blocks are present, performing exome sequencing and overlapping the data with the HM results would help identify the candidate gene locus easily.
- Although gene therapy treatments are not available readily at present, the encouraging results from clinical trials of *RPE65* and *MERTK* are promising. In our study cohort also we have two families (3 affected patients) with *RPE65* mutation and one family with four affected members with *MERTK* mutation. Hence appropriate molecular diagnosis is very essential for therapeutic gene based trials and treatment in future.

SPECIFIC CONTRIBUTION

- The appropriate molecular diagnosis is very essential for a patient/family for genetic counseling and disease management. In the LCA family with *IQCB1* mutation, the affected sib without renal complication has been specifically advised and recommended for regular renal function examination and evaluation. This is possible only because the causative gene and mutation is identified and other possible systemic involvement is known.

FUTURE SCOPE OF WORK

In our present study the causative gene and mutation was not identified in one (LCA family) of the fifteen families studied. Performing exome sequencing and combining with the homozygosity data available would help to identify the possible novel locus/gene in this family. This would further add on to the repertoire of candidate genes and increase the sensitivity of molecular diagnosis and lead to designing of further therapeutic studies. Studying larger cohort would reveal the spectrum and prevalence of mutations in our population.

REFERENCES

1. Pascolini, D. and S.P. Mariotti, *Global estimates of visual impairment: 2010.* Br J Ophthalmol, 2012. **96**(5): p. 614-8.
2. Neena, J., et al., *Rapid Assessment of Avoidable Blindness in India.* PLoS One, 2008. **3**(8): p. e2867.
3. Smith, J.R., F. Mackensen, and J.T. Rosenbaum, *Therapy insight: scleritis and its relationship to systemic autoimmune disease.* Nat Clin Pract Rheumatol, 2007. **3**(4): p. 219-26.
4. Kolb, *The neural organization of the human retina.* Principles and practices of clinical electrophysiology of vision.St. Louis: Mosby Year Book 1991: p. 25-52.
5. Kandel E.R., S., J.H., Jessell, T.M., *Principles of Neural Science.* 2000(4th edition): p. pp.507-513.
6. Purves D, A.G., Fitzpatrick D, et al, *"Vision:The Eye"* in *Neuroscience* G.J.A. Dale Purves, David Fitzpatrick, Lawrence C Katz, Anthony-Samuel LaMantia, James O McNamara, and S Mark Williams, Editor, Sinauer Associates;2001: Sunderland.
7. Wright, A.F., et al., *Photoreceptor degeneration: genetic and mechanistic dissection of a complex trait.* Nat Rev Genet, 2010. **11**(4): p. 273-84.
8. Perusek, L. and T. Maeda, *Vitamin A derivatives as treatment options for retinal degenerative diseases.* Nutrients, 2013. **5**(7): p. 2646-66.
9. *OpenWetWare contributors. BIO254:Phototransduction [database on the Internet]*. [updated 2006 Nov 6] [cited 7th Sep 2015]; Available from: http://openwetware.org/index.php?title=BIO254:Phototransduction&oldid=85424
.

10. Kramer, R.H. and E. Molokanova, *Modulation of cyclic-nucleotide-gated channels and regulation of vertebrate phototransduction.* Journal of Experimental Biology, 2001. **204**(17): p. 2921-2931.
11. Huang, Y., V. Enzmann, and S.T. Ildstad, *Stem cell-based therapeutic applications in retinal degenerative diseases.* Stem Cell Rev, 2011. **7**(2): p. 434-45.
12. Sullivan, L.S. and S.P. Daiger, *Inherited retinal degeneration: exceptional genetic and clinical heterogeneity.* Mol Med Today, 1996. **2**(9): p. 380-6.
13. Veleri, S., et al., *Biology and therapy of inherited retinal degenerative disease: insights from mouse models.* Dis Model Mech, 2015. **8**(2): p. 109-29.
14. Cooke Bailey, J.N., et al., *Advances in the genomics of common eye diseases.* Hum Mol Genet, 2013. **22**(R1): p. R59-65.
15. Bowne, S.J., et al., *A dominant mutation in RPE65 identified by whole-exome sequencing causes retinitis pigmentosa with choroidal involvement.* Eur J Hum Genet, 2011. **19**(10): p. 1074-81.
16. Huang, X.F., et al., *Genotype-phenotype correlation and mutation spectrum in a large cohort of patients with inherited retinal dystrophy revealed by next-generation sequencing.* Genet Med, 2015. **17**(4): p. 271-8.
17. Travis, G.H., *Mechanisms of cell death in the inherited retinal degenerations.* Am J Hum Genet, 1998. **62**(3): p. 503-8.
18. Pierce, E.A., *Pathways to photoreceptor cell death in inherited retinal degenerations.* Bioessays, 2001. **23**(7): p. 605-18.
19. Sohocki, M.M., et al., *Mutations in a new photoreceptor-pineal gene on 17p cause Leber congenital amaurosis.* Nat Genet, 2000. **24**(1): p. 79-83.
20. Nichols, L.L., 2nd, et al., *Two novel CRX mutant proteins causing autosomal dominant Leber congenital amaurosis interact differently with NRL.* Hum Mutat, 2010. **31**(6): p. E1472-83.

21. Stone, E.M., *Leber congenital amaurosis - a model for efficient genetic testing of heterogeneous disorders: LXIV Edward Jackson Memorial Lecture.* Am J Ophthalmol, 2007. **144**(6): p. 791-811.
22. Koenekoop, R.K., *An overview of Leber congenital amaurosis: a model to understand human retinal development.* Surv Ophthalmol, 2004. **49**(4): p. 379-98.
23. den Hollander, A.I., et al., *Leber congenital amaurosis: genes, proteins and disease mechanisms.* Prog Retin Eye Res, 2008. **27**(4): p. 391-419.
24. Roger, J.E., et al., *OTX2 loss causes rod differentiation defect in CRX-associated congenital blindness.* J Clin Invest, 2014. **124**(2): p. 631-43.
25. Abu-Safieh, L., et al., *Autozygome-guided exome sequencing in retinal dystrophy patients reveals pathogenetic mutations and novel candidate disease genes.* Genome Res, 2013. **23**(2): p. 236-47.
26. Wang, X., et al., *Comprehensive molecular diagnosis of 179 Leber congenital amaurosis and juvenile retinitis pigmentosa patients by targeted next generation sequencing.* J Med Genet, 2013. **50**(10): p. 674-88.
27. Wang, X., et al., *Whole-exome sequencing identifies ALMS1, IQCB1, CNGA3, and MYO7A mutations in patients with Leber congenital amaurosis.* Hum Mutat, 2011. **32**(12): p. 1450-9.
28. Chacon-Camacho, O.F. and J.C. Zenteno, *Review and update on the molecular basis of Leber congenital amaurosis.* World J Clin Cases, 2015. **3**(2): p. 112-24.
29. Ferrari, S., et al., *Retinitis pigmentosa: genes and disease mechanisms.* Curr Genomics, 2011. **12**(4): p. 238-49.
30. Hartong, D.T., E.L. Berson, and T.P. Dryja, *Retinitis pigmentosa.* Lancet, 2006. **368**(9549): p. 1795-809.
31. Sen, P., et al., *Prevalence of retinitis pigmentosa in South Indian population aged above 40 years.* Ophthalmic Epidemiol, 2008. **15**(4): p. 279-81.
32. Kajiwara, K., E.L. Berson, and T.P. Dryja, *Digenic retinitis pigmentosa due to mutations at the unlinked peripherin/RDS and ROM1 loci.* Science, 1994. **264**(5165): p. 1604-8.

33. Daiger, S.P., S.J. Bowne, and L.S. Sullivan, *Perspective on genes and mutations causing retinitis pigmentosa.* Arch Ophthalmol, 2007. **125**(2): p. 151-8.
34. Millan, J.M., et al., *An update on the genetics of usher syndrome.* J Ophthalmol, 2011. **2011**: p. 417217.
35. Boughman, J.A., M. Vernon, and K.A. Shaver, *Usher syndrome: definition and estimate of prevalence from two high-risk populations.* J Chronic Dis, 1983. **36**(8): p. 595-603.
36. Moore, S.J., et al., *Clinical and genetic epidemiology of Bardet-Biedl syndrome in Newfoundland: a 22-year prospective, population-based, cohort study.* Am J Med Genet A, 2005. **132A**(4): p. 352-60.
37. Saunier, S., R. Salomon, and C. Antignac, *Nephronophthisis.* Curr Opin Genet Dev, 2005. **15**(3): p. 324-31.
38. Colville, D.J. and J. Savige, *Alport syndrome. A review of the ocular manifestations.* Ophthalmic Genet, 1997. **18**(4): p. 161-73.
39. de Vries, J., et al., *Jeune syndrome: description of 13 cases and a proposal for follow-up protocol.* Eur J Pediatr, 2010. **169**(1): p. 77-88.
40. Fousteri, M., et al., *Cockayne syndrome A and B proteins differentially regulate recruitment of chromatin remodeling and repair factors to stalled RNA polymerase II in vivo.* Mol Cell, 2006. **23**(4): p. 471-82.
41. Mathews, L., K. Narayanadas, and G. Sunil, *Thiamine responsive megaloblastic anemia.* Indian Pediatr, 2009. **46**(2): p. 172-4.
42. Hamel, C.P., *Cone rod dystrophies.* Orphanet J Rare Dis, 2007. **2**(1): p. 1-7.
43. Michaelides, M., D.M. Hunt, and A.T. Moore, *The cone dysfunction syndromes.* Br J Ophthalmol, 2004. **88**(2): p. 291-7.
44. Szlyk, J.P., et al., *Perceived and actual performance of daily tasks: relationship to visual function tests in individuals with retinitis pigmentosa.* Ophthalmology, 2001. **108**(1): p. 65-75.
45. Maugeri, A., et al., *Mutations in the ABCA4 (ABCR) gene are the major cause of autosomal recessive cone-rod dystrophy.* Am J Hum Genet, 2000. **67**(4): p. 960-6.

46. Ostergaard, E., et al., *Mutations in PCDH21 cause autosomal recessive cone-rod dystrophy.* J Med Genet, 2010. **47**(10): p. 665-9.
47. Nikopoulos, K., et al., *Identification of two novel mutations in CDHR1 in consanguineous Spanish families with autosomal recessive retinal dystrophy.* Sci Rep, 2015. **5**: p. 13902.
48. Aleman, T.S., et al., *CERKL mutations cause an autosomal recessive cone-rod dystrophy with inner retinopathy.* Invest Ophthalmol Vis Sci, 2009. **50**(12): p. 5944-54.
49. Hameed, A., et al., *Evidence of RPGRIP1 gene mutations associated with recessive cone-rod dystrophy.* J Med Genet, 2003. **40**(8): p. 616-9.
50. McKibbin, M., et al., *Genotype-phenotype correlation for leber congenital amaurosis in Northern Pakistan.* Arch Ophthalmol, 2010. **128**(1): p. 107-13.
51. K. Semagn, Å.B., M. N. Ndjiondjop, *Principles, requirements and prospects of genetic mapping in plants* in *African Journal of Biotechnology*2006, Academic Journal: Nairobi,Kenya. p. 2569-2587.
52. Brown, T.A., *Introduction to Genome*, in *Genomes*: 2nd ed. Oxford:Wiley-Liss; 2002.
53. Hudson, T.J., et al., *An STS-based map of the human genome.* Science, 1995. **270**(5244): p. 1945-54.
54. Trask, B.J., et al., *Mapping of human chromosome Xq28 by two-color fluorescence in situ hybridization of DNA sequences to interphase cell nuclei.* Am J Hum Genet, 1991. **48**(1): p. 1-15.
55. Sturtevant, A.H., *The linear arrangement of six sex-linked factors in Drosophila, as shown by their mode of association.* Journal of Experimental Zoology, 1913. **14**: p. 43-59.
56. Botstein, D., et al., *Construction of a genetic linkage map in man using restriction fragment length polymorphisms.* Am J Hum Genet, 1980. **32**(3): p. 314-31.

57. Wang, D.G., et al., *Large-scale identification, mapping, and genotyping of single-nucleotide polymorphisms in the human genome.* Science, 1998. **280**(5366): p. 1077-82.
58. Morton, N.E., *Sequential tests for the detection of linkage.* Am J Hum Genet, 1955. **7**(3): p. 277-318.
59. Lander, E.S. and D. Botstein, *Homozygosity mapping: a way to map human recessive traits with the DNA of inbred children.* Science, 1987. **236**(4808): p. 1567-70.
60. den Hollander, A.I., et al., *Identification of novel mutations in patients with Leber congenital amaurosis and juvenile RP by genome-wide homozygosity mapping with SNP microarrays.* Invest Ophthalmol Vis Sci, 2007. **48**(12): p. 5690-8.
61. Zhang, L., et al., *Homozygosity mapping on a single patient: identification of homozygous regions of recent common ancestry by using population data.* Hum Mutat, 2011. **32**(3): p. 345-53.
62. *Autozygosity mapping Online Sir Jules Thorn International Resource for Autozygosity Mapping [database on the internet]*. [updated 2011 Feb 8] [cited 20th Aug 2015]; Available from: http://autozygosity.org.
63. Singh, H.P., et al., *Genetic analysis of Indian families with autosomal recessive retinitis pigmentosa by homozygosity screening.* Invest Ophthalmol Vis Sci, 2009. **50**(9): p. 4065-71.
64. Hildebrandt, F., et al., *A systematic approach to mapping recessive disease genes in individuals from outbred populations.* PLoS Genet, 2009. **5**(1): p. e1000353.
65. Ropers, H.H., *New perspectives for the elucidation of genetic disorders.* Am J Hum Genet, 2007. **81**(2): p. 199-207.
66. Bittles, A.H. and M.L. Black, *Evolution in health and medicine Sackler colloquium: Consanguinity, human evolution, and complex diseases.* Proc Natl Acad Sci U S A, 2010. **107 Suppl 1**: p. 1779-86.

67. Woods, C.G., et al., *Quantification of homozygosity in consanguineous individuals with autosomal recessive disease.* Am J Hum Genet, 2006. **78**(5): p. 889-96.
68. Hamamy, H., et al., *Consanguineous marriages, pearls and perils: Geneva International Consanguinity Workshop Report.* Genet Med, 2011. **13**(9): p. 841-7.
69. Hamamy, H., *Consanguineous marriages : Preconception consultation in primary health care settings.* J Community Genet, 2012. **3**(3): p. 185-92.
70. Benayoun, L., et al., *Genetic heterogeneity in two consanguineous families segregating early onset retinal degeneration: the pitfalls of homozygosity mapping.* Am J Med Genet A, 2009. **149A**(4): p. 650-6.
71. Miano, M.G., et al., *Pitfalls in homozygosity mapping.* Am J Hum Genet, 2000. **67**(5): p. 1348-51.
72. Quail, M.A., et al., *A tale of three next generation sequencing platforms: comparison of Ion Torrent, Pacific Biosciences and Illumina MiSeq sequencers.* BMC Genomics, 2012. **13**: p. 341.
73. Grada, A. and K. Weinbrecht, *Next-generation sequencing: methodology and application.* J Invest Dermatol, 2013. **133**(8): p. e11.
74. Schneiderman, H., *The Funduscopic Examination*, in *Clinical Methods: The History, Physical, and Laboratory Examinations*, H.K. Walker, W.D. Hall, and J.W. Hurst, Editors. 1990: Boston.
75. Chrispell, J.D., T.I. Rebrik, and E.R. Weiss, *Electroretinogram analysis of the visual response in zebrafish larvae.* J Vis Exp, 2015(97).
76. Grover, S., G.A. Fishman, and J. Brown, Jr., *Patterns of visual field progression in patients with retinitis pigmentosa.* Ophthalmology, 1998. **105**(6): p. 1069-75.
77. Yannuzzi, L.A., et al., *Ophthalmic fundus imaging: today and beyond.* Am J Ophthalmol, 2004. **137**(3): p. 511-24.
78. Scholl, H.P., et al., *Fundus autofluorescence in patients with leber congenital amaurosis.* Invest Ophthalmol Vis Sci, 2004. **45**(8): p. 2747-52.

79. Fujimoto, J.G., et al., *Optical coherence tomography: an emerging technology for biomedical imaging and optical biopsy.* Neoplasia, 2000. **2**(1-2): p. 9-25.
80. Shintani, K., D.L. Shechtman, and A.S. Gurwood, *Review and update: current treatment trends for patients with retinitis pigmentosa.* Optometry, 2009. **80**(7): p. 384-401.
81. Sahni, J.N., et al., *Therapeutic challenges to retinitis pigmentosa: from neuroprotection to gene therapy.* Curr Genomics, 2011. **12**(4): p. 276-84.
82. Rivas, M.A. and E. Vecino, *Animal models and different therapies for treatment of retinitis pigmentosa.* Histol Histopathol, 2009. **24**(10): p. 1295-322.
83. Acland, G.M., et al., *Gene therapy restores vision in a canine model of childhood blindness.* Nat Genet, 2001. **28**(1): p. 92-5.
84. Bainbridge, J.W., et al., *Effect of gene therapy on visual function in Leber's congenital amaurosis.* N Engl J Med, 2008. **358**(21): p. 2231-9.
85. Cideciyan, A.V., et al., *Human gene therapy for RPE65 isomerase deficiency activates the retinoid cycle of vision but with slow rod kinetics.* Proc Natl Acad Sci U S A, 2008. **105**(39): p. 15112-7.
86. Maguire, A.M., et al., *Safety and efficacy of gene transfer for Leber's congenital amaurosis.* N Engl J Med, 2008. **358**(21): p. 2240-8.
87. Cideciyan, A.V., et al., *Human RPE65 gene therapy for Leber congenital amaurosis: persistence of early visual improvements and safety at 1 year.* Hum Gene Ther, 2009. **20**(9): p. 999-1004.
88. Cideciyan, A.V., et al., *Vision 1 year after gene therapy for Leber's congenital amaurosis.* N Engl J Med, 2009. **361**(7): p. 725-7.
89. Cideciyan, A.V., et al., *Human retinal gene therapy for Leber congenital amaurosis shows advancing retinal degeneration despite enduring visual improvement.* Proc Natl Acad Sci U S A, 2013. **110**(6): p. E517-25.
90. Bainbridge, J.W., et al., *Long-term effect of gene therapy on Leber's congenital amaurosis.* N Engl J Med, 2015. **372**(20): p. 1887-97.

91. Ghazi, N.G., et al., *Treatment of retinitis pigmentosa due to MERTK mutations by ocular subretinal injection of adeno-associated virus gene vector: results of a phase I trial.* Hum Genet, 2016. **135**(3): p. 327-43.
92. Lewin, A.S., et al., *Ribozyme rescue of photoreceptor cells in a transgenic rat model of autosomal dominant retinitis pigmentosa.* Nat Med, 1998. **4**(8): p. 967-71.
93. O'Reilly, M., et al., *RNA interference-mediated suppression and replacement of human rhodopsin in vivo.* Am J Hum Genet, 2007. **81**(1): p. 127-35.
94. Redmond, T.M., et al., *Rpe65 is necessary for production of 11-cis-vitamin A in the retinal visual cycle.* Nat Genet, 1998. **20**(4): p. 344-51.
95. Van Hooser, J.P., et al., *Recovery of visual functions in a mouse model of Leber congenital amaurosis.* J Biol Chem, 2002. **277**(21): p. 19173-82.
96. Koenekoop, R.K., et al., *Oral 9-cis retinoid for childhood blindness due to Leber congenital amaurosis caused by RPE65 or LRAT mutations: an open-label phase 1b trial.* Lancet, 2014. **384**(9953): p. 1513-20.
97. Hamel, C., *Retinitis pigmentosa.* Orphanet J Rare Dis, 2006. **1**: p. 40.
98. Sieving, P.A., et al., *Ciliary neurotrophic factor (CNTF) for human retinal degeneration: phase I trial of CNTF delivered by encapsulated cell intraocular implants.* Proc Natl Acad Sci U S A, 2006. **103**(10): p. 3896-901.
99. Comyn, O., E. Lee, and R.E. MacLaren, *Induced pluripotent stem cell therapies for retinal disease.* Curr Opin Neurol, 2010. **23**(1): p. 4-9.
100. Garcia, J.M., et al., *Stem cell therapy for retinal diseases.* World J Stem Cells, 2015. **7**(1): p. 160-4.
101. Klassen, H.J., et al., *Multipotent retinal progenitors express developmental markers, differentiate into retinal neurons, and preserve light-mediated behavior.* Invest Ophthalmol Vis Sci, 2004. **45**(11): p. 4167-73.
102. MacLaren, R.E. and R.A. Pearson, *Stem cell therapy and the retina.* Eye (Lond), 2007. **21**(10): p. 1352-9.

103. Radtke, N.D., et al., *Transplantation of intact sheets of fetal neural retina with its retinal pigment epithelium in retinitis pigmentosa patients.* Am J Ophthalmol, 2002. **133**(4): p. 544-50.

104. Ramsden, C.M., et al., *Stem cells in retinal regeneration: past, present and future.* Development, 2013. **140**(12): p. 2576-85.

105. Hirami, Y., et al., *Generation of retinal cells from mouse and human induced pluripotent stem cells.* Neurosci Lett, 2009. **458**(3): p. 126-31.

106. Daiger, S.P. *Summaries of Genes and Loci Causing Retinal Diseases [database on the Internet]*. [updated 2015 June 19] [cited 2015 July 7]; Available from: https://sph.uth.edu/Retnet/sum-dis.htm#A-genes.

107. Wang, H., et al., *Comprehensive Molecular Diagnosis of a Large Chinese Leber Congenital Amaurosis Cohort.* Invest Ophthalmol Vis Sci, 2015. **56**(6): p. 3642-55.

108. Ramprasad, V.L., et al., *Identification of a novel splice-site mutation in the Lebercilin (LCA5) gene causing Leber congenital amaurosis.* Mol Vis, 2008. **14**: p. 481-6.

109. Verma, A., et al., *Mutational screening of LCA genes emphasizing RPE65 in South Indian cohort of patients.* PLoS One, 2013. **8**(9): p. e73172.

110. Sundaresan, P., et al., *Mutations that are a common cause of Leber congenital amaurosis in northern America are rare in southern India.* Mol Vis, 2009. **15**: p. 1781-7.

111. Lotery, A.J., et al., *Mutation analysis of 3 genes in patients with Leber congenital amaurosis.* Arch Ophthalmol, 2000. **118**(4): p. 538-43.

112. Falk, M.J., et al., *NMNAT1 mutations cause Leber congenital amaurosis.* 2012. **44**(9): p. 1040-5.

113. Goyal, S., et al., *Confirmation of TTC8 as a disease gene for nonsyndromic autosomal recessive retinitis pigmentosa (RP51).* Clin Genet, 2016. **89**(4): p. 454-460.

114. Zhou, Y., et al., *Whole-exome sequencing reveals a novel frameshift mutation in the FAM161A gene causing autosomal recessive retinitis pigmentosa in the Indian population.* J Hum Genet, 2015. **60**(10): p. 625-30.

115. Kannabiran, C., et al., *Mutations in TULP1, NR2E3, and MFRP genes in Indian families with autosomal recessive retinitis pigmentosa.* Mol Vis, 2012. **18**: p. 1165-74.

116. Sampangi, R., et al., *Cone-rod dystrophy and acquired dissociated vertical nystagmus.* J Pediatr Ophthalmol Strabismus, 2005. **42**(2): p. 114-6.

117. Fogla, R. and G.K. Iyer, *Keratoconus associated with cone-rod dystrophy: a case report.* Cornea, 2002. **21**(3): p. 331-2.

118. Singh, H.P., et al., *Homozygous null mutations in the ABCA4 gene in two families with autosomal recessive retinal dystrophy.* Am J Ophthalmol, 2006. **141**(5): p. 906-13.

119. Agarwal, S., et al., *Sankara Nethralaya-Diabetic Retinopathy Epidemiology and Molecular Genetic Study (SN-DREAMS 1): study design and research methodology.* Ophthalmic Epidemiol, 2005. **12**(2): p. 143-53.

120. Vijaya, L., et al., *Prevalence of primary angle-closure disease in an urban south Indian population and comparison with a rural population. The Chennai Glaucoma Study.* Ophthalmology, 2008. **115**(4): p. 655-660 e1.

121. Desmet, F.O., et al., *Human Splicing Finder: an online bioinformatics tool to predict splicing signals.* Nucleic Acids Res, 2009. **37**(9): p. e67.

122. Schwarz, J.M., et al., *MutationTaster2: mutation prediction for the deep-sequencing age.* Nat Methods, 2014. **11**(4): p. 361-2.

123. Adzhubei, I.A., et al., *A method and server for predicting damaging missense mutations.* Nat Methods, 2010. **7**(4): p. 248-9.

124. Kumar, P., S. Henikoff, and P.C. Ng, *Predicting the effects of coding non-synonymous variants on protein function using the SIFT algorithm.* Nat Protoc, 2009. **4**(7): p. 1073-81.

125. Reva, B., Y. Antipin, and C. Sander, *Predicting the functional impact of protein mutations: application to cancer genomics.* Nucleic Acids Res, 2011. **39**(17): p. e118.

126. Li, B., et al., *Automated inference of molecular mechanisms of disease from amino acid substitutions.* Bioinformatics, 2009. **25**(21): p. 2744-50.

127. Ferrer-Costa, C., et al., *PMUT: a web-based tool for the annotation of pathological mutations on proteins.* Bioinformatics, 2005. **21**(14): p. 3176-8.

128. Stone, E.M., et al., *Variations in NPHP5 in patients with nonsyndromic leber congenital amaurosis and Senior-Loken syndrome.* Arch Ophthalmol, 2011. **129**(1): p. 81-7.

129. Otto, E.A., et al., *Mutation analysis in nephronophthisis using a combined approach of homozygosity mapping, CEL I endonuclease cleavage, and direct sequencing.* Hum Mutat, 2008. **29**(3): p. 418-26.

130. Estrada-Cuzcano, A., et al., *IQCB1 mutations in patients with leber congenital amaurosis.* Invest Ophthalmol Vis Sci, 2011. **52**(2): p. 834-9.

131. Schuster, A., et al., *The phenotype of early-onset retinal degeneration in persons with RDH12 mutations.* Invest Ophthalmol Vis Sci, 2007. **48**(4): p. 1824-31.

132. Kirin, M., et al., *Genomic runs of homozygosity record population history and consanguinity.* PLoS One, 2010. **5**(11): p. e13996.

133. Thompson, D.A., et al., *Retinal degeneration associated with RDH12 mutations results from decreased 11-cis retinal synthesis due to disruption of the visual cycle.* Hum Mol Genet, 2005. **14**(24): p. 3865-75.

134. Valverde, D., et al., *Complexity of phenotype-genotype correlations in Spanish patients with RDH12 mutations.* Invest Ophthalmol Vis Sci, 2009. **50**(3): p. 1065-8.

135. Mullins, R.F., et al., *Autosomal recessive retinitis pigmentosa due to ABCA4 mutations: clinical, pathologic, and molecular characterization.* Invest Ophthalmol Vis Sci, 2012. **53**(4): p. 1883-94.

136. Cideciyan, A.V., et al., *ABCA4 disease progression and a proposed strategy for gene therapy.* Hum Mol Genet, 2009. **18**(5): p. 931-41.
137. Sohocki, M.M., et al., *Prevalence of AIPL1 mutations in inherited retinal degenerative disease.* Mol Genet Metab, 2000. **70**(2): p. 142-50.
138. Sohocki, M.M., et al., *Localization of retina/pineal-expressed sequences: identification of novel candidate genes for inherited retinal disorders.* Genomics, 1999. **58**(1): p. 29-33.
139. van der Spuy, J., et al., *The Leber congenital amaurosis gene product AIPL1 is localized exclusively in rod photoreceptors of the adult human retina.* Hum Mol Genet, 2002. **11**(7): p. 823-31.
140. Carver, L.A. and C.A. Bradfield, *Ligand-dependent interaction of the aryl hydrocarbon receptor with a novel immunophilin homolog in vivo.* J Biol Chem, 1997. **272**(17): p. 11452-6.
141. Ramamurthy, V., et al., *AIPL1, a protein implicated in Leber's congenital amaurosis, interacts with and aids in processing of farnesylated proteins.* Proc Natl Acad Sci U S A, 2003. **100**(22): p. 12630-5.
142. Gallon, V.A., et al., *Purification, characterisation and intracellular localisation of aryl hydrocarbon interacting protein-like 1 (AIPL1) and effects of mutations associated with inherited retinal dystrophies.* Biochim Biophys Acta, 2004. **1690**(2): p. 141-9.
143. Haeseleer, F., et al., *Dual-substrate specificity short chain retinol dehydrogenases from the vertebrate retina.* J Biol Chem, 2002. **277**(47): p. 45537-46.
144. Weleber, R.G., et al., *Leber Congenital Amaurosis*, in *GeneReviews(R)*, R.A. Pagon, et al., Editors. 1993: Seattle (WA).
145. Sun, W., et al., *Novel RDH12 mutations associated with Leber congenital amaurosis and cone-rod dystrophy: biochemical and clinical evaluations.* Vision Res, 2007. **47**(15): p. 2055-66.
146. Moiseyev, G., et al., *RPE65 is the isomerohydrolase in the retinoid visual cycle.* Proc Natl Acad Sci U S A, 2005. **102**(35): p. 12413-8.

147. Mata, N.L., et al., *Rpe65 is a retinyl ester binding protein that presents insoluble substrate to the isomerase in retinal pigment epithelial cells.* J Biol Chem, 2004. **279**(1): p. 635-43.

148. Gu, S.M., et al., *Mutations in RPE65 cause autosomal recessive childhood-onset severe retinal dystrophy.* Nat Genet, 1997. **17**(2): p. 194-7.

149. Morimura, H., et al., *Mutations in the RPE65 gene in patients with autosomal recessive retinitis pigmentosa or leber congenital amaurosis.* Proc Natl Acad Sci U S A, 1998. **95**(6): p. 3088-93.

150. Thompson, D.A., et al., *Genetics and phenotypes of RPE65 mutations in inherited retinal degeneration.* Invest Ophthalmol Vis Sci, 2000. **41**(13): p. 4293-9.

151. Mamatha, G., et al., *Screening of the RPE65 gene in the Asian Indian patients with leber congenital amaurosis.* Ophthalmic Genet, 2008. **29**(2): p. 73-8.

152. den Hollander, A.I., et al., *Mutations in a human homologue of Drosophila crumbs cause retinitis pigmentosa (RP12).* Nat Genet, 1999. **23**(2): p. 217-21.

153. Izaddoost, S., et al., *Drosophila Crumbs is a positional cue in photoreceptor adherens junctions and rhabdomeres.* Nature, 2002. **416**(6877): p. 178-83.

154. Jacobson, S.G., et al., *Crumbs homolog 1 (CRB1) mutations result in a thick human retina with abnormal lamination.* Hum Mol Genet, 2003. **12**(9): p. 1073-8.

155. den Hollander, A.I., et al., *Leber congenital amaurosis and retinitis pigmentosa with Coats-like exudative vasculopathy are associated with mutations in the crumbs homologue 1 (CRB1) gene.* Am J Hum Genet, 2001. **69**(1): p. 198-203.

156. McKay, G.J., et al., *Pigmented paravenous chorioretinal atrophy is associated with a mutation within the crumbs homolog 1 (CRB1) gene.* Invest Ophthalmol Vis Sci, 2005. **46**(1): p. 322-8.

157. Lotery, A.J., et al., *Mutations in the CRB1 gene cause Leber congenital amaurosis.* Arch Ophthalmol, 2001. **119**(3): p. 415-20.

158. Bujakowska, K., et al., *CRB1 mutations in inherited retinal dystrophies.* Hum Mutat, 2012. **33**(2): p. 306-15.

159. Beryozkin, A., et al., *Mutations in CRB1 are a relatively common cause of autosomal recessive early-onset retinal degeneration in the Israeli and Palestinian populations.* Invest Ophthalmol Vis Sci, 2013. **54**(3): p. 2068-75.
160. Boye, S.E., *A Mini-review: Animal Models of GUCY2D Leber Congenital Amaurosis (LCA1).* Adv Exp Med Biol, 2016. **854**: p. 253-8.
161. Perrault, I., et al., *Retinal-specific guanylate cyclase gene mutations in Leber's congenital amaurosis.* Nat Genet, 1996. **14**(4): p. 461-4.
162. Kelsell, R.E., et al., *Mutations in the retinal guanylate cyclase (RETGC-1) gene in dominant cone-rod dystrophy.* Hum Mol Genet, 1998. **7**(7): p. 1179-84.
163. Camuzat, A., et al., *A gene for Leber's congenital amaurosis maps to chromosome 17p.* Hum Mol Genet, 1995. **4**(8): p. 1447-52.
164. Hanein, S., et al., *Leber congenital amaurosis: comprehensive survey of the genetic heterogeneity, refinement of the clinical definition, and genotype-phenotype correlations as a strategy for molecular diagnosis.* Hum Mutat, 2004. **23**(4): p. 306-17.
165. Tucker, C.L., et al., *Functional analyses of mutant recessive GUCY2D alleles identified in Leber congenital amaurosis patients: protein domain comparisons and dominant negative effects.* Mol Vis, 2004. **10**: p. 297-303.
166. Ugur Iseri, S.A., Y.K. Durlu, and A. Tolun, *A novel recessive GUCY2D mutation causing cone-rod dystrophy and not Leber's congenital amaurosis.* Eur J Hum Genet, 2010. **18**(10): p. 1121-6.
167. Rozet, J.M., et al., *Complete abolition of the retinal-specific guanylyl cyclase (retGC-1) catalytic ability consistently leads to leber congenital amaurosis (LCA).* Invest Ophthalmol Vis Sci, 2001. **42**(6): p. 1190-2.
168. Otto, E.A., et al., *Nephrocystin-5, a ciliary IQ domain protein, is mutated in Senior-Loken syndrome and interacts with RPGR and calmodulin.* Nat Genet, 2005. **37**(3): p. 282-8.

169. Nomura, N., et al., *Prediction of the coding sequences of unidentified human genes. I. The coding sequences of 40 new genes (KIAA0001-KIAA0040) deduced by analysis of randomly sampled cDNA clones from human immature myeloid cell line KG-1.* DNA Res, 1994. **1**(1): p. 27-35.

170. Eblimit, A., et al., *Spata7 is a retinal ciliopathy gene critical for correct RPGRIP1 localization and protein trafficking in the retina.* Hum Mol Genet, 2015. **24**(6): p. 1584-601.

171. Zhang, X., et al., *A novel gene, RSD-3/HSD-3.1, encodes a meiotic-related protein expressed in rat and human testis.* J Mol Med (Berl), 2003. **81**(6): p. 380-7.

172. Wang, H., et al., *Mutations in SPATA7 cause Leber congenital amaurosis and juvenile retinitis pigmentosa.* Am J Hum Genet, 2009. **84**(3): p. 380-7.

173. Mackay, D.S., et al., *Screening of SPATA7 in patients with Leber congenital amaurosis and severe childhood-onset retinal dystrophy reveals disease-causing mutations.* Invest Ophthalmol Vis Sci, 2011. **52**(6): p. 3032-8.

174. Carr, A.J., et al., *Molecular characterization and functional analysis of phagocytosis by human embryonic stem cell-derived RPE cells using a novel human retinal assay.* Mol Vis, 2009. **15**: p. 283-95.

175. Graham, D.K., et al., *Cloning and mRNA expression analysis of a novel human protooncogene, c-mer.* Cell Growth Differ, 1994. **5**(6): p. 647-57.

176. Ostergaard, E., et al., *A novel MERTK deletion is a common founder mutation in the Faroe Islands and is responsible for a high proportion of retinitis pigmentosa cases.* Mol Vis, 2011. **17**: p. 1485-92.

177. Allikmets, R., et al., *A photoreceptor cell-specific ATP-binding transporter gene (ABCR) is mutated in recessive Stargardt macular dystrophy.* Nat Genet, 1997. **15**(3): p. 236-46.

178. Gerber, S., et al., *Complete exon-intron structure of the retina-specific ATP binding transporter gene (ABCR) allows the identification of novel mutations underlying Stargardt disease.* Genomics, 1998. **48**(1): p. 139-42.

179. Yatsenko, A.N., et al., *An ABCA4 genomic deletion in patients with Stargardt disease.* Hum Mutat, 2003. **21**(6): p. 636-44.
180. Martinez-Mir, A., et al., *Retinitis pigmentosa caused by a homozygous mutation in the Stargardt disease gene ABCR.* Nat Genet, 1998. **18**(1): p. 11-2.
181. Ducroq, D., et al., *The ABCA4 gene in autosomal recessive cone-rod dystrophies.* Am J Hum Genet, 2002. **71**(6): p. 1480-2.
182. Gerber, S., et al., *A gene for late-onset fundus flavimaculatus with macular dystrophy maps to chromosome 1p13.* Am J Hum Genet, 1995. **56**(2): p. 396-9.
183. Allikmets, R., et al., *Mutation of the Stargardt disease gene (ABCR) in age-related macular degeneration.* Science, 1997. **277**(5333): p. 1805-7.
184. Tsybovsky, Y., R.S. Molday, and K. Palczewski, *The ATP-binding cassette transporter ABCA4: structural and functional properties and role in retinal disease.* Adv Exp Med Biol, 2010. **703**: p. 105-25.
185. Weng, J., et al., *Insights into the function of Rim protein in photoreceptors and etiology of Stargardt's disease from the phenotype in abcr knockout mice.* Cell, 1999. **98**(1): p. 13-23.
186. Sieving, P.A., et al., *Inhibition of the visual cycle in vivo by 13-cis retinoic acid protects from light damage and provides a mechanism for night blindness in isotretinoin therapy.* Proc Natl Acad Sci U S A, 2001. **98**(4): p. 1835-40.
187. Littink, K.W., et al., *Homozygosity mapping in patients with cone-rod dystrophy: novel mutations and clinical characterizations.* Invest Ophthalmol Vis Sci, 2010. **51**(11): p. 5943-51.
188. Rattner, A., et al., *A photoreceptor-specific cadherin is essential for the structural integrity of the outer segment and for photoreceptor survival.* Neuron, 2001. **32**(5): p. 775-86.
189. Henderson, R.H., et al., *Biallelic mutation of protocadherin-21 (PCDH21) causes retinal degeneration in humans.* Mol Vis, 2010. **16**: p. 46-52.
190. Dharmaraj, S., et al., *The phenotype of Leber congenital amaurosis in patients with AIPL1 mutations.* Arch Ophthalmol, 2004. **122**(7): p. 1029-37.

191. Ehrenberg, M., et al., *CRB1: one gene, many phenotypes.* Semin Ophthalmol, 2013. **28**(5-6): p. 397-405.
192. Mackay, D.S., et al., *Novel mutations in MERTK associated with childhood onset rod-cone dystrophy.* Mol Vis, 2010. **16**: p. 369-77.
193. Kjellstrom, U., *Association between genotype and phenotype in families with mutations in the ABCA4 gene.* Mol Vis, 2014. **20**: p. 89-104.
194. Karrin W.Littink, A.I.d.H., Frans P.M. Cremers, and Rob W.J.Collin, *The Power of Homozygosity Mapping:Discovery of New Genetic Defects in Patients with Retinal Dystrophy*, in *Retinal Degenerative Diseases*, J.D.A. Matthew M. LaVail., Robert E. Anderson., (Eds), Editor, Springer Science + Business Media,LLC 2012. p. 353-362.
195. Glockle, N., et al., *Panel-based next generation sequencing as a reliable and efficient technique to detect mutations in unselected patients with retinal dystrophies.* Eur J Hum Genet, 2014. **22**(1): p. 99-104.
196. Maria, M., et al., *Homozygosity mapping and targeted sanger sequencing reveal genetic defects underlying inherited retinal disease in families from pakistan.* PLoS One, 2015. **10**(3): p. e0119806.

APPENDICES

1. Blood collection:

Venous blood was collected from cases and the families after obtaining their consent. The blood was collected using 10ml vacutainers with sodium heparin/Acid-Citrate-Dextrose (ACD) as the anticoagulant.

2. DNA Extraction:

Principle

The genomic DNA was extracted from heparinised/ACD whole blood by Nucleospin Blood XL Kit (Macherey-Nagel, GmbH, Düren, Germany). Lysis is achieved by incubating the whole blood in a solution containing large amounts of chaotropic ions in the presence of Proteinase K. Appropriate conditions for binding of DNA to the silica membrane of the columns are created by addition of ethanol to the lysate. The binding process is reversible and specific to nucleic acids. Washing steps efficiently remove contaminants. Finally, pure genomic DNA is eluted under low ionic strength conditions in a slightly alkaline elution buffer. The average yield of DNA is 200-300 ng/µl.

Reagent Preparation

Proteinase K: 126 mg of proteinase K [lyophilized form] was dissolved in 5.75 ml of proteinase buffer. It was stored at 4°C.

Wash Buffer: To 50 ml of wash buffer [BQ2] provided in the kit, 200 ml of absolute alcohol (ethanol) was added.

Procedure

Lysis of blood samples

- 500 µl of proteinase K was taken in a 50 ml collection tube.
- Blood sample was added along the sides of the tube containing proteinase K.
- If the volume of the blood was <10 ml, the volume was made up to 10 ml with PBS.
- If the volume of the blood was <5 ml, the volume was made up to 5 ml with PBS and the volume of proteinase K, lysis buffer and ethanol was also reduced to half the volume mentioned.
- 10 ml of lysis buffer was added to the blood samples.
- The tube was shaken vigorously for 4 min.
- The tube was placed in 56°C shaking water bath for 15 min.

Adjusting DNA binding conditions

- 10 ml of chilled absolute alcohol was added to the lysate after it had cooled to room temperature and shaken vigorously for 4 min.

Binding of DNA

- Half of the lysate was transferred to the Nucleospin® Blood XL column placed in a 50 ml collection tube and centrifuged at 4500 rpm for 3 min.
- The flow through was discarded into 3% sodium hypochloride solution after removing the column.
- The sides and the rim of the collection tubes are wiped clean and the remaining lysate transferred and centrifuged at 4500 rpm for 4 min.
- The flow through was discarded and the sides of the tubes are wiped clean.

Washing and drying of the silica membrane

- The column was washed with 7.5 ml of wash buffer and centrifuged at 4500 rpm for 2 min.
- The above step was repeated with the centrifugation time increased to 20 min to ensure complete drying of the column.
- The column was transferred to a fresh 50 ml elution tube.

Elution of DNA

- 750 µl of elution buffer pre-heated to 70°C was added to the column and left at room temperature, overnight.
- The DNA was eluted completely by centrifuging at 5000 rpm for 6 min.
- This was transferred to a 1.5 ml vial labeled as first elute. It was stored at 4°C for immediate use or at -20°C for long term storage.
- 1000 µl of elution buffer pre-heated to 70°C was added to the column and left at room temperature, overnight.
- The column was centrifuged at 5000 rpm for 6 min.
- The eluted DNA was transferred onto the same column and this process was repeated everyday till fifth day.
- At the end of fifth day, the final elute was transferred into a 1.5 ml vial labeled as 2-5 elute and stored at 4°C or -20°C.

3. Quantification of extracted DNA

Nucleic acid was quantified using Nanodrop (ND 1000) spectrophotometer. Initialization was done by placing 2 µl of sterile water. The elution buffer from the Nucleospin Blood XL kit was used as a blank. Two µl of the sample was placed on the pedestal and the absorbance read and noted.

4. Affymetrix HMA GeneChip processing work flow:

Precaution:

- All the reactions were performed on ice in a cooling chamber
- The reaction protocol were set only in ABI 9700 Thermocycler (Applied Biosystems, Foster City, California)

i) **Genomic DNA preparation:** The genomic DNA concentrations were determined and dilutions were made to obtain a working stock of 50ng/µl using reduced EDTA TE buffer (pH 8.0). 5.0 µl of each DNA aliquot was taken for the next step.

ii) **Restriction Enzyme Digestion:** The digestion master mix was prepared as below.

Reaction protocol for restriction enzyme digestion

Reagent stock	**Per sample (in µl) for 10K array**	**Per sample (in µl) for 250K array**
Water	10.5	11.55
NE buffer	2	2
BSA	2 (10X (1mg/mL))	0.2 (100X (10mg/mL))
Restriction enzyme	0.5 Xba1 (20U/µl)	1.0 Nsp1 (10U/µl)
Total	15	14.75

Five µl of genomic DNA was added to the digestion reaction mixture, vortexed and the digestion performed in ABI 9700 thermocycler at 37˚C (120min) followed by 70˚C (20min) for 10K array and at 37˚C (120min) followed by 65˚C (20min) for 250K array and hold at 4˚C.

iii) **Ligation:** The ligation master mix

Reaction protocol for preparation of ligation mixture

Reagent	**Per sample (in µl) for 10K array**	**Per sample (in µl) for 250K array**
Adaptor	1.25 XbaI (5µM)	0.75 NspI (50 µM)
T4 DNA Ligase buffer (10X)	2.5	2.5
T4 DNA Ligase (400U/ µl)	1.25	2
Total	3.75	5.25

The digested genomic DNA was added to the ligation mixture, vortexed and placed in thermocycler with the profile; 16˚C (120min for 10K array; 180min for 250K array) followed by inactivation at 70˚C (20min) and 4˚C hold. The ligated product was diluted with 75 µL molecular biology grade water giving a total volume of 100 µL.

iv) PCR: PCR master mix

PCR reaction protocol

Reagent	**Per sample (in µl) for 10K array**	**Per sample (in µl) for 250K array**
PCR buffer (10X)	10	10
dNTP (2.5mM)	10	14
MgCl2 (25mM)	10	-
GC-Melt (5M)	-	20
PCR Primer	7.5 XbaI (10µM)	4.5 primer 002 (100 µM)
Taq (5U/µL)	2 (Amplitaq Gold) (Applied biosystems, Fostercity, California)	2 (Titanium *Taq)* (Clontech Laboratories, Takara BioCompany, Canada)
Water	50.5	39.5
Total	90	90

A total four reactions were set for 10K array while 3 reactions for 250K array. Ninety µL of PCR master mix was added to 10 µL of diluted ligated DNA making a total of 100 µL. The PCR was performed in the thermal cycler and programmed as follows.

Thermal cycler profile for PCR for 10K GeneChip

Phase of the cycle	**Temperature ˚C**	**Time (secs)**	**Cycles**
Initial Denaturation	94	180	1x
Denaturation	94	20	35x
Annealing	60	15	
Extension	68	15	
Final extension	68	420	
Hold	4	Infinity	

Thermal cycler profile for PCR for 250K GeneChip

Phase of the cycle	**Temperature ˚C**	**Time (secs)**	**Cycles**
Initial Denaturation	95	180	1x
Denaturation	95	20	35x
Annealing	59	15	
Extension	72	15	
Final extension	72	420	
Hold	4	Infinity	

3 µL of the PCR product was mixed with 3 µL of 2X gel loading dye on 2% TBE agarose gel and electrophorised at 120V for 1hr.

2% Agarose gel photograph of 10K array PCR product

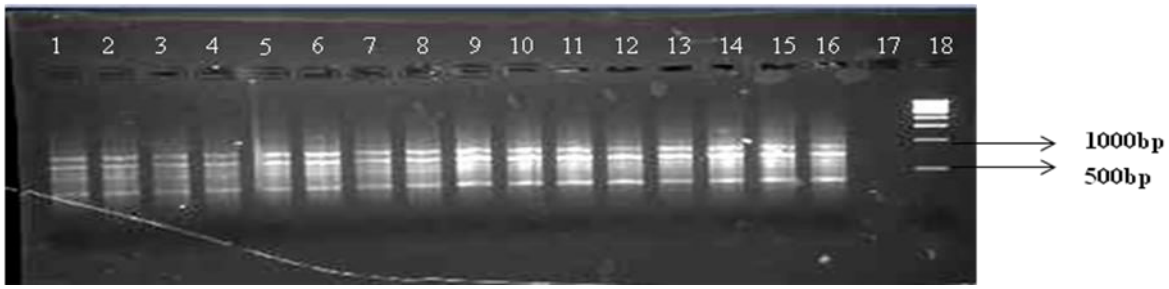

Legend:

Lane 1 - 4: Sample 1

Lane 5 – 8: Sample 2

Lane 9 – 12: Sample 3

Lane 13 – 16: Sample 4

Lane 17: Negative control

Lane 18: 500bp ladder

2% Agarose gel photograph of 250K array PCR product

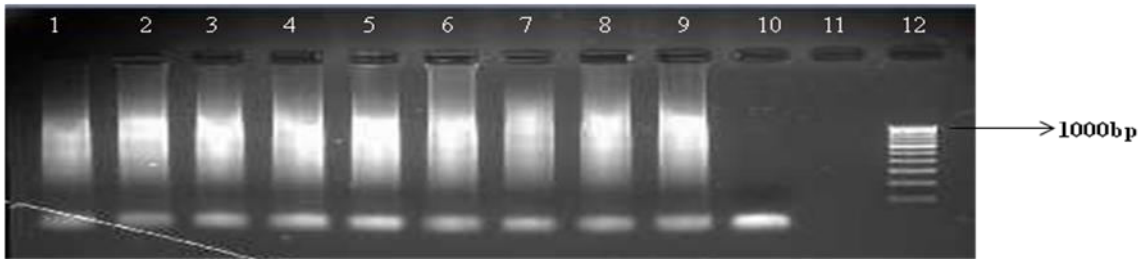

Legend:

Lane 1 - 3: Sample 1

Lane 3 – 6: Sample 2

Lane 7 – 9: Sample 3

Lane 10: Negative control

Lane 11: Empty well

Lane 12: 100bp ladder

v) **Purification, elution and quantification of PCR product:** Purification was performed using 96 Ultra Filter (UF) PCR purification plate and vacuum manifold. All four or three PCR products were consolidated into a single well of the purification plate and vacuum of ~ 800mbar (10K array)/ ~ 600mbar (250K array) was applied, respectively. The PCR products of the 250K assay were diluted with 0.1M EDTA (8 µL) before proceeding with purification. The process of purification and drying takes approximately 90-120 minutes. The PCR products were washed three times with 50µL of molecular biology grade water for approximately 20 mins. Following this 40 µL elution buffer (10K array)/ 45µL of RB buffer (250K array) was added to elute the product. After elution, a 40 fold (10K array)/ 100 fold (250K array) dilution with water was performed for each sample and quantified using NanoDrop 1000 spectrophotometer.

Further, final dilutions were made to get a concentration of 20 µg/45 µL (10K array)/ 90 µg /45µL (250K array) with elution buffer and RB buffer, respectively. This was further taken for fragmentation.

vi) **Fragmentation:** 5 µL of fragmentation buffer (10X) was added to the purified diluted PCR product making a total volume of 50µL fragmentation mix. The fragmentation reagent was prepared separately according the manufacturer's instructions. Depending on the concentration of Fragmentation reagent (2U/µL or 3U/µL) the preparation of Fragmentation mix varies.

Fragmentation Mix Reagent Preparation

Reagent	**Fragment Reagent Concentration**	
	2U/ µL	3U/ µL
Accugene water	5.25	5.30
Fragmentation Buffer	0.6	0.6
Fragmentation	0.15	0.1
Total	**6.0**	**6.0**

Five µL fragmentation reagents was then added to the fragmentation mix. The fragmentation thermal cycler protocol included incubation at 37˚C (30min, 10K array /35min, 250K array), denaturation at 95˚C (15mins) and 4˚C hold. Four µL of fragmented PCR product was diluted with 4 µL gel loading dye and run on 4% agarose gel at 120V for 30 min-1hr.

4% Agarose gel photograph of 10K array Fragmented PCR products

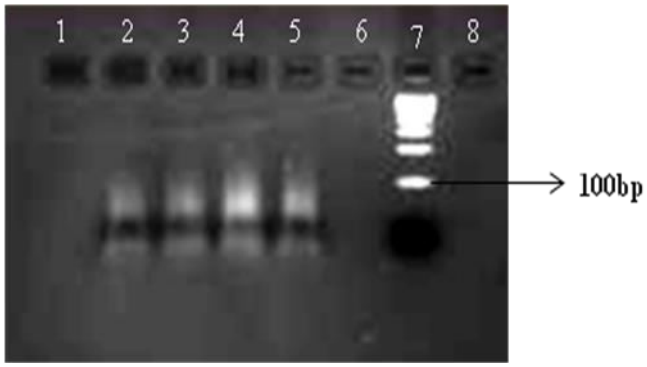

Legend:
Lane 1 & 6 & 8: Empty wells
Lane 2: Sample 1
Lane 3: Sample 2
Lane 4: Sample 3
Lane 5: Sample 4
Lane 7: 100bp ladder

4% Agarose gel photograph of 250K array Fragmented PCR products

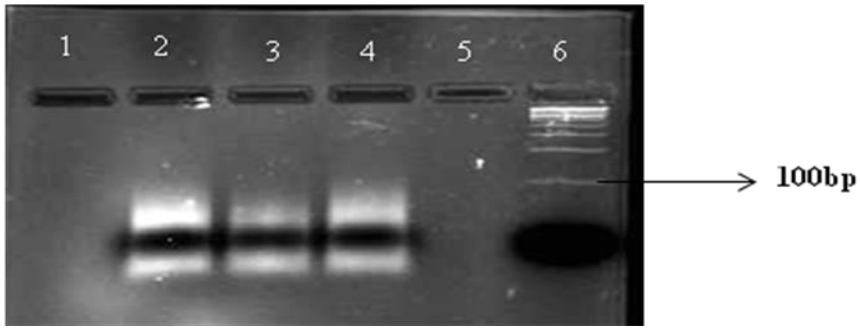

Legend:
Lane 1& 5: Empty wells
Lane 2: Sample 1
Lane 3: Sample 2
Lane 4: Sample 3
Lane 6: 100bp ladder

vii) **Labeling:** The labeling master mix was prepared as below

Reagent	**Per sample (in µl) for 10K array**	**Per sample (in µl) for 250K array**
5 TdT buffer	14	14
Gene chip DNA labeling reagent	2	2
TdT (30U/ µL)	3.4	3.5
Total	19.4	19.5

To 20µl of labeling mixture, 50µl of fragmented DNA was added. After brief vortexing the mixture was thermal cycled at 37˚C (2hrs, 10K array/4hrs, 250K array), 95˚C (15min) and 4˚C hold.

viii) **Hybridization:** The hybridization cocktail was prepared as follows. It was same for both 10K and 250K array.

Reagent	**Per sample (in µl)**	**Final concentration**
MES (12;1.22M)	12	0.056M
DMSO (100%)	13	5%
Denhardt's solution (50X)	13	2.5
EDTA (0.5M)	3	5.77mM
HSDNA (10mg/mL)	3	0.115mg/mL
Oligonucleotide control	2	1X
Human Cot-1 (1mg/mL)	3	11.5µg/mL
Tween-20 (3%)	1	0.0115%
TMACL (5M)	140	2.69M
Total	190	-

Seventy µL of labeled sample was transferred to the 190 µL hybridization mix. This was then subjected to denaturation at 95˚C in a heat block for 10min and cooled in crushed ice for 10secs.

Following this 80 µL (10K array) and 200 µL (250K array) of hybridization mix was injected respectively, into the array GeneChip and placed in hybridization oven (GeneChip®Hybridisation Oven 640, Affymetrix, Santa Clara, CA) at 48˚C (10K array)/ 49˚C (250K array) for 16-18hrs at 60rpm.

Washing & Staining: After hybridization, the cocktail was removed from the probe array and in turn filled with 80 µL (10K array)/ 270 µL (250K array) of array holding buffer. Following this, staining of the array probe was done in the Affymetrix Fluids Station (GeneChip® Fluidics Station 450, Affymetrix, Santa Clara, CA). This involves 3 major steps, Streptavidin Phycoerythin (SAPE) stain, followed by antibody amplification step and final stain with SAPE again. The washing and staining procedures were done using programmed protocol in the automated fluidics station. The washing and staining steps are complete in 120 minutes. After staining the array was filled with the array holding buffer.

Preparation of wash buffers and stains for the Affymetrix GeneChip:

i) Stain buffer:

Components	**1x (in µl)**	**Final concentration**
Water	800.04	
SSPE (20X)	360	6x
Tween-20 (3%)	3.96	0.01%
Denhardt's solution (50X)	24	1x
Subtotal	1188	

ii) SAPE solution:

Components	1x (in µl)	Final concentration
Stain buffer	594	1x
1mg/ml SAPE	6	10µg/mL
Total	600	

iii) Antibody stain solution

Components	1x (in µl)	Final concentration
Stain buffer	594	1x
0.5 mg/ml SAPE	6	5µg/mL
Total	600	

iv) Array holding buffer

Components	Volume (ml)
MES stock buffer (12X)	8.3
5M NaCl	18.5
Tween-20 (10%)	0.1
Water	73.1
Total	100

ix) **Scanning:** Following washing and staining, the arrays are checked for large bubble or air pockets; if present they are removed and refilled with array holding buffer with respective volumes as mentioned earlier. Scanning was performed in the GeneChip® Scanner 3000 7G (Affymetrix, Santa Clara, CA) using Affymetrix GeneChip Operating Software 1.4. The .CEL files generated were analyzed either by GTYPE (10K array) or GCOS software (250K array).

5. Primer Sequence

Gene	Exon	Primer sequence 5'-3'
MERTK		
	1	FP:GTTCGGGACGTCCATCTGT RP:TTTGCAAACTTGTCCAGCAG
	2a	FP: TTATCTTTTCCTGGGGCACA RP:AACTGTGTGTTTGAAGGCAAGA
	2b	FP: TGACCACACACCGCTGTTAT RP: GGCATCATGGTGAAACCTCA
	3	FP: AAGAAGTTGAAGAAGTTTCCATCC RP: CAGAGTTATAAATAGGCAGGCAAAA
	4	FP: TCCAGTTTCCATTCCCCTTT RP: ATCTGTCTCCACTGCCTGCT
	5	FP:CCAAAAGCCATGAACCAAGA RP:CCCTGACACCAAAGAGGAGA
	6	FP: GCTGTAGCCTGTCATCTATAATTGTG RP: GAAGAAAAATCCTTAAACCCACAG
	7	FP: AAATGTGTGTGTGCCCAGAA RP: TGGGAAGGGTTTGTTGAATC
	8	FP: CACTTGAAAACCCAGATGAGAA RP: TTCTAAAACTGAAGTAAACCAGCAA
	9	FP: GCTGTGGAAGTGTGGCTTCT RP: ATCCATCCCCCAGGTTACTT
	10	FP: TTCGCATGGTCTCAGCTTAC RP: CCAACAGGAAAGGCATAATCA
	11	FP: CATCCTTGTGGAATCAGTGC RP: TTTGGCTTTTGTTAGAAATCTGTC
	12	FP:TTTAATTATCAAGTGAAAGAAAACACG RP: TGTGCCAGATCTGAGTTTCAA
	13	FP: TGGGTGAGTTGCTCTCATACC RP: CCTCATGGAGCACCCAATAC
	14	FP: CTCCCCTAGCCCTACTAGCC RP: TCTGGGTGAAAACCTCAATG
	15	FP: GGCTTCAGTTTTTCCAGTGGT RP: TGGCTTCACTTTCAAGATTAGATG
	16	FP: TGTTTCCTTATTTCATCACTACACTG RP: AGGCAGTGAAAACTCCCAAA
	17	FP: GGCTGGTGGTGTCTCTGTGT RP: GCCATACCAGCTGAGGTCAT
	18	FP: GAGCAGTGCGTCTCACACAT

		RP: TGGCTAACAGCAGTCCCTTT
	19a	FP: TCTGTAAAAACAAAGGCATGGA RP: CAGGGTCGATGTTCAAGTCC
	19b	FP: CGGAACCAAGCAGACGTTAT RP: AAACATCAGGTACAATTGGATTCTC
RPE65		
	1	FP:GAGAGCTGAAAGCAACTTCTG RP:ATAGCACATTTATCATGAATCCATG
	2	FP:CTATCTCTGCGGACTTTGAGC RP : GCCAGAGAAGAGAGACTGAC
	3	FP : GGCAGGGATAAGAAGCAATG RP : CTGAGTTCAGAGGTGAAAAC
	4 & 5	FP : CTGTACGGATTGCTCCTGTC RP : TTAGAATCATACATTCGCAGCATG
	6	FP : TATAATGTATCTTCCTTCTCTCAAC RP : CTCACAATACAGTAACTTTCTCAC
	7 & 8	FP : AAATAAGAGGCTGTTCCAAAGC RP : TTAAACACATCTTCTTCAGAATCAC
	9	FP : GTACACTTTTTTCCTTTTTAAATGCATC RP : GTTTTAGATGTGATTCAGATTGAGTG
	10	FP : TTGTCATTGCCTGTGCTCATG RP : TGAGAGAGATGAAACATTCTGG
	11	FP : AATTCTTTCCTGCTCACTGA RP : GTTACC TCCCGTGTGAAGTT
	12	FP : GAGTTTTCCTAAGCATGTGC RP : AGCATATACTACAAGCAGTG
	13	FP : GCATATTGACTGATTGCTTG RP : GCAGTAAGAAGAGTATTCAG
	14	FP : AGTCAGAAAAAGAAGTCAGGTC RP : ATTGCTTGCTCAACTCAGTGC
CRB1		
	1	FP:AAGAAAACTCGCAGCAAAGG RP:TTTTATAGAACATGCAACATTATCCA
	2A	FP: GCAGCACAAAGGTCACAAAG RP:TCTTCCAGCATATCCAGCAG
	2B	FP: TCTGTGCAAATGTCCTCCTG RP: AAATGTCACCTCTGCTTCTGC
	3	FP: TGACAAGTGCTCTGGTAAACAAA RP: TAAGCCGAGAACGTGAGAGC
	4	FP: GGGTTGATAGACAGTTGAAGAAA RP: TCATTTGCTATAAGCGATATGTG
	5	FP: CCTCCTTTTAGGCAAATGCTC

		RP: AAAGCCATGGTCTGCCATAA
	6A	FP: GCTATTCATGCACTTCTGCAA RP:CAAACTGAGCCCTTGGTTGT
	6B	FP: CGGGTCCCTGTGTGAAAT RP:GCCTACAAACGAAGGTGTGG
	6C	FP:CAGAACTCCTTTTTGGGTGGT RP: TTTCATAGCAGGCAGAAGCA
	7	FP: TTCGTCTTCCATCCCTTCTG RP: GGCCTCATTTCTATGGCTCA
	8	FP: TTTCACCGTCAACATTTTTCT RP: TTGCTCTTGGAACAACTCAAA
	9A	FP: TGGCATGCATTAGGATTTCA RP: TGTTTCGTTGTCCACTTCCA
	9B	FP:TCAATTGCAAAGTGGCAACA RP: CAGTGTTTCCCTGACCATCC
	9C	FP:TTCTCAAAATCTCTACCAATTCAGTG RP: CAGTGTCACCCTGTTCAGCA
	10	FP: AGCTTGGCATTGACTACATACA RP: TCCCATCATTCTTTAGCTCAG
	11	FP: TTCCCATTTCACAACCAATGT RP: GCTCGTCATTCATACGCAAA
	12A	FP: GCTTGCTCTGGTTGGTCTTC RP: GCGGAACCACTGTGAAAGTT
	12B	FP:ACCTGACAATGTTAATCTGCAA RP: AATTCATAAGCAGGTTCTTCAAA
	CRB1 TRANSCRIPT 3 EXON1	FP:AGCCAACGAACACGTCAAC RP: GCACCTCGGCAAACTACTTC
	EXON2	FP: TTGCCACAGCCATCTCAG RP: AATATTCCCCCACATTTTGC
	EXON3	FP:CCCCAAAATCTTCATAGCACA RP: TGAAGGCTGAGCAAGTCAAC
	EXON 10	FP:CCCAGGACAAACACAGTTCAT RP: GCACAAGGAGGGTTTTTCAA
IQCB1		
	1	FP: AGCGTCTCACGTTCTGATTG RP:AGTCCTGGCCTCCTGGTAG
	2	FP: ATTTAGGATCAGCCGCAACA RP:TTCAACACTTCTCCCATCTTTACA
	3	FP: GAATCTTGAGCTCTTTTACACTGG RP: CATCCAGGAGCTATTTGTATTTTT
	4	FP:AAAAATACAAATAGCTCCTGGATG

		RP:GCAAATGTTGAAAATCAGAATCA
	5	FP:GCACAGTGTCTCTAGAAGCTTGA RP:CTTTCAGCCAAATATTGCACA
	6	FP:AAGGCAACAAAATCATGTCC RP:CATGGTTTCATTTCAGTGTGG
	7	FP:AAGTTTAGCAGAGATGGTCATGC RP:TGGTGATGGAACTTCAGCATT
	8	FP:CACAGTCCGGCATCAAGTTA RP:TTTTCTGAATTGGTATCTGTTGTGA
	9	FP: AGAATTCTCAGGAGGGAGGAA RP:GTGGCTACTCATGGGTGTGA
	10	FP: TTGCCTTACCAAGCCTAACA RP: GGATTGCATATTTGACACATCAG
	11	FP: CACAACAGCAGCAGATGACA RP: TCATCACGTAGCTAGAAAAGTTGG
	12	FP: TCATTGTCCTGATTCCAGAACTT RP: CAGGTAATTAGCAAAGTCAGTTTTGA
	13	FP:TCCCCTCCTTATACACACTCAGA RP: CAATGCATTACCTTATACCAGCA
	14	FP: CCTCTGCTAAGTGGTTGGGTA RP: TTCCTGAGGTTAGGGGATGA
	15A	FP: TCAAAAGTAGTACATTCAGAGTTGGAA RP: TTTGCTTACTGCAGGTCTTGTC
	15B	FP: TTTTAGGAGATTATATTGGTTCTGC RP: GCTTTGAGATTCCTAGGAGAAAA
AIPL1		
	1	FP:GGACACCTCCCTTTCTCC RP:GCTGGGGCTGCCTGGCTG
	2	FP:GGGCCTTGAACAGTGTGTCT RP:TTTCCCGAAACACAGCAGC
	3	FP:AGTGAGGGAGCAGGATTC RP:TGCCCATGATGCCCGCTGTC
	4	FP: TCCTGTTTTTCGGGTCTCTG RP: CCAGAGTCAGCGCCACTT
	5	FP:GCAGCTGCCTGAGGTCATG RP:GTGGGGTGGAAAGAAAAG
	6	FP:CTGGGAAGGGAGCTGTAG RP:AAAAGTGACACCACGATCC
RPGRIP1		
	1	FP: GACATCCTAAAGTTGCATG RP: GTTCCACAGTGAGAGTTC
	2	FP: CTCTCTGGACAAGATGTG

		RP: AAATTTAAGGAGAACTCTA
	3	FP: TAACTGTCATGAAAGGAGAAG RP: AGTCCTTCCCAGTGTCTT
	4	FP: GTTCCGGAGGGTACTGTT RP: CTTCCCTGATCATGCTGAA
	5	FP: CCTCGACATGTACCAAGGT RP: TTCCTCTGAGATGGAGGAA
	6	FP: AGGGCATAGTCAAGGAGAA RP: CTGAATTGTGGCTTCTCATA
	7	FP: GACTACTTGGCAAGCTAGG RP: TACTTGGAGATGAACATAGAT
	8	FP: CGTGCTGAGTGATATGACC RP: ACACATTCTAACATCCCTGA
	9	FP: GAAATCCTGTGCAGGGGAA RP: TCATAGTAACACTGCTCTG
	10	FP: ACGTCATATCACACCCCTT RP: GAGGTAGAGGATGCCACA
	11	FP: TGGTGATAAATAACTACAGAAT RP: GCCAGAGATCTCTCTGCAG
	12	FP: CCTGTCATATTTATACTCCCT RP: TTCCCACGTTCCTGTTATC
	13	FP: TTGGTTTTAGGCCACTGAGA RP: CTGTGGAAGGGTCCCGAA
	14	FP: GAAAGAGCTCCCTACCCTT RP: GGAAATTCTGCATTGGTGC
	15	FP: CTTGCCACACCATCTGTAT RP: GTTTGGCTGAGGCTCCTC
	16	FP: ACAGTCTCAAGCTGCCCTT RP: AGACAACACTGGGAAGAGG
	17	FP: CTTATTTCATGTGATCAGGTC RP: CATAGGATTGGCAGAGATC
	18	FP: GTTGTTAAACTACCAGCTTG RP: GGGACACTACAACCCACAA
	19	FP: CCAAGATATTACCAGCTATG RP: AGCCTGATCTCGTGATCTG
	20	FP: GGCTAAAGTGCTTTGAAACA RP: TATCGTCTTATCTCGTATGC
	21	FP: CTTGGAGCCTCACTAACC RP: TTCATCAGACTTCCTCACC
	22	FP: CACTGCAACAGTATATGATTC RP: CTGTCTCAATATCTCCTTTG
	23	FP: GCATTAAGAGTATCAACAGTG

		RP: TTAGGATGATTTCCTTGGAA
	24	FP: AGTGTTCAACTGAGTGATGC RP: ACTATGGTTCCCTCAGAGAC
RDH12		
	1	FP:AAGCAGCCAAGAGCTGGAG RP:TGCCCTGACTTTCTCCTCTG
	2	FP:ACCCTTCTTTGAGGCTGGAT RP:TTGAATCCCAGGTTCCTTGA
	3	FP:AAGGATGGCTGGGAGAATG RP:TAGTGGGGTGGATGATGGTT
	4	FP:GGGCAATTATGCAGGTCTGT RP:AACAACAAGCCAATGGGTCTA
	5	FP:GGCATCAAAATTGGTTCACA RP:GGGGCAAGCACTCTGTTTT
	6	FP:TTGCTGCAGGAGATAAGCTG RP:GAAAAGCGGCACACGAGTAT
	7	FP:TCTGCTCGCCACTACTTTGA RP:AGCTGGCCAAGAGGACAAT
SPATA7		
	1	FP: GTCGGCTCCTCTTTTCCAG RP: CCCTGACAGCTGCCCTTTAC
	2	FP:TGAATATTGTTGTTTTTGTAAAAGTTG RP: TTGCCAGTAAAGGAAACACTCA
	3	FP: CATTGGCATTATCAGTGCAAG RP: CCAAACAAATACAAATCCTCTCA
	4	FP: ACAGCTGCAAGGTCTGGAAC RP: GCAGTATAAAGAGAGTTCTGGAGGT
	5	FP: TCTAGAGGCACATGTGAAATAAAT RP: CAAAGTCAGATTGTACCACTAAAGAA
	6A	FP: AAACCCTTGAGGCTATCATTTTT RP: CTTCTCAGGACCATTTGTGATG
	6B	FP: AACCGCAAATTGAGGATGAC RP: ATCTTAAGGCTGGCAGCAGA
	7	FP: TTCTAGCCAGTAAACCTTGTTACC RP: CCACCAACAGATTATTCTTCACA
	8	FP: AAAAAGTGCTGGATGGATAGAA RP: CATTTCAACTTTTACTAAGCACTTCA
	9	FP: TCCAAACATCTAAGATAAGGGCTAT RP: CAATCCTGACTTATTTAATATGGTTTC
	10	FP: TGATTGCGCCTTGTCCTT RP:ATGGGATTATGGAGCTTTGC
	11	FP: CAACCTTTGTAGTTTCAGTGTTACG

		RP: GCACTTGCTTTTAATGTATTGTTTG
	12A	FP: AGATTTTCAGCACTGCAGTCA RP: CATCCTTTGGTGCCGACAAT
	12B	FP: CCTGCTGCATGTCCTGAAAG RP: ACATTCACAGAAGTTTCCCGA
	12C	FP: AGAACGAGATATTCCCTTCACCA RP: TGAGTTACTGGCCATTTGAGG
ABCA4	11	FP: ATGGACTTGGGGAAATGGGA RP: AGCTTTCATTTTCCCCACTGA
CDHR1	13	FP: GGAGACACGGCAGATGGAT RP: GGACAGCTAATGAGTGTGGG

6. **Annealing Temperature and the product size for nine candidate genes that were screened are listed.**

Genes	**Exons**	**Annealing Temperature**	**Product size**
MERTK			
	1	60	238
	2a	60	362
	2b	62	616
	3	60	293
	4	60	355
	5	60	354
	6	60	250
	7	60	391
	8	59	300
	9	60	366
	10	59	395
	11	59	250
	12	59	343
	13	60	262
	14	59	399
	15	60	300
	16	59	409
	17	60	365
	18	60	385
	19a	60	291

	19b	60	484
RPE65			
	1	54	244
	2	54	199
	3	52	282
	4 & 5	54	501
	6	56	269
	7 & 8	54	545
	9	56	292
	10	56	226
	11	48	197
	12	48	176
	13	47	199
	14	53	453
CRB1			
	1	60	458
	2A	60	441
	2B	60	445
	3	60	392
	4	60	300
	5	60	317
	6A	60	453
	6B	60	496
	6C	60	399
	7	60	816
	8	60	300
	9A	60	687
	9B	60	492
	9C	60	499
	10	60	280
	11	60	283
	12A	60	481
	12B	60	596
	CRB1 TRANSCRIPT 3 EXON1	60	287
	EXON2	60	615
	EXON3	60	352
	EXON 10	60	355

GUCY2D			
	1	60	108
	2	60	835
	3	60	381
	4	62	444
	5	62	294
	6	62	205
	7	60	204
	8	62	179
	9	64	295
	10	63/56-56	235
	11	62	220
	12	64	260
	13	64	277
	14	64	253
	15	64	260
	16	60	199
	17	60	166
	18	60	152
	19	66/59-59	189
	20	63/56-56	210
IQCB1			
	1	60	250
	2	60	231
	3	60	494
	4	60	297
	5	60	294
	6	60	364
	7	60	406
	8	60	424
	9	60	529
	10	60	499
	11	60	383
	12	60	300
	13	60	400
	14	60	351
	15A	60	499
	15B	60	595
AIPL1			
	1	69/61-61	240

	2	63/56-56	297
	3	63/56-56	364
	4	60	315
	5	60	279
	6	63/56-56	497
RPGRIP1			
	1	56	231
	2	46	245
	3	50	366
	4	54	262
	5	52	450
	6	50	282
	7	53	282
	8	56	257
	9	51	175
	10	56	311
	11	53	261
	12	56	278
	13	53	247
	14	52	553
	15	56	251
	16	56	450
	17	53	278
	18	65/58-58	301
	19	56	258
	20	54	194
	21	56	287
	22	53	181
	23	52	228
	24	56	203
RDH12			
	1	60	284
	2	60	359
	3	60	375
	4	60	326
	5	60	493
	6	60	492
	7	60	469
SPATA7			
	1	60	144

	2	60	211
	3	60	390
	4	60	312
	5	60	397
	6A	60	249
	6B	60	558
	7	60	250
	8	60	477
	9	60	250
	10	60	700
	11	60	243
	12A	60	300
	12B	60	390
	12C	60	396
ABCA4	11	60	493
CDHR1	13	60	350

7. Agarose Gel Electrophoresis:

The amplified products were loaded in 2% agarose gel to check for specific amplification.

Requirements

1. Gene Ruler 100bp: Molecular weight marker (Thermo Fisher scientific, Waltham, MA, USA)
2. Agarose (SRL, Mumbai, India)
3. 10X TBE buffer

Tris	-	50.0gms
Boric acid	-	27.5 gms
EDTA	-	3.72gms
Distilled water	-	500ml

4. Ethidium bromide (2mg/ml concentration)

5. Tracking dye- Bromophenol blue (BPB)

   Bromophenol blue - 0.1gm

   1X TBE buffer - 100ml

   Sucrose - 40 gms in 100 ml water

   Mix equal volumes of 0.1% BPB and sucrose.

Agarose gel preparation

The gel trough was cleaned with ethanol and the ends were sealed with the cellophane tape. The combs were placed in the respective positions to form wells. Weighed 0.5gm of agarose and dissolved in 25ml of 1X TBE buffer (2% agarose gel). The agarose was melted in microwave oven and 10µl of ethidium bromide was added to the molten agarose. This was poured on to the sealed trough and allowed it to set in dark.

Agarose gel Electrophoresis

After the gel solidified, the cellophane tapes and combs were removed and the trough was placed in electrophoresis tank containing 250ml of 1X TBE Buffer. Five µl of amplified DNA product was mixed with 5µl of 0.1% bromo phenol blue and loaded on to the wells. One µl of Molecular weight marker was diluted with 10µl of autocloaved milliQwater and mixed with 5µl of bromo phenol blue and loaded onto the wells. The productes were electrophorised at 120V for 20 to 30 min. The gel was captured by gel documentation system Bio-Rad Gel Doc XR System, (Bio-Rad, California, United States) and analysed using Quantity one 1-D software.

8. Exo SAP digestion:

Shrimp alkaline phosphotase (SAP) dephosphorylates unutilized nucleotides and exonuclease (ExoI) degrades unutilized primers which may interfere with downstream process like sequencing.

ExoSap digestion protocol:

Reagents	Reaction volume in µl
SAP (ThermoFisherScientific, Waltham, MA USA)	1.0
Exo (ThermoFisher Scientific, Waltham, MA USA)	0.5
PCR product	5.0

Thermal cycler profile of ExoSap digestion

Temperature ˚C	Time (min)
37	15
85	15

9. Cycle Sequencing:

Cycle Sequencing combines enzymatic amplification and termination using labeled dye terminators in a reaction that is subjected to annealing, extension and denaturation in thermal cycler. In the sequencing reaction, amplified extended products are terminated by one of the four dye labeled dideoxynucleotides. The ratio between the deoxynucelotides and dideoxynucleotides is optimized such that it produces a balanced population of short and long extension products. The terminated fragments are dye labeled at their 3' end. The Big Dye ready reaction mix (Applied Biosystems, Foster City,California) contains, deoxynucleoside triphosphate, dye labeled dideoxynucleoside triphosphate, AmpliTaq DNA polymerase, FS, rTth pyrophosphate, magnesium chloride and buffer which are

all premixed and is suitable for performing fluorescence based cycle sequencing reactions on single stranded or double stranded templates. The four dideoxynucleotides are labeled with four different dyes.

Cycle Sequencing Protocol

Reagents	**Volume (µl)**
Amplified Product	1.0
Primer (1pmoles)	1.0
5X Sequencing buffer	2.0
RR mix	0.5
Milli QWater	5.5

Reaction conditions of Cycle Sequencing

Initial denaturation	96°C	60 seconds
Denaturation	96°C	10 seconds
Annealing	50°C	5 seconds
Extension	60°C	4 minutes

The reaction was carried out for 25 cycles.

10. <u>Purification of Cycle Seqeunced Extension Products</u>

Purifying the extended products helps to remove the unincorporated dye terminators before the samples are analysed by capillary electrophoresis. Excess dye terminators in sequencing reactions obscure data in the early part of the sequence and can interfere with base calling.

Reagents Required:

i. 50mM EDTA.
ii. 3M Sodium acetate (pH 4.6).
iii. Absolute ethanol.
iv. 70% ethanol.

Procedure

- A one in four dilution of 50mM EDTA with milliQwater was done.
- In a 0.5ml vial 10µl of autoclaved milliQ water followed by 2µl of diluted EDTA (final concentration 125mM) was added.
- Added 50µl of absolute ethanol and 2µl of 3M sodium acetate.
- To the above mixture 10µl of the cycle sequencing product was added and mixed throughly by vortexing.
- This was left at room temperature for 15 minutes. Microfuged at 10,000rpm for 20 minutes. Discarded the supernatant and added 200µl of 70% ethanol.
- Vortexed and microfuged at 10000rpm for 10 minutes.
- The 70% ethanol wash was repeated twice.
- Discarded the supernatant and the vial was left at room temperature overnight for drying.
- Before loading 10-12uL of Hi-Di formamide was added, vortexed, denatured at 95^0C for 3 minutes and then loaded on to the genetic analyzer.

11. <u>Sequencing in *ABI Prism Avant 3100 & 3730*</u> Genetic Analyzer (Applied Biosystems, Foster City, California)

Automated sequencer adopts capillary eletrophoresis where the amplififed and dye lebeled terminated fragmments are seperated. Each dye emits light at a different wavelength when extited by an argon ion laser. This is captured as raw data. Hence all four bases can be detected and distinguished in a single lane or capillary.The cycle seqeunced and purified products were subjected to capillary electrophoresis by an automated sample injection. During electrophoresis, when the labeled fragments pass through the window region of the capillary, the dyes get exited and the emitted raw data is collected at the rate of one per second by cooled, charge-coupled device (CCD) camera at particular wavelength bands (virtual filters) and stored as digital

signals. These are further analysed by Seqeunce Analysis v2.5 software. The seqeunce data was also analyzed by BioEdit software.

The four nucleotide bases with the respective acceptor dyes and colour emission.

Terminator	Acceptor dye	Colour of raw data on electrophoretogram
A	dR6G	Green
C	dROX	Red
G	dR110	Blue
T	dTAMRA	Black

12. cDNA primers seqeunce encompassing exons 11-13 of *IQCB1* gene

Exons	Primer sequence 5'-3'
11,12,13	FP: TCCATCTGCTGTGATTGCTT RP: AGCTCCCTACTGACCACATC

13. Primers sequence for allele specific PCR for the identified mutation in *MERTK* c.721C>T p.(Gln241Ter), *AIPL1* c.247G>A p.(Glu83Lys) in the Fam 01 and Fam 09, respectively

Gene	**Exon**	**Primer sequence**	**Product size (bp)**
MERTK	Exon4	FP:TCCAGTTTCCATTCCCCTTT RP:ATCTGTCTCCACTGCCTGCT	355bp
	Exon4 Wild type allele specific primer	FP:AACAGTAGCCGTGTTAAgGAAC	161bp
	Exon4 Mutant allele specific primer	FP:AACAGTAGCCGTGTTAAgGAAT	161bp
AIPL1	Exon2	FP: GGGCCTTGAACAGTGTGTCT RP: TTTCCCGAAACACAGCAGC	316bp
	Exon2 Wild type allele specific primer	RP: CCAGAACTCGGCCtCCTC	217bp
	Exon2 Mutant allele specific primer	RP: CCAGAACTCGGCCtCCTT	217bp

14. Details of Bioinformatic tools

a) **Human Splice Finder (HSF) 2.4.1:** It is a tool which is used to predict the effect of mutations on splice-sites or to identify the splicing motifs in any human sequence. The HSF algorithm presents consensous value (CV) which indicate strength of the splice-site and ranges from 0 to 100. The splice-sites of CV higher than 80 are considered as strong splice-sites, 70-80 as less strong and 65-70 as weak, and a CV below 70 is considered to be non-functional. The threshold is defined at 65 for HSF. Every signal with a score above the threshold is considered to be a splice-site (donor or acceptor). When a mutation occurs, if the WT score is above the threshold and the score variation (between WT and Mutant) is under -10% for HSF, the mutation is considered to break the splice-site. Conversely, if the WT score is under the threshold and the score variation is above +10% for HSF, the mutation is considered to create a new splice-site. Thus potential splice-sites can be predicted using this software.

b) **Mutation Taster:** This tool is useful in predicting of the probable effect of missense, insertion, deletion and splice-site mutations. The scoring is based on aminoacid substitution matrix (Grantham matrix). For missense mutations a score of above 100 is significant and predicts it to be disease causing. For splice-site changes, the wild type and the mutant are scored and a confidence score of >0.3 for the mutant indicates gain of completely new splice-site.

c) **Polyphen-2:** Polymorphism Phenotyping is a tool which predicts possible impact of an amino acid substitution on the structure and function of a human protein using physical and comparative considerations. It uses eight sequence-based and three structure-based predictive features which were selected by an iterative greedy algorithm. Majority of them involves comparison of a property of the wild type (ancestral, normal) allele and the corresponding property of the mutant (derived, disease causing) allele which together define the amino acid replacement. The functional significance of an allele replacement is predicted from its individual features by Naive Bayes classifier and a mutation is appraised qualitatively as benign, possibly damaging and probably damaging.

d) **SIFT (Sorting Intolerant from Tolerant):** SIFT is a program that predicts whether the amino acid substitution affects protein function. SIFT presumes that important amino acids will be conserved in the protein family and so changes at well conserved position tend to be predicted as deleterious.It considers the position at which the change occurred and the type of the amino acid change and based on the normalized value predicts if an amino acid change is tolerated or deleterious (if the normalized value is less than the cutoff).

e) **Mutation Assessor:** It creates a multiple sequence alignment with the aim of identifying evolutionary conserved positions in turn contributing to the protein functional specificity. A conservation score is combined with a specificity score to determine a functional impact score (FIS). Variants classed as 'neutral' or 'low' are predicted not to impact protein function, whereas variants classed as 'medium' or 'high' are predicted to result in altered function.

f) **MutPred:** It is a web based application to classify whether an amino acid substitution as disease associated or neutral in human. The output gives a general score (*g*) i.e the probability that the amino acid substitution is deleterious/disease-associated and property score (*p*) where *p* is the p-value that certain structural and functional properties are impacted. Certain combination of high values of general scores and low values of property scores are referred to as hypotheses. Scores with $g > 0.5$ and $p < 0.05$ are referred to as actionable hypotheses, the prediction is considered to be Confident hypothesis if the general score corresponds to $g > 0.75$ and $p < 0.05$ and a very confident hypothesis is said when the general score corresponds $g > 0.75$ and $p < 0.01$.

g) **PMut (Pathogenic mutation prediction):** This tool mainly works based on the Neural Network scoring. The scoring of >0.5 signals pathological mutations. It also allows the fast scanning of mutation hot spots which are obtained by three procedures such as a) The pathogenecity index associated with the mutation through Ala (alanine-scanning) of all residues b) Maximum, mean and minimum pathogenecity index at each mutation site c) then maximum, mean, and minimum pathogenecity indexes associated with the genetically accessible mutations i.e (implying only one nucleotide change in each position of the protein).

LIST OF PUBLICATIONS

Pertaining to thesis

- **Srilekha S**, BhavnaRao, Divya M, Sudha D. Sathya Priya C, Pandian A.J, Soumittra, N, Sripriya, S. "Strategies for Gene Mapping in Inherited Ophthalmic Diseases". Asia Pac J Ophthalmol (Phila), 2016. **5**(4): p. 282-92.

- **Srilekha S**, Meenakshi S, Parveen Sen, Arokiasamy T, Swati Deshpande, Neetha John, Rupali Gadkari, Ashraf Mannan, Soumittra N. "Homozygosity mapping guided next generation sequencing to identify the causative genetic variation in inherited retinal degenerative diseases". J Hum Genet, 2016. doi:10.1038/jhg.2016.83. [Epub ahead of print].

- **Srilekha S**, Arokiasamy T, Srikrupa N N, Umashankar V, Meenakshi S, Sen P, Kapur S, Soumittra N. "Homozygosity Mapping in Leber Congenital Amaurosis and Autosomal Recessive Retinitis Pigmentosa in South Indian Families". *PLoS One*, 2015. **10**(7): p. e0131679.

Other publications

- M.Neuillé, S.Malaichamy, M.Vadalà,C.Michiels, C.Condroyer, R.Sachidanandam , **S.Srilekha**, T.Arokiasamy, M.Letexier, V.Démontant, J.A.Sahel, P. Sen, I.Audo, N. Soumittra and C. Zeitz. "Next-generation sequencing confirms the implication of *SLC24A1* in autosomal-recessive congenital stationary night blindness". Clin Genet, 2016. 89(6): p. 690-9.

- Khan NA, Govindaraj P, Soumittra N, **Srilekha S**, Ambika S, Vanniarajan A, Meena AK, Uppin MS, Sundaram C, Taly AB, Bindu PS, Gayathri N, Thangaraj K. "Haplogroup heterogeneity of LHON patients carrying m.14484T>C mutation in India". *Invest Ophthalmol Vis Sci*. 2013 May 14. pii: iovs.13-11925v1. doi: 10.1167/iovs.13-11925.

- Gandra Mamatha, Sundaramurthy **Srilekha**, Swaminathan Meenakshi, Govindasamy Kumaramanickavel "Screening of the RPE65 gene in thre asian Indian patients with Leber Congenital Amaurosis". *Ophthalmic genetics*. 07/2008; 29(2):73-8.

- Mamatha Gandra, Venkataramana Anandula, Vidhya Authiappan, **Srilekha** Sundaramurth**y**, Rajiv Raman, Shomi Bhattacharya, Kumaramanickavel Govindasamy "Retinitis pigmentosa: mutation analysis of RHO, PRPF31, RP1, and IMPDH1 genes in patients from India". *Molecular Vision*.2008. 14:1105-13.

POSTERS AND PRESENTATIONS

Pertaining to thesis

- **Srilekha Sundaramurthy**, Meenakshi Swaminathan, Parveen Sen, Tharigopala Arokiasamy, Swati Deshpande, Neetha John, Rupali Gadkari, Nagasamy Soumittra. Homozygosity mapping guided next generation sequencing (NGS) to identify the causative genetic variations in inherited retinal degenerative diseases. **Travel Fellowship award**, IERG ARVO India Chapter, Hyderabad, 2015.

- **Srilekha Sundaramurthy,** Meenakshi S, Arokiasamy T, Nagasamy Soumittra. Identification of causative gene/mutation in South Indian consanguineous Leber congenital amaurosis families by homozygosity mapping. **Best paper,** MGR University, Chennai, 2014.

- Nagasamy Soumittra, **Srilekha Sundaramurthy**, Tharigopal Arokiasamy, Parveen Sen, Meenakshi Swaminathan. Homozygosity mapping in Leber congenital amaurosis (LCA) in consanguineous south Indian families. **Best paper**, Asia Arvo, Delhi, 2013.

Other posters

- **Srilekha Sundaramurthy,** Jayaprakash Mani, Ambika SelvaKumar, Nagasamy Soumittra. Screening the three primary mitochondrial mutations in suspected Leber Hereditary Optic Neuropathy (LHON) patients of Asian Indian origin. ISHG, Chennai, 2016.
- **Srilekha Sundaramurthy,** Ambika SelvaKumar, Jagadeesan Madhavan, Nagasamy Soumittra. Screening of Mitochondrial Genes for the three primary Mutations in suspected Leber Hereditary Optic Neuropathy (LHON) patients of Asian Indian origin. ISHG, Chandigarh, 2012.

CONFERENCES AND WORKSHOP ATTENDED

- Attended International Conference 41st Indian Society of Human Genetics, Annual Meeting and International Conference (ISHG 2016) on "Celebrating Genetics – The Human Way", Chennai 2016.
- Attended a National conference on "Sanger to NGS – The Genomics Era" at Vision Research Foundation Chennai 2015.
- Attended a workshop on "Microarray Data Analysis" organized by DBT at M.G.R University, Chennai 2014.
- Attended International Conference on "Opthalmic Genetics and Genetic Counseling" at Narayana Nethralaya, Bangalore 2014.
- Attended a symposium on "Genetic counseling and Gene Testing" at Vision Research Foundation Chennai 2013.

LIST OF AWARDS

- **Travel Fellowship grant** at IERG ARVO India Chapter 2015 at Hyderabad.
- Received **Senior Research Fellowship** award ICMR January 2015. (Ref No.45/2/2014-HUM-BMS)
- Received **Best paper award** in a National Seminar on Function Genomics at Dr.M.G.R. University in February 2014.
- Bangalore Genei Private Endowment Award for Clinical Genetics May 2011.
- Ranbaxy Laboratories Limited Immuno Diagnostic Division Endowment for Clinical Immunology May 2011.
- Sankara Nethralaya Silver Jubliee Award for Diagnostic Microbiology May 2011.
- High Media performance Private Limited Endowment Award Clinical Microbiology May 2011.
- Dr.S.Ramaswamy & Dr.Narasimhan Endowment Award for Anatomy & Physiology May 2011.
- Endowment Award in Biochemistry for the best biochemistry Internship Award May 2011.
- Dr.H.N.Madhavan Endowment Award for best outstanding student in Master of Science in Medical Lab Technology from August 2008 to May 2011.
- Received Best Outstanding employee award for the year 2003 & 2004.
- Received Top 3rd award in P.G.D.M.LT (2000).

BIOGRAPHY OF THE CANDIDATE

Ms.S.Srilekha is a PhD student in Biological sciences at Birla Institute of Technology and Sciences, Hyderabad. She did her bachelor's degree in Microbiology at Valliammal College for women (University of Madras) in Chennai. Following it she completed her P.G.DMLT in Stella Maris College, Chennai. After completion she joined as Lab Technician at Sankara Nethralaya in the year 2000. Then she received her three years Master degree (MS) in MLT from BITS, Pilani (2008-2011) in collaboration with Medical Research Foundation (MRF), Sankara Nethralaya, Chennai. Her thesis for post graduation was "Molecular Genetic Screening of Mitochondrial Genes for Mutations m.11778G>A, m.14484T>C and m.3460G>A in patients with Leber hereditary optic neuropathy (LHON) & controls of Asian Indian origin". She had received "**Dr.H.N.Madhavan Endowment Award** for best outstanding student in Master of Science in Medical Lab Technology from August 2008 to May 2011" along with six other awards while completing her master's degree programme. She joined back in the the Department of Genetics and Molecular Biology as Research scholar in the year 2011, received ten years of service award and was deputed for 3 years under the ICMR project titled "Characterization of consanguineous Leber Congenital Amaurosis (LCA) families – homozygosity based approach". She had registered for PhD in 2011 under the supervision of Dr.N.Soumittra from Vision Research Foundation (VRF) and under the co-supervision of Prof.Suman Kapur and aimed in her thesis for "Genetic Analysis of Consanguineous south Indian Families with Leber Congenital Amaurosis and Retinitis Pigmentosa using Homozygosity Mapping". She had received the **best paper** award in a National Seminar on Function Genomics at Dr.M.G.R. University in February 2014. She also received her **SRF Fellowship award** in the year of 2015, received the **travel fellowship award** for IERG ARVO India chapter, 2015 and the fifteen years of service award at Sankara Nethralaya.

BRIEF BIOGRAPHY OF THE SUPERVISOR

Dr. N.Soumittra, Associate Professor and Principal Scientist, joined as Senior Scientist in the department of Genetics and Molecular Biology, Vision Research Foundation, Chennai in 2006. She completed her PhD from University of Madras and her doctoral work was on genetics of hereditary cancers. She is a recipient of Best outgoing student in biochemistry and overall Best outgoing student in the post graduate programme, MSMLT. She is UGC-CSIR lectureship qualified and was awarded "Best Paper award" by the Indian Society of Oncology Conference, 2004, "Young Scientist award" for the year 2004 by the Indian Society of Human Genetics and "Best free paper" in Genetics at Asia ARVO 2013 conference. Her current research interests are genetics of retinal diseases and corneal dystrophies. Her technical areas of expertise include medium and high through put genotyping and expression analyses studies like linkage analyses, homozygosity mapping, next generation sequencing analyses (targeted re-sequencing and whole exome sequencing) and whole transcriptome expression using microarray. She has received grants from DBT and ICMR, Govt. of India, as principal and co-investigator and has two current and four completed grants to her credit including an ICMR-INSERM collaborative project. She has published twenty-two research articles in international journals with two publications in Nature Genetics and two book chapters. She is involved in teaching genetics and molecular biology courses to post graduate students and is also a recognized PhD guide by SASTRA University, Thanjavore and University of Madras. Currently she has three PhD students under her supervision. Dr. N. Soumittra is a genetic counselor and is involved in molecular diagnostics of inherited ocular diseases.

BRIEF BIOGRAPHY OF THE CO-SUPERVISOR

Dr. Suman Kapur joined BITS, Pilani as Professor in the Centre for Biotechnology, Biological Sciences Group. She has worked in the capacity of Unit Chief, Community Welfare and International Relations since 1st January 2007. From 16th April 2010 she has taken charge as Dean, International Programmes & Collaborations at the Hyderabad Campus of BITS. With her team of a dozen research scholars has been instrumental in building a state of the art Human Genomics laboratory from funds received as Principal and/or Co-Investigator of now more than eighteen grants awarded since her joining BITS in 2004. As a mentor she has been able to motivate younger faculty to submit and execute independent grants in the form Women scientist (DST), Research Associate and senior research fellows (ICMR & CSIR). She has published more than 80 research articles in International and journals. Her research interests life in identifying biomarkers for unraveling the genetic basis of human diseases such as psychianic disorders like depression, schizophrenia, addiction and alzheimeres disease and metabolic disorders such as diabetes (T2DM), obesity, cataract and metabolic syndrome. The group is specifically studying several genes,viz., APOE, CAPN, PPARi5, it-4C ALDH2, ADM.% ADH1C, OPRM1, OB, TPH, CRVGA, CRVGB, D2, D5, ADCV4, ADCV3, CCKAR, CCKBR, cm, CF508, SPNK-1, PS-1, CVP2E1, CTSB, HSP70, TNFii, IC PRSS-1 and several micro-satellite markers on chromosome segments 2, 6 and 10. Chronic diseases have a long latency period and genetic markers can be effectively used for identifying individuals at an increased risk for developing these diseases and advocating appropriate lifestyle measures to delay the onset and progression of such diseases. Dr. Suman Kapur has ably conducted the day to day activities of this unit and was instrumental in orchestrating several student exchanges introduction of new fellowships and opportunities for both students and faculty at BITS campuses.